

The Use of Different Measurement Tools Including Quantitative Ultrasonography to Assess
Tissue Properties of Breast Cancer-Related Stage 2 Lymphedema: An Observational Study

Stefanie Fallone

A Thesis in
The Department
of
Health, Kinesiology and Applied Physiology

Presented in Fulfillment of the Requirements
for the Degree of Master of Science (Health and Exercise Science) at
Concordia University
Montreal, Quebec, Canada

March 2019
©Stefanie Fallone, 2019

CONCORDIA UNIVERSITY

School of Graduate Studies

This is to certify that the thesis prepared

By: **Stefanie Fallone**

Entitled: **The Use of Different Measurement Tools Including Quantitative
Ultrasonography to Assess Tissue Properties of Breast Cancer-
Related Stage 2 Lymphedema: An Observational Study**

and submitted in partial fulfillment of the requirements for the degree of

Master of Science

complies with the regulations of the University and meets the expected standards with respect to originality and quality.

Signed by the final Examining Committee:

Dr. Andreas Bergdahl Chair
Dr. Anna Towers Examiner
Dr. Hassan Rivaz Examiner
Dr. Nancy St-Onge Examiner
Dr. Robert Kilgour Supervisor

Approved by: _____
Chair of Department or Graduate Program Director

Dean of Faculty

Date: _____

ABSTRACT

The Use of Different Measurement Tools Including Quantitative Ultrasonography to Assess Tissue Properties of Breast Cancer-Related Stage 2 Lymphedema: An Observational Study

Stefanie Fallone

Breast cancer-related lymphedema is a growing concern for patients and clinicians as it is chronic and leads to debilitating physical and social effects. The condition characterized by a swelling in the arm and hand is accompanied by numerous changes including fibrosis, adipose tissue deposits and fluid accumulation that are not easily detectable in clinical practice. There is no standardized affordable method that is used to objectively detect and assess the underlying tissue changes. Patients are staged based on subjective palpation and circumferential measures. The aim of this project was to obtain a better understanding of the muscle, fat and skin changes that occur in the lymphedematous limb. A total of 20 women with unilateral stage 2 breast cancer related lymphedema as well as 20 healthy control women were recruited to participate. They underwent a DXA body composition scan, a Perometer arm volume determination as well as circumferential arm measurements along 6 pre-determined landmarks, and handgrip strength measures. Of the 20 patients, 7 were randomly selected to collect muscle, fat and skin strain values along the same 6 landmarks through ultrasound elastography. This study suggested that the onset of lymphedema may be localized in the mid-forearm spreading proximally and raised questions regarding simultaneous development of lymphedematous fluid in the unaffected arm. Furthermore, results showed that ultrasound elastography is a tool that can be used to assess elastic tissue properties in a safe and time-efficient manner and can provide details on the pathology, thus helping clinicians determine more detailed staging of the lymphedema and the best treatment alternative for their patients.

Acknowledgements

I would like to start by thanking my supervisor Dr. Robert Kilgour for his continuous guidance and support throughout my thesis, without him this thesis would have never been possible. Dr. Kilgour, taught me about the research process and provided me with continuous feedback from the very beginning. I am very grateful for having been given the opportunity to work by his side and I have learned an incredible amount thanks to him. A thank you for inviting me to attend weekly team meetings at the McGill Nutrition and Performance Laboratory and making me a part of the research team. Dr. Kilgour was more than just a supervisor to me, he was a mentor.

A big thank you to Dr. Anna Towers who taught me an incredible amount about lymphedema and for always being available for questions. She gave me private tutorials and lessons about the pathology of the condition and provided me with the great opportunity to shadow her in clinical practice. Thank you for allowing me to be a part of the McGill Lymphedema Research Program and thank you to the entire clinic staff for teaching me how to complete arm circumference measures, and Perometer measures and for being such an amazing support throughout the recruitment and data collection process.

I am just as grateful for the help of Dr. Hassan Rivaz who taught me about ultrasound and elastography and showed me how to use this tool. He invited me into many of his lab meetings and guided me throughout the more technical aspect of this project. He played a crucial role in the completion of this thesis, and for that I am very thankful. Another thank you to Hoda Hashemi and Zara Vajihi who were both of such amazing help from the very beginning. They were there to assist with the data collection of all ultrasound measures, and this thesis would have never been possible without them. Another thank you to Hoda for assisting in the analysis of the strain measurements. A thank you to Dr. Nancy St-Onge for joining my committee and for all her comments that have assisted in making this project stronger. Another thank you to both Anthony Thorburn and Jesse Whyte who have also assisted with some data collection.

A thank you to Dr. Sarkis Meterissian and his team at the McGill Cedars Breast Centre for collaborating in this project and assisting in the recruitment of participants. A thank you to Dr.

Leonard Rosenthal for all his assistance with the statistics for this project. Another thank you to the Dr. Louis G. Johnson Foundation and the PERFORM Centre of Equipment for providing funding to complete this study.

A thank you to the Concordia University Graduate Fellowship Award as well as the William. R. Sellers award for providing me with financial support throughout this thesis.

Contribution of Authors

Manuscript 1:

Stefanie Fallone: Generation of study, recruitment, data collection, writing of the chapter

Dr. Robert Kilgour: Generation of study

Dr. Anna Towers: Generation of study and clinical expertise

Dr. Hassan Rivaz: Generation of study

Manuscript 2:

Stefanie Fallone: Generation of study, recruitment, data collection, writing of the chapter

Hoda Hashemi: Assistance with data collection, calculations of strain values

Dr. Robert Kilgour: Generation of study

Dr. Anna Towers: Generation of study and technical expertise

Dr. Hassan Rivaz: Generation of study

Manuscript 3:

Hoda Hashemi: Generation of study, data collection, calculation of strain values, writing of chapter

Stefanie Fallone: Recruitment and data collection

Dr. Robert Kilgour: Generation of study

Dr. Hassan Rivaz: Generation of study and technical expertise

Dr. Anna Towers: Generation of study and clinical expertise

Dr. Mathieu Boily: Validation of anatomical landmarks obtained from ultrasound measurements

Table of Contents

Chapter I

Introduction and Background.....	1
Overview of lymphedema.....	2
1. What is lymphedema	
2. Clinical importance of lymphedema	
3. Staging of lymphedema	
Techniques to monitor lymphedema.....	5
Ultrasound and body composition.....	16
Ultrasound and lymphedema.....	18
Project overview.....	23

Chapter II

Segmental Tissue Composition and Handgrip Strength Relationships in Stage 2 Breast Cancer Related Lymphedema.....	25
---	----

Chapter III

Tissue Strain in a Cohort of Stage 2 Breast Cancer Related Lymphedema Patients Using Ultrasound Elastography.....	46
---	----

Chapter IV

Assessment of Mechanical Properties of Tissue in Breast Cancer-Related Lymphedema Using Ultrasound Elastography.....	63
--	----

Chapter V

Concluding Remarks.....	74
-------------------------	----

Chapter VI

References.....	79
-----------------	----

List of Figures

Chapter 1

Figure 1: Lymphedema stages.....	4
Figure 2: (A) Circumference landmarks along the arm (B) in order to obtain the volume of the limb	6
Figure 3: The Perometer device and software application. (A) The Perometer. (B) An example of the volume measurement of each arm. (C) The incremental measurements along the length of the arm used to calculate the overall volume.....	8
Figure 4: The water displacement technique. (A) The limb is submerged in a present container filled with water. Once the arm is removed (B) the difference in water is measured and represents the volume of the limb.....	9
Figure 5: Bioimpedance Spectroscopy (full body). Electrodes are placed onto the skin in the affected area of interest. While one pair of electrodes supply the current, the other measure the resistance to the current.....	10
Figure 6: (A) The DXA, (B) An example of a DXA scan as displayed on the computer (C) with the measurements obtained.....	11
Figure 7: Contrast Enhanced MRI of a lymphedematous calf.....	12
Figure 8: (A) A CT machine displaying (B) a CT cross-sectional image of a medial right thigh demonstrating skin thickening and edema.....	13
Figure 9: A simplified representation of the basics of ultrasound.....	14
Figure 10: Ultrasound images of (A) a lymphedematous calf with (B) minimal amount of water and (C) a stone paved image from excess water.....	19
Figure 11: The higher the grade of fluid accumulation, the more important the relative reduction of lymphedema volume.....	19
Figure 12: Definition of subcutaneous echogenicity grade and subcutaneous echo-free space grade.....	21
Figure 13: Changes in muscle thickness (measured through ultrasonography) and changes in limb volume (measured through tape circumference) of the lymphedematous proximal and distal limb over time.....	22

Chapter 2

Figure 1: Circumference tape landmarks along the segment of the arm. The numbers on the figure represent the landmarks indicated in the text.....31

Figure 2: Chart illustrating the arm circumference ratio of dominant over non-dominant arm in the healthy control women across the 6 locations along the limb and the ratio of the affected over unaffected arm in women diagnosed with stage 2 BCRL across the 6 locations along the limb ..38

Chapter 3

Figure 1: Tape landmarks along the segment of the arm. The numbers in the figure represent the landmarks indicated in the text.....51

Figure 2: (A) Fat strain differences found across the 6 landmarks along the affected and unaffected arms. (B) Muscle strain differences found across the same 6 landmarks along the affected and unaffected arm of women with stage 2 breast cancer-related lymphedema.....56

List of Tables

Chapter 1

Table 1: CTC v.3.0 staging of lymphedema..... 4

Table 2: Summary of the techniques used to diagnose and monitor lymphedema..... 15

Chapter 2

Table 1: Demographic and body composition data between women diagnosed stage 2 breast cancer related lymphedema compared to women without lymphedema.....33

Table 2: Volume of the affected and unaffected arms of women with lymphedema.....34

Table 3: (A) DXA fat measures and (B) DXA lean measures on the affected and unaffected arms of women with lymphedema.....35

Table 4: Body composition ratios between the right and left arm of the control group and the affected and unaffected arms of the experimental group.....36

Table 5: Arm circumference ratios of the affected over unaffected sides of women with lymphedema.....39

Chapter 3

Table 1: Comparisons between the cohort of 20 lymphedema patients recruited in this study and the 7 normal participants.....53

Table 2: General comparisons between the affected lymphedema arm and the unaffected arm..54

Table 3: Comparisons of the affected and unaffected tissue strain measurements for skin, fat and muscle.....55

List of Abbreviations

BCRL	Breast cancer-related lymphedema
US	Ultrasound
BIS	Bioelectric Impedance Spectroscopy
HGS	Handgrip Strength
DXA	Dual X-Ray Absorptiometry
MRI	Magnetic Resonance Imaging
CT	Computed Tomography
BMI	Body Mass Index
MUHC	McGill University Health Centre
MNUPAL	McGill Nutrition and Performance Laboratory
CDT	Complete Decongestive Therapy
BMD	Bone mineral density

I

Introduction and Background

Overview of Lymphedema

1. What is Lymphedema?

The lymphatic system plays an important role in the immune system of the body and is responsible for the transportation of lymphatic fluid. Its primary functions include the drainage of excess interstitial fluid, the transportation of dietary lipids, and the initiation of immune responses against antigens. Interstitial fluid is mainly composed of blood plasma and some protein, and filters through the capillary walls. The excess fluid drains into the lymphatic vessels and becomes lymph. This excess fluid includes approximately 3 liters per day. The lymph travels into the lymphatic ducts and into the internal jugular and subclavian vein as blood (Tortora et al. 2012). Damage to the lymphatic system can consequently lead to a condition known as lymphedema.

The initial stages of lymphedema are defined as an accumulation of protein-rich interstitial fluid in an area of the body, resulting from impaired lymphatic flow or damage to the lymphatic vessels. This can be as a result of malformation in the lymphatics, known as primary lymphedema, or from damage or removal of lymph nodes, such as from surgery or cancer treatment, known as secondary lymphedema (Cheville et al, 2003, Szuba et al, 1998). Secondary lymphedema is reported as the most common form of lymphedema (Cheville et al. 2003). Several factors may lead to secondary lymphedema although the most common are caused by a tumor in the lymphatics, a tumor metastasis to the lymph nodes consequently blocking the lymphatic flow, or from cancer surgery or radiation therapy.

There are four main types of secondary lymphedema. The first, known as iatrogenic lymphedema is caused by surgery or radiation therapy and can lead to fibrosis. The cause can be either intentional, for instance during lymph node dissection for cancer surgery, or accidental. Lymphedema of the arm following axillary lymph node dissection for breast cancer and lymphedema of the leg following pelvic lymph node dissection for pelvic neoplasms are the most common forms of this type of secondary lymphedema. The second, called traumatic lymphedema is caused from traumatic injuries. The third, is known as post-infectious lymphedema and can

develop as result of an infection, such as filiaris, which is caused by a parasite that is directly transmitted by a mosquito, and usually is present in more tropical areas. The fourth is called neoplastic disease and represents the involvement of tumors in the lymphatic vessels, lymph nodes and lymphatic ducts (Szuba et al. 1998).

2. Clinical Importance of Lymphedema

Breast cancer-related lymphedema occurs as a result of breast cancer treatment including surgery, radiation therapy and chemotherapy, and typically affects the ipsilateral upper limb. Patients who undergo axillary lymph node dissection as well as patients with an elevated BMI, particularly over 30 kg/m², are at increased risk of developing the condition. Although the onset of the condition may occur any time following the cancer treatment, the majority of patients will begin to experience symptoms of lymphedema within the first 2-3 years after breast cancer treatment. However, some patients develop the condition as early as 30 days following their cancer treatment, and as late as 30 years after. It has been reported that lymphedema affects over 90 million people worldwide (Garza et al. 2017, Park et al. 2007), and that lymphedema following breast cancer will develop in about 1 in 8 Canadian women (Canadian Cancer Society, 2019). This chronic condition, although not life-threatening, is followed by multiple debilitating complications and a negative impact on the patient's quality of life. Symptoms are described as swelling, feelings of tightness and heaviness, weakness, pain, and tension. Furthermore, it causes feelings of anxiety, social isolation and stress (Tassenoy et al. 2016). The condition also puts patients at high risk of cellulitis, and results in frequent hospital visits (Moffatt et al. 2003).

3. Staging of Lymphedema

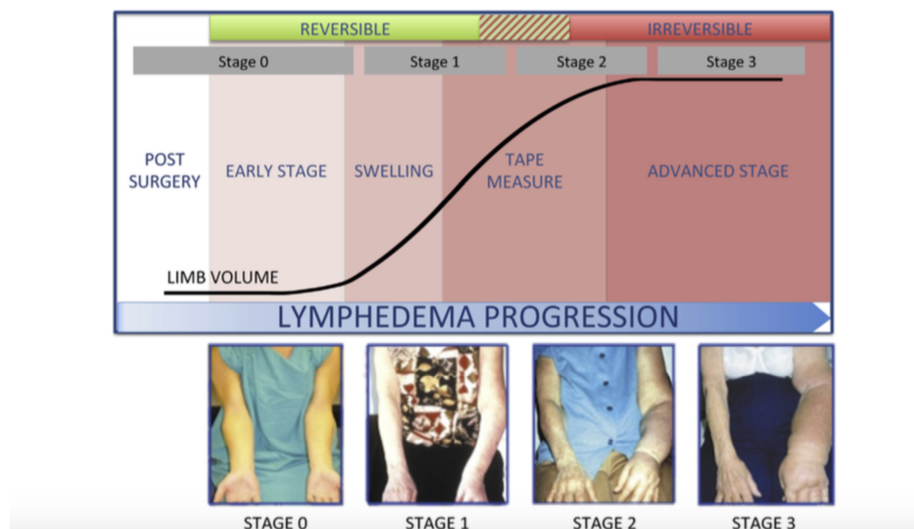
The diagnosis of lymphedema is based mainly on changes in limb volume. Ideally, one would want to detect the condition as early as possible, as early detection and treatment may lead to reversibility. However, there currently exists no technique that can identify very early limb volume or subcutaneous tissue changes, nor is there any tool that can identify patients that may be predisposed to this chronic condition that requires continuous self-management and treatment (Dixon et al. 2015).

Once diagnosed, the disease is staged based upon a subjective assessment of tissue texture and skin changes. There have been multiple ways to stage the severity of lymphedema (Cheville et al. 2003). According to the Common Toxicity Criteria version 3 (CTC v.3.0), lymphedema can be staged based on a 3-point criteria scale (Common Toxicity Criteria 2006). The details of the criteria are presented in table 1, where the very subjective nature of these criteria is clearly seen. Some methods also use a 4-point criteria scale, as described by Dixon et al. (2015) and illustrated on figure 2.

TABLE 1: CTC v.3.0 staging of lymphedema (Common Toxicity Criteria v. 3.0 2006).

Adverse Event	Short Name	1	2	3
Lymphedema-related fibrosis	Lymphedema-related fibrosis	Minimal to moderate redundant soft tissue, unresponsive to elevation or compression, with moderately firm texture or spongy feel	Marked increase in density and firmness, with or without tethering	Very marked density and firmness with tethering affecting $\geq 40\%$ of the edematous area

FIGURE 1: Lymphedema Stages (Dixon et al. 2015)



In this method, Stage 0 is known as a subclinical stage through which limb volume assessment will not be capable of identifying lymphedema, as the changes in limb size from swelling only begin to occur late during Stage 1 or early in Stage 2. At this point, however, the lymphatic fluid transport system is already damaged. In Stage 1 lymphedema, there may be a noticeable swelling

in the limb especially at the end of the day, along with a feeling of heaviness. Pitting edema is also present; however, it disappears with elevation or overnight. At this stage, the disease may still be reversible, as the swelling is characterized by an accumulation of lymph fluid that can be drained by combined decongestive physiotherapy (for example, manual lymphatic drainage techniques, compressive bandaging, elastic sleeves). It is usually during the latter part of Stage 1 and most often in Stage 2 that lymphedema is usually diagnosed. Therefore, the majority of patients fall under Stage 2 and remain at that stage if the disease is properly controlled. Stage 2 is the stage that involves multiple subcutaneous tissue changes, including the beginning of fibrosis, an accumulation of adipose tissue deposits, a hardening of the tissue and non-pitting edema. These changes are now mostly irreversible and one can only hope to prevent further deterioration. In Stage 3 we begin to see skin thickening (pachydermia), changes in dermal papillae and inflammatory skin changes (dermatitis and hyperpigmentation). Although it is rare for patients to progress to the late Stage 3, this stage is defined as the most advanced stage of swelling and is called elephantiasis (Dixon et al. 2015). In this stage, the skin changes in shape and form and the extremities of the limb begin to resemble the legs of an elephant (Garza et al. 2017). This stage is also categorized by the absence of pitting, further fat deposition, fibrosis, and the development of wart-like nodules (Hoffner et al. 2017).

Given that the condition becomes irreversible at the onset of stage 2, and that this stage involves multiple subcutaneous changes, it is essential to have a technique that can objectively quantify these changes along with accurate limb volume measurements at this early stage. This would then allow for treatment early in the course of the disease and thus potentially improve long term patient outcomes.

Techniques to Monitor Lymphedema

1. Tools to Measure Volume

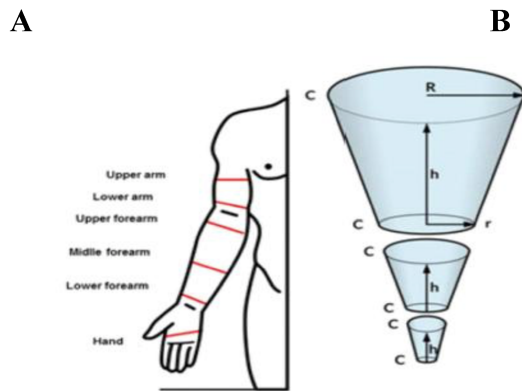
Typically, lymphedema diagnosis and monitoring is limited to the identification of changes in the limb shape and size. These mainly involve indirectly calculating the volume of the limb and comparing it to the unaffected limb, as well as monitoring change of volume over time. There exist several tools to monitor lymphedema, but there is a large variability in their use

across research trials, thus limiting their applicability to particular clinical settings (Stout et al. 2008). The most common clinical method to monitor the progression of lymphedema is through circumferential tape measurements. This technique involves measuring the circumference of the arm at specific segments and converting these measurements to total limb volumes using the formula for a truncated cone (Johnson et al. 2015), as illustrated in figure 1 and calculated as

$$V = \frac{\pi \cdot h}{3} \cdot (R^2 + R \cdot r + r^2)$$

where V is the volume, h is the height of the cone, R is the radius of the larger base of the cone and r is the radius of the smaller base (Ferreira et al. 2015).

FIGURE 2: (A) Circumference landmarks along the arm (B) in order to obtain the volume of the limb, where **h**= the height of the cone section, corresponding to the length of the arm between the two landmark points, **R**= the radius at the base of the cone, **r**= the radius at the apex of the cone (Ferreira et al. 2015).

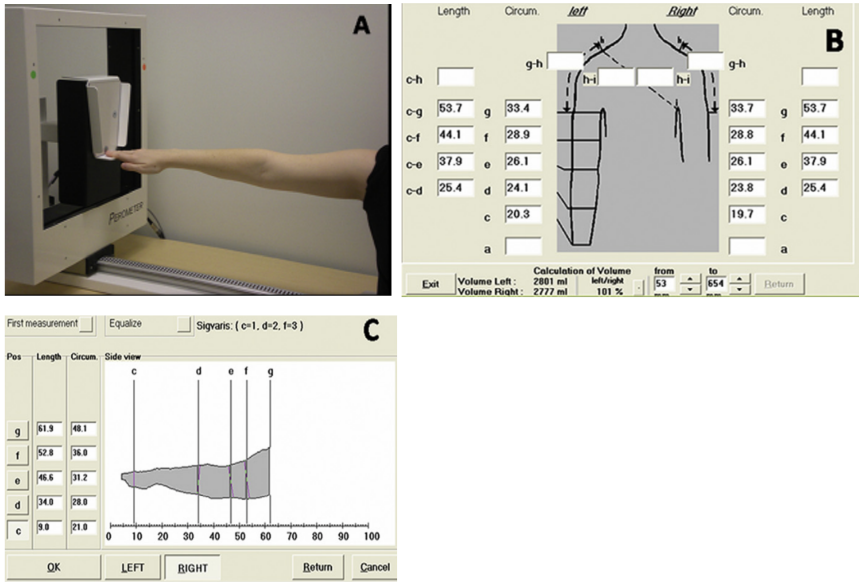


The main difficulty with tape measurements is that they do not provide any information on the structural changes and tissue properties of the skin (e.g., skin thickness) and subcutaneous tissues (e.g., fat, interstitium, and skeletal muscle). Hence this technique is unable to differentiate lymphedema from adipose tissue nor to determine if a decrease in circumference or volume is due to a reduction of lymphedema or from muscular atrophy, for example. Technical errors are also possible due to inaccurate marking of measurement landmarks, applying an inadequate amount of pressure on the tape or if the angle of tape is improperly positioned relative to the limb (Newman et al. 2013).

Apart from tape measurement, other techniques have been developed to measure the volume of a limb. One common technique for lymphedema volume measurement is perometry: a 3D scanning technique that measures the volume of a limb using 360 degrees of infra-red light (Dixon et al. 2015). The tool consists of a square-measuring frame that moves along the long axis of the limb being measured (Hwang et al. 2014). The machine measures the surface area of the limb at 0.5 cm increments, from which volume is calculated. Although the measurement is time efficient, the machine is rather large and expensive (Garza et al. 2017). An image of the perometer device along with the software application and image output is illustrated on figure 3.

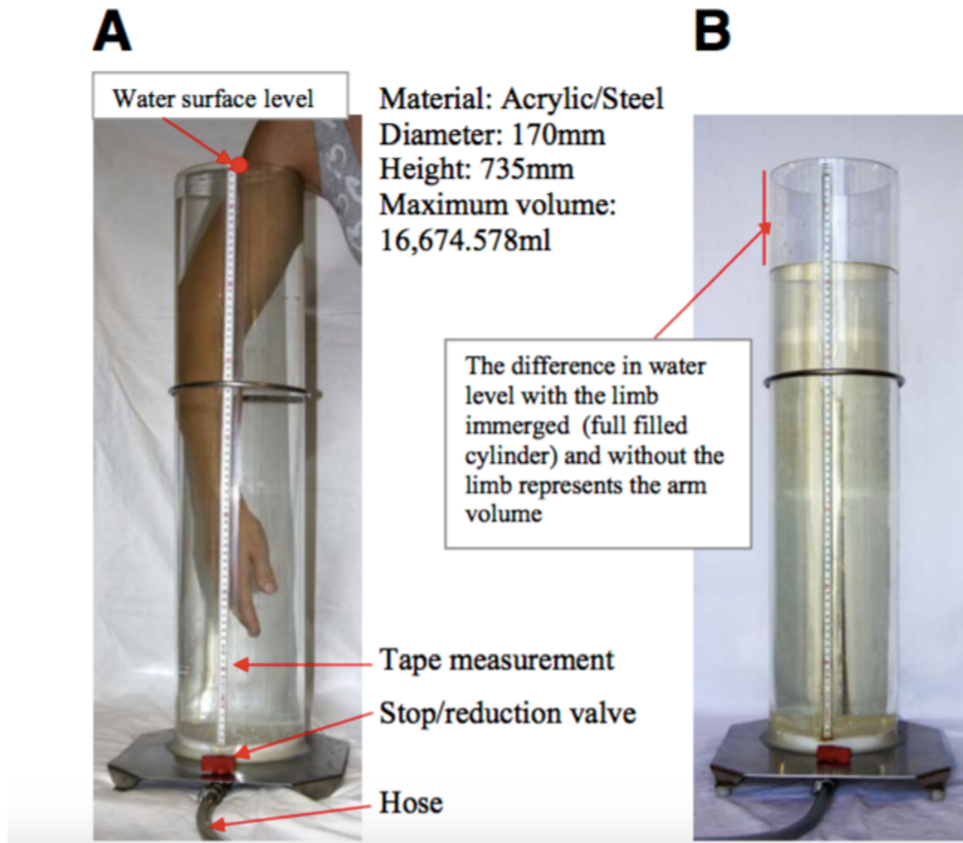
The main issue with this technique is that when measuring the volume of the limb, it omits the extremities, such that any swelling in a hand, for instance will not be taken into consideration. This can lead to the possibility of under-diagnosing the disease. Under certain circumstances, tape measurements have been shown to diagnose lymphedema at a higher sensitivity than perometry (Armer et al. 2009). Both techniques; however, are limited in their ability to differentiate between weight gain and swelling from lymphedema (Garza et al. 2017).

FIGURE 3: The perometer device and software application. (A) The perometer. (B) An example of the volume measurement of each arm. (C) The incremental measurements along the length of the arm used to calculate the overall volume (Ancukiewicz et al. 2011).



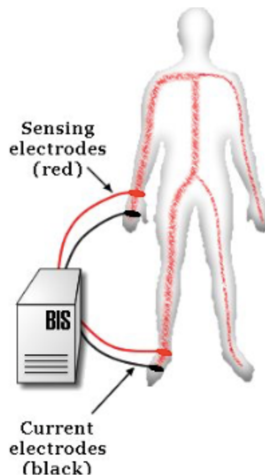
Water displacement and bioelectrical impedance spectroscopy (BIS) are also tools used to assess swelling and volume measurements of the lymphatic limb. Water displacement simply measures the fluid displaced by dipping the arm in a water-filled bath. The entire arm until the level of the armpit is immersed in a container of a height of 735 mm filled with a preset volume of water. The arm is then removed and the amount of water that is displaced is then measured. The displacement is representative of the volume of the limb (Sagen et al. 2009). This technique is illustrated in figure 4. Although this technique is considered a gold standard for obtaining limb volume measurements, it is rather impractical in a clinical setting as it is large, messy and contraindicated for individuals with open wounds. It may also be subject to challenges with both inter-rater and intra-rater reliability due to difficulties in identifying and reproducing the landmark on the limb up to which the arm is submerged (Garza et al. 2017).

FIGURE 4: The water displacement technique. (A) The limb is submerged in a preset container filled with water. Once the arm is removed (B) the difference in water is measured and represents the volume of the limb (Sagen et al. 2009).



Bioelectric impedance has the advantage of measuring extracellular fluid and total fluid volume. It measures opposition or resistance to the flow of an electrical current that passes through the area of interest, as per the illustration in figure 5 (Ward LC. 2015), from which fluid volume is then calculated. It is based on the principle that fluid accumulation will decrease the resistance to the electrical current and therefore represent a more severe lymphedema. In this technique, however, the control limb is used as a reference point, thus eliminating this tool in the use of bilateral lymphedema. The tool could also be used to monitor the volume changes in the lymphatic limb over time; however, it fails to provide any changes in tissue composition that accompany lymphedema, such as fibrosis. Furthermore, increases in fibrotic tissue may lead to increases in electrical current, falsely giving the impression of an improvement in the lymphedema condition. (Garza et al. 2017).

FIGURE 5: Bioelectric impedance Spectroscopy (full body). Electrodes are placed onto the skin in the affected area of interest. While one pair of electrodes supply the current, the other measure the resistance to the current.



<https://www.bcm.edu/bodycomplab/biaschemapage.htm>

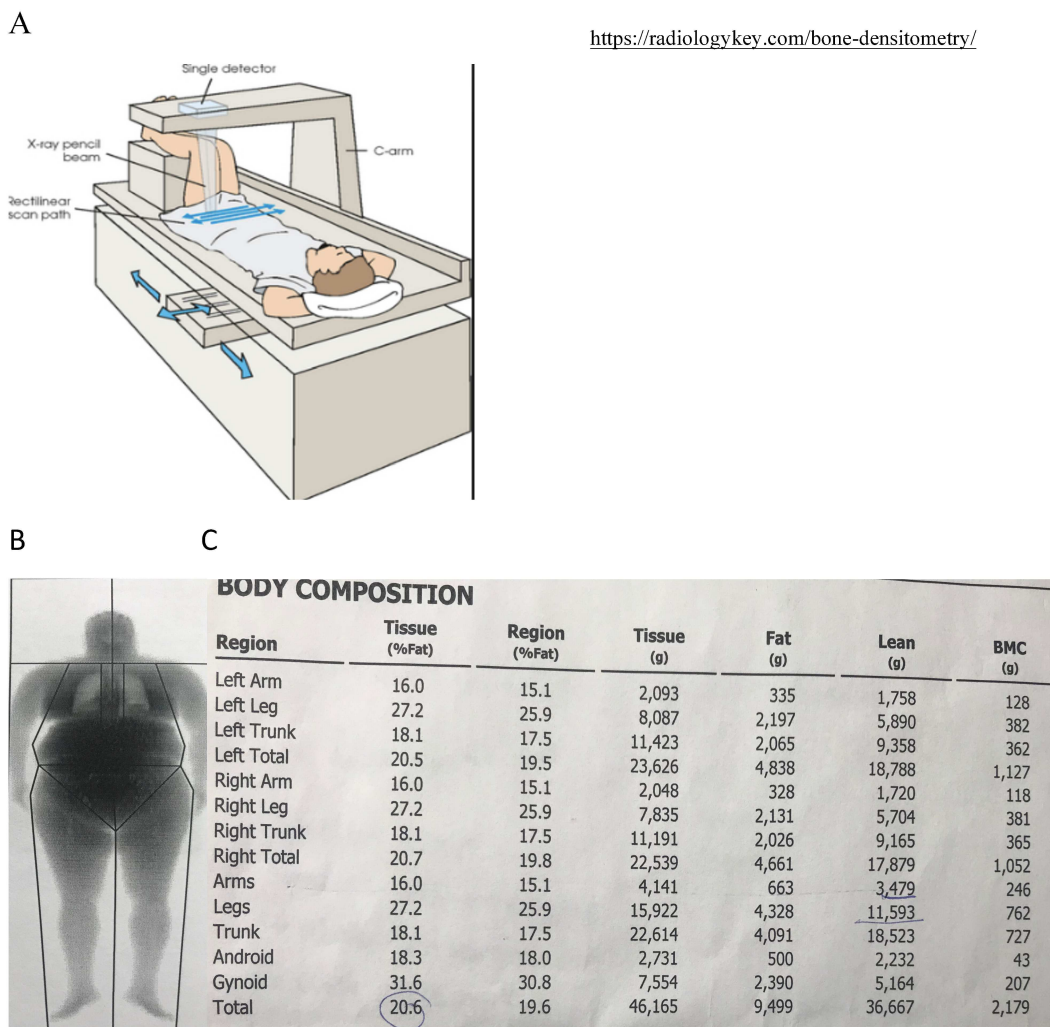
2. *Tools to Measure Body Composition*

Subcutaneous tissue changes in a lymphedema population are currently monitored through pitting edema. This involves the subjective judgment of the therapist to palpate the affected area of the patient's limb and identify the tissue texture based on skin and subcutaneous tissue elasticity. The main changes in tissue texture that occur as lymphedema progresses include edema, from an excess of fluid, and fibrosis, which involves a hardening of the tissue from an accumulation of protein-rich lymph fluid (Johnson et al. 2015). This technique involves the clinician to push down onto the skin for about 10 seconds and check for an indentation in the skin, which would represent an accumulation of fluid in the region of interest. This type of measurement is subjective as it does not provide a quantifiable amount of edema or tissue elasticity.

Dual energy X-ray absorptiometry (DXA) is another tool that provides a measurement of body composition. It is a two-dimensional scanning technology that uses a minimal amount of x-rays and provides a measure of fat, lean and bone mineral masses. During a scan, an x-ray beam

travels across a person in a rectilinear motion. A single detector is then used to acquire the data where it is then registered on a computer. Measurements obtained from the DXA can be regional, total body and appendicular skeletal muscle mass (Visser et al. 1999). This technique is illustrated in figure 6. Newman et al. (2013) investigated the precision of DXA and BIS in 24 women with stage 2 lymphedema and concluded that these two measurements provided an acceptable measure of precision of arm lean mass, fat mass and extracellular fluid volume. A particular limitation of DXA, is that the measure of lean mass can also include other tissue components such as water, proteins, glycogen, and non-bone minerals, therefore leading to an overestimation of muscular content.

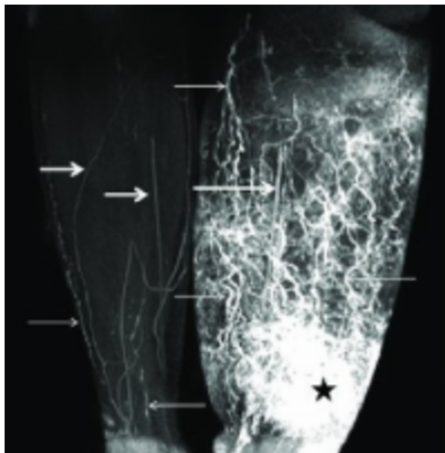
FIGURE 6: (A) The DXA, (B) An example of a DXA scan as displayed on the computer (C) with the measurements obtained



The issue remains that none of the above techniques consistently measure the tissue components of the lymphedematous limb across the different stages of the disease. Furthermore, these methods lack accuracy in differentiating between lymphedema and other types of edema (Righetti et al. 2007) such as swelling from chronic venous insufficiency (Nicolaidis, 2000).

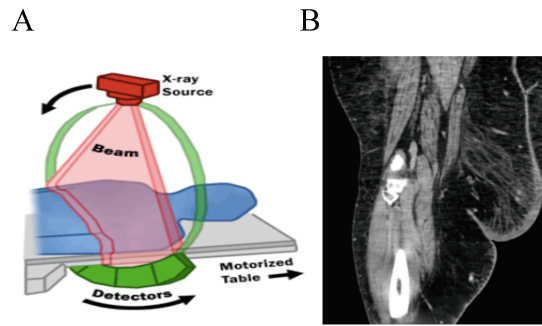
In contrast, magnetic resonance imaging (MRI) and computed tomography (CT) have been shown to precisely measure lymphedema at a localized area and can be useful in the differentiation of the etiology of the lymphedema. MRI, more specifically contrast enhanced MRI involves the injection of a contrast agent into the lymphatic system that will provide visualization of soft tissues and water (Tassenoy et al. 2016, Garza et al. 2017), as shown on figure 7. However, this method is costly and not readily available in clinics (Hwang et al. 2014), which limits its usage for the lymphedema population given that it is a chronic condition requiring multiple follow-ups (Righetti et al. 2007).

FIGURE 7: Contrast Enhanced MRI of a lymphedematous calf (Lu et al. 2012).



A CT scan involves a narrow beam of X-rays that are rotated around the patient and produce signals. The signals get processed by the computer and produces cross-sectional images (figure 8). With lymphedema, the images have been shown to differentiate between skin and subcutaneous thickening. The main issue with CT is that it provides high exposure to ionizing radiation (Tassenoy et al. 2016).

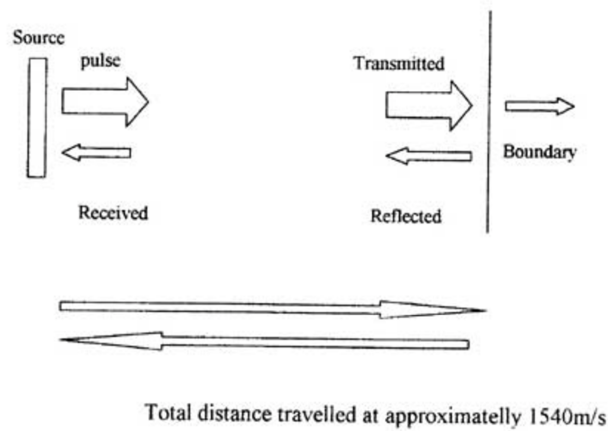
FIGURE 8: (A) A CT machine displaying (B) a CT cross-sectional image of a medial right thigh demonstrating skin thickening and edema (Porino J et al. 2016)



<https://www.fda.gov/>

Ultrasonography is a real time, safe and inexpensive tool that has recently began to be studied as an alternative method to evaluate the tissue properties in upper and lower limb lymphedema (Hwang et al. 2014). This medical imaging technique, is a form of acoustic oscillation that uses high frequency sound waves and their echoes (e.g., echo density) in order to display images of the underlying tissue structures. Any oscillation frequency above 20KHz is considered ultrasound. The device emits a selected frequency of sound pulses through the transducer probe. The pulses then penetrate into the skin until they reach a boundary, through which some of the sound wave rebounds back towards the probe. The ultrasound device then records the amount of time it takes for this echo to return back to the probe, which allows it to compute the distance of the boundary to the probe using a constant speed of sound (1540 m/s) and displays this on an image. The machine transmits and receives millions of pulses every second, allowing it to display an image of the tissue at that moment in time. This process is illustrated on figure 9.

FIGURE 9: A simplified representation of the basics of ultrasound



<http://dynamicultrasound.org/dugphysics.htm>

The ability of a tissue to reflect a sound reflection or echo, is known as the principle of echogenicity. Structures are said to be hyperechoic when the surface reflects a stronger echo. Hyperechoic structures are represented by a brighter point on an ultrasound scan. An example of a hyperechoic structure is skin. When a structure has a lower tendency to bounce back an echo, it is known as a hypoechoic structure and is represented by a darker point on the image. An example of a hypoechoic structure is fat. Certain tissue components such as fluid are known to be anechoic as the sound pulses pass straight through it, and are displayed in black on the ultrasound image. The main disadvantage of ultrasound is its inability to penetrate through bone or air, but this would not be an issue in the evaluation of lymphedema. This classic form of ultrasound is known as brightness-mode or B-mode ultrasound.

Ultrasonography is an imaging technique that is continuously evolving. One recent advancement of this technique is ultrasound elastography, which has the ability to measure the mechanical properties of tissue, including tissue elasticity and muscle stiffness. Strain elastography is a technique that involves manually applying a compression with the ultrasound transducer over the tissue. The strain is then measured in a 2-dimensional region and displayed on an elastogram. The measurements, although qualitative, can be converted to quantitative data using the Young modulus. In fact, once the strain differences are displayed in color or in grey-

scale on the elastogram, the elastography software calculates the strain ratio between the reference area and the diseased area. (Brandenburg et al. 2014).

A summary identifying the advantages, disadvantages and applicability of the different lymphedema measuring techniques mentioned above can be found in Table 2.

TABLE 2: Summary of the techniques used to diagnose and monitor lymphedema (This table was generated from data presented in the following references: Dixon et al. 2015; Garza et al. 2017; Szuba et al. 1998; Newman et al. 2013; Righetti et al. 2007, Semelka, 2007)

Technique	Cost	Time-efficiency	Safety	Reliability and applicability	Measurement
Tape Measure	Very low	Time-intensive	Safe	Susceptible to poor inter-observer variability, but can be reproducible using specific anatomical landmarks, portable	Volume, circumference
Perometry	Moderate	Quick	Safe	Accurate but lacks information on distal part of limb (Hand/foot)	Volume
Water Displacement	Low	Quick	Safe	Gold Standard, but may be subject to challenges with inter-rater and intra-rate reliability.	Volume
BIS	Low	Quick	Safe	Can detect early changes of inflammation, no information on tissue structure, portable	Extracellular fluid content, lean mass and fat mass measures for stage II patients
DXA	Expensive	Quick	Safe (minimal x-ray)	Has been shown to provide acceptable precision in measuring	Measurement of lean mass, fat

				the body composition, but more useful in unilateral lymphedema	mass and bone mineral mass
MRI	Very Expensive	Long	Safe	Accurate	Provides structural tissue information, especially soft tissue and water visualization
CT	Very Expensive	Moderate	Exposure to radiation	Accurate	Provides tissue structure information, can identify skin thickening
US	Moderate	Quick	Safe	Good reliability and reproducibility, portable	Provides information on structure changes, can detect lymphedema

Another tool that is often used to assess breast cancer survivors and could be used with lymphedema patients is the handgrip dynamometer. This tool is an indicator of muscle capacity and provides a measure of forearm muscle strength which can be used to assess changes in muscle function as a result of lymphedema. In fact, it has been shown that changes in handgrip and body composition can occur six months after breast cancer surgery (Gomes et al. 2014).

Ultrasound and Body Composition

Some of the first literature that evaluated the use of ultrasonography as a measure of body composition was conducted by Ikai et al (1968). Ultrasound has been widely used since then as a measure of body composition. For example, in a study conducted by Young et al (1980), ultrasonography was used to assess the severity of quadriceps muscle wasting following an injury and immobilization of the leg and was compared to the standard measure of circumference tape measurement. The authors assessed the knees of 21 participants (5 females and 16 males). They took bilateral ultrasound scans of each participant's knee at a frequency of 2.5 MHz. The authors

compared the difference in muscle wasting between the uninjured and injured leg and also tested the reproducibility of the results by re-assessing the thighs of seven subjects at four different occasions. The authors concluded that assessing the composition of the thigh through ultrasound revealed more severe muscle wasting than through the tape measurement. The authors described that anthropometric measures overestimate the size of the muscle since a layer of subcutaneous fat surrounds it, but ultrasonography can provide an image that distinguishes the muscle from the fat.

It is interesting to note that over thirty years ago, the literature identified the lack of validity in using a tape measure as an assessment tool for body composition, yet this is still the most common method for monitoring lymphedema. Young et al (1980) did however describe certain limitations regarding the use of ultrasound in their study, such as issues when scanning very lean thighs due to the difficulty to apply a stable compression with the transducer causing the outer border of the muscle to be hidden, and the method being time-consuming. Nevertheless, there have since been multiple advancements in this technique. In fact, in a study conducted by Minetto et al. (2015), 44 older adults with a mean age of 82 ± 7 years and 60 younger individuals with a mean age of 26 ± 3 years were assessed by bioelectric impedance and ultrasonography in order to establish muscle specific and population specific cut-off values for low muscle mass. Three consecutive B-mode static ultrasound scans of lower body muscles were taken by the same evaluator. The authors assessed the intersession and intra-rater reliability of the ultrasound measures by determining the intraclass correlations and coefficients of variations of the three scans for each muscle being assessed. The authors obtained the following correlations and coefficients of variations for the rectus femoris muscle, the vastus lateralis, the tibialis anterior, and medial gastrocnemius respectively: 0.98 and 3.2%, 0.99 and 3.3%, 0.98 and 1.5%, 0.97 and 3.7%. Ultrasound was suggested to be a highly sensitive tool for the assessment of low muscle mass. The authors therefore suggested using ultrasound to identify site-specific cut-off points for sarcopenia diagnosis. They also showed that the bioelectric impedance derived criteria and cut-off points underestimate the prevalence of low muscle mass, as it ranged from 2 to 75% depending on the diagnostic criteria being used and therefore concluded that ultrasound would be the modality of choice.

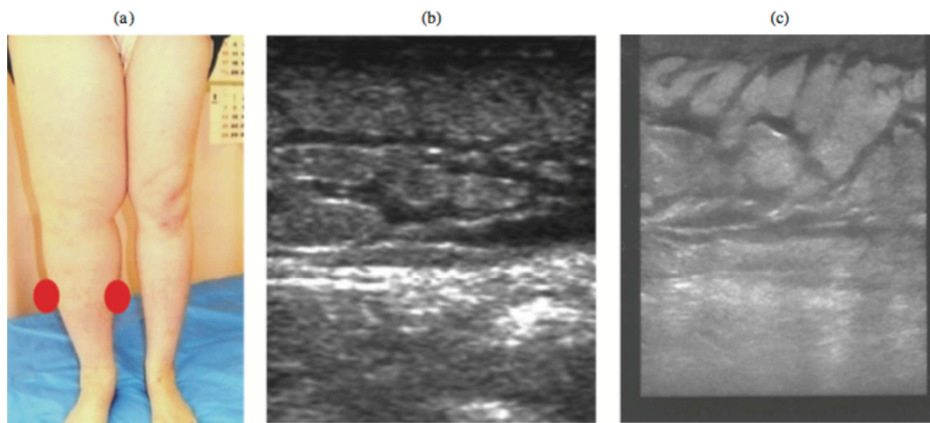
Recent studies have also used ultrasound as a tool to investigate muscle architecture. In fact, Rastelli et al. (2015) assessed the muscle architecture of the muscle bellies of the quadriceps femoris. Specifically, the authors measured muscle fascicle length and pennation angle of the muscles of five obese women and six normal weight women in order to determine if changes in muscle composition from fat infiltration and changes in muscle architecture from reduced fascicle length or increased pennation angle were associated with less force production regardless of increased muscle cross-sectional area in obese women. Ultrasound images of the quadriceps were obtained by moving the transducer probe along the muscle bellies. The operator would then identify the proximal and distal edge of each muscle of the quadriceps and divided the length into three landmarks. Images were taken for each of those landmarks. The pennation angle was determined as the angle between the muscle fascicular paths and their insertion in the deep aponeurosis. Four different fascicles were measured in each image and the average value was analyzed. The ultrasound images found the pennation angle of obese women to be significantly greater than the normal weight women, concluding that steeper pennation angle has a negative effect on muscle performance. Abe et al. (2016) also used ultrasound to investigate muscle quality. The authors tested the relationships between age-related declines in muscle strength, as measured by a handgrip dynamometer, and loss of muscle thickness and muscle forearm quality through ultrasound and suggested that age-related decline in handgrip strength is associated with muscle quality. The authors described ultrasound as a portable alternative to DXA to estimate muscle quality of the forearm.

Ultrasound and Lymphedema

The use of ultrasound has recently begun to gain interest in the assessment of lymphedema. Many studies have used ultrasonography as a tool that can predict or monitor treatment outcomes in lymphedema patients. In fact, in a study conducted by Niimi et al (2014), 178 outpatients and 29 inpatients with unilateral leg lymphedema following cancer were studied in order to test whether fluid accumulation as visualized through ultrasound can be a predictor of the patient's response to compression physical therapy. Ultrasound images were taken at three different time periods including at the onset of their therapy, at one month and at two months. The ultrasound measures were taken from linear 7.5 MHz to 10 MHz probes and fluid

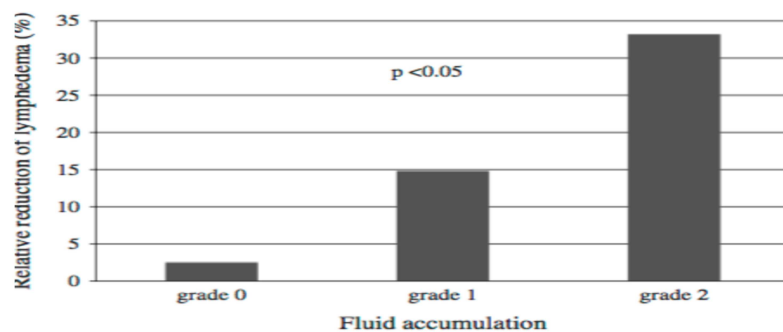
accumulation was determined by low echogenicity, that is the darker areas on the image. The fluid accumulation was then classified into three grades: grade 0 defined as no fluid present, grade 1 defined by a minimal amount of water, and grade 2 defined by a stone paved image due to excess water. Visual representation of the ultrasound images is shown on figure 10:

FIGURE 10: Ultrasound images of (A) a lymphedematous calf with (B) minimal amount of water (grade 1) and (C) a stone paved image from excess water (grade 2) (Niimi et al. 2014).



The authors suggested that the higher the grade of fluid accumulation as viewed from ultrasound echogenic images, the higher the reduction of lymphedema volume with physical therapy, thus predicting the treatment results. These results are shown in figure 11.

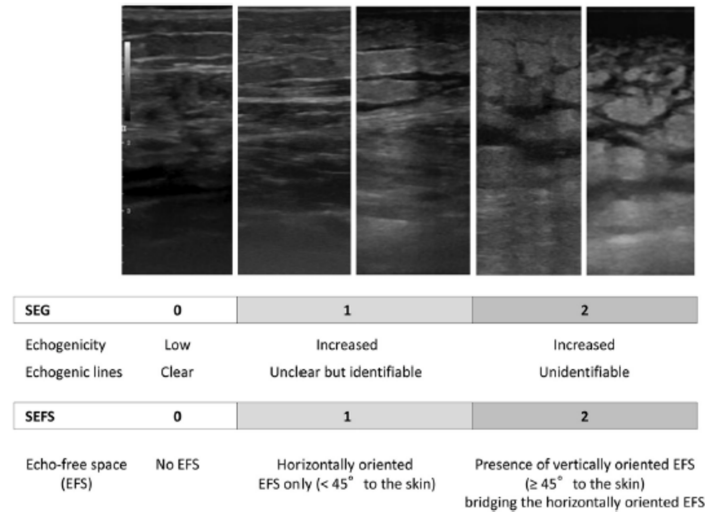
FIGURE 11: The higher the grade of fluid accumulation, the more important the relative reduction of lymphedema volume (grade 0: 2.5%, grade 1: 14.8%, grade 3: 33.2%, $p < 0.01$) (Niimi et al. 2014).



Hacard et al. (2013) also assessed the effectiveness of treatment outcomes through ultrasound. They evaluated thirty patients with lymphedema undergoing a five-day intensive decongestive treatment. The authors took the circumferential measurements of the affected limb and correlated it to the dermal thickness of the skin as measured through ultrasound. The authors also assessed the biomechanical properties of the skin using a Cutometer and the quality of life of the patients using a visual analogue scale. The ultrasound scans were taken at 15 frames per second 15mm wide and 7 mm deep. Images were taken at three locations on the limb: 15 cm above and below the elbow and at the top of the hand for an individual affected with upper limb lymphedema and 20 cm above and below the knee and at the top of the foot for individuals with leg lymphedema. Dermal thickness was measured from the surface of skin down to the deepest point of dermal echogenicity. Measurements were taken before the physiotherapy treatment and 6 months later. Reductions in skin thickness as a result of the physiotherapy were observed. Spearman coefficient correlations between the relative changes in volume and changes in dermal thickness were found to be statistically significant ($r=0.37$, $p=0.02$), meaning that ultrasound determines that treatment reduced lymphedema by a reduction in dermal thickness. Interestingly, none of the parameters correlated with quality of life improvement following the treatment.

Suehiro et al. (2015) used ultrasonography of subcutaneous tissue in order to test the effectiveness of physiotherapy treatment on leg lymphedema outcomes. The authors describe that the current outcome measurement tool for lymphedema monitoring is through volumetric volume measurements but that circumferential measurements alone are not enough to understand the nature of extremity volume changes in lymphedema patients. For example, a limb enlargement can be due to tissue fluid accumulation just as it can be due to tissue proliferation. The authors therefore identified the need for a tool to monitor treatment results using tissue echogenicity assessments of lower limbs with lymphedema. They defined tissue echogenicity as inflammatory tissue changes, and the subcutaneous echo-free space as fluid accumulation between the superficial fasciae. The criteria used to define both echogenicity and echo-free space are illustrated on figure 12.

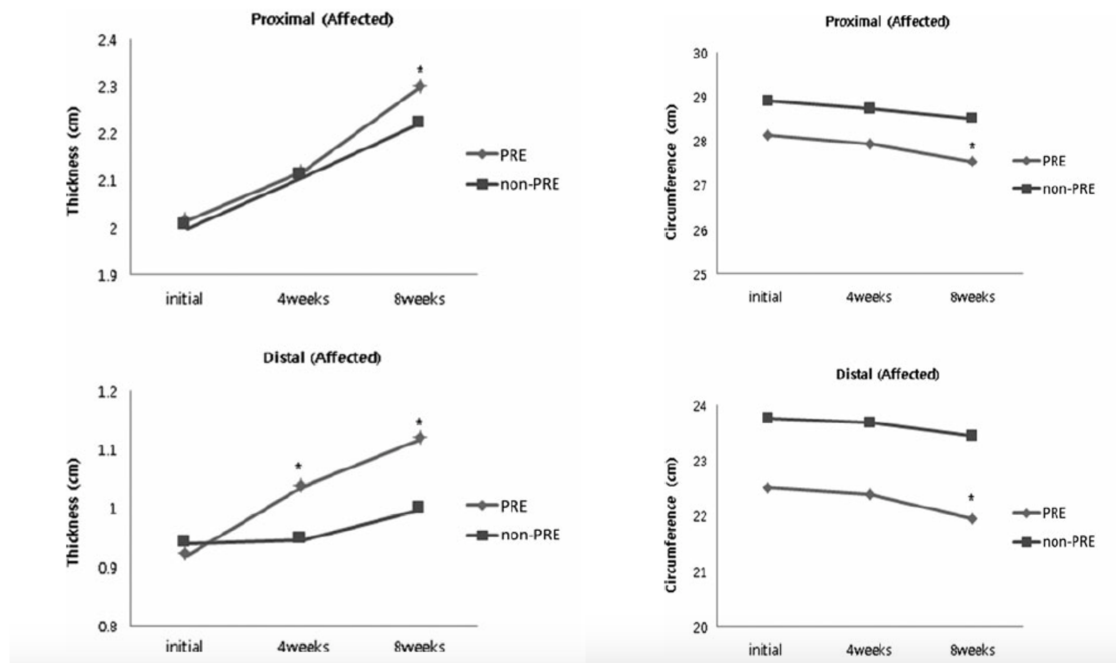
FIGURE 12: Definition of subcutaneous echogenicity grade (SEG) and subcutaneous echo-free space grade (SEFS) (Suehiro et al. 2015).



Combined physical therapy (CDT) was described as manual lymph drainage, bandaging, exercise and skin care. Patients’ leg volumes were monitored at every follow-up visit using circumference tape measurements. Ultrasound measurements were taken at the first and last visit using a 12-MHz linear transducer. The authors took ultrasound scans at eight points on the leg. Using ultrasonography, the authors were able to see increases in subcutaneous thickness, subcutaneous echogenicity and subcutaneous echo-free space, suggesting possible tissue proliferation.

Bok et al. (2016) used ultrasound to assess the changes in muscle thickness and subcutaneous tissue thickness of the arms of 32 women with breast cancer related lymphedema. Subjects were divided into two groups, one that received CDT along with progressive resistance exercise training and one that received only CDT. Changes in arm volume, assessed through tape measurements, and arm composition were assessed at baseline, 4 weeks and 8 weeks. Results showed a decrease in arm volume through tape measures at the 8-week mark, but no significant difference was observed at the 4-week point. However, ultrasonography showed a significant increase in muscle thickness and a decrease in subcutaneous fat at week 4 in the distal limb. These results are shown on figure 13.

FIGURE 13: Changes in muscle thickness (measured through ultrasonography) and changes in limb volume (using tape circumferential measurements) of the lymphedematous proximal and distal limb over time.



*p<0.05 by repeated measures ANOVA, PRE: Progressive resistance exercise

This highlights the importance of understanding the tissue composition underneath the skin, as this gives more information on treatment results than does circumference measurements alone. Furthermore, changes in tissue structure were observed sooner through ultrasonography than through volumetric measures. The authors of this study also described ultrasonography as an easily accessible tool, safe from radiation, less expensive than computed tomography (CT) or magnetic resonance imaging (MRI), and therefore arguably an ideal tool for both diagnosis of lymphedema and for monitoring changes in muscle and tissue thickness.

Ultrasonography has also been used to assess musculoskeletal pathologies resulting from lymphedema. Jang et al. (2015) observed forty-seven patients with breast cancer related lymphedema and assessed them for shoulder pathologies using ultrasonography. The researcher was blinded to the shoulder abnormalities and took ultrasound scans from 5 different views and made diagnoses of various shoulder pathologies. The researcher diagnosed abnormalities 87.2% of the time (such as tendon tears, bursal thickening and distention of the bicep tendon sheath).

The authors described ultrasound as a useful examination tool for patients with lymphedema of the arm following breast cancer.

Project Overview

Breast cancer-related lymphedema is a chronic condition that leads to multiple physical and psychosocial complications in the patient's life. Stage 2 lymphedema is the stage in which there are the most dynamic tissue changes in the affected arm. These changes can include a hardening of the tissue, fibrosis, and non-pitting edema (Dixon et al. 2015). However there exists no standardized criteria to diagnose, stage and monitor the condition. Presently the most common ways of assessing the condition in clinical practice is through subjective measures, such as palpation, pitting tests, and circumferential arm measures. The main issue with this is that it does not provide any descriptions nor information of the changes in the underlying tissue of the arm. Furthermore, circumference measurements can lead to errors when marking the landmarks on the limb and applying an inadequate amount of tension on the tape and can therefore lead to problems with precision. There is currently a large gap in the literature involving the use of objective measurement techniques in lymphedema patients. To our knowledge there are no published findings on the changes in lymphedema through objective measurement tools such as ultrasound by comparing a cohort of patients affected with the condition to a cohort of healthy controls. There also seem to be no such findings comparing the affected arms of unilateral lymphedema patients with the unaffected healthy limb.

The purpose of this thesis project was to obtain a better understanding of the tissue changes in arm lymphedema following breast cancer treatment. Specifically, with the use of several lymphedema measurement techniques, lymphedema in breast cancer patients was extensively characterized and compared to normal controls. The project was divided into two parts; The first part (Chapter II) consisted of obtaining an overall understanding of the pathology by comparing a group of women diagnosed with lymphedema to a group of healthy controls. Comparisons were done using the currently most common methods to assess the condition, that is circumferential tape volumetric measurements, Perometry, DXA as well as an assessment of

handgrip strength. The primary aim of this study was to assess the arm fat and arm lean tissue of the arm affected with lymphedema and to compare it to the unaffected side, as well as to look at differences in arm volume, segmental arm circumferences, and forearm muscle strength. The secondary aim of this study was to assess the correlation between lean tissue and forearm muscle strength. This study had the following hypotheses: 1) We hypothesize that the arm affected with lymphedema will have significantly more lean mass and fat mass compared to the unaffected side as well as significantly higher volume and arm circumference measurements along the arm affected with lymphedema. 2) We hypothesize no significant difference in these measurements between the right and left arms of the control women. 3) We hypothesize a strong correlation in lean mass and handgrip strength in both groups.

The second part of the study (chapters III and IV) include an assessment of the lymphedematous limb through a novel ultrasonic technique called ultrasound elastography to obtain measurements of fat, skin and muscle tissue. The aim was to assess the tissue characteristics, including the tissue compliance of the arms of women with lymphedema. Comparisons were made to the opposing unaffected limb of these women. Our hypothesis is the following, we foresee as significant difference in fat strain, muscle strain and skin strain between both arms of women with lymphedema, where the arm affected with lymphedema will have lower strain values and be less compliant.

II

Segmental Tissue Composition and Handgrip Strength Relationships in Stage 2 Breast Cancer Related Lymphedema

Abstract

Background: Breast cancer is one of the commonest cancers in women. With modern treatments, the survival rates are increasing. Breast cancer-related lymphedema (BCRL) is a condition defined as swelling in the upper extremity due to damage to the lymphatic transport system from breast cancer surgery or radiation therapy. This condition is characterized by an accumulation of fluid and adipose tissue deposits followed by various tissue changes including fibrosis. In clinical practices, the most common tools used to assess the progression of the condition include arm circumferential measurements, and palpation. These methods are subjective and fail to provide any detail of muscular or fat or tissue changes that occur underneath the skin. The aim of this study was to obtain a better understanding of arm tissue composition following lymphedema diagnosis. **Methods:** A total of 20 women diagnosed with unilateral breast cancer-related Stage 2 lymphedema and 21 healthy controls underwent a series of tests including assessments of lean and fat tissue through a DXA scan, a volume measurement of the arms through a Perometer, circumferential measurements at 6 spots along the arms and assessments of forearm strength through a handgrip dynamometer. Paired t-tests were used to compare differences between the affected lymphedema arm and the unaffected side in the patient group and between the left and right arms of the control group. **Results:** The affected arm was found to be significantly larger in volume compared to the unaffected side ($3613\text{mL} \pm 909$ vs. $3161\text{ mL} \pm 939$, $p=0.01$). There was a 12.9% (95%CI: 6.2-19.6%) larger fat mass and 13% (95%CI: 6.2-19.8%) larger lean mass in the affected limb compared to the opposite limb. Arm circumference ratios of the affected over unaffected arms were larger around the mid-forearm region as compared the more proximal or distal regions of the arm (1.134 ± 0.149 vs. 1.018 ± 0.062 , $p<0.01$). There was no correlation between handgrip and lean mass in the lymphedema arm ($r=-0.03$, $p=0.87$, $n=19$). **Conclusion:** This study suggests that lymphedema is most important around the mid-forearm area according to volume measurements, and that lymphedema may be spreading towards from the affected to the unaffected side since there was no correlation between lean mass as measured by DXA and handgrip strength in the both arms of women lymphedema. The increased lean mass measured by DXA may simply have been due to a false high reading because of the additional fluid accumulation rather than a true increase in muscle mass.

Introduction

With an increasing number of breast cancer survivors, more women are developing lymphedema. In fact, worldwide there are over 1.38 million new cases of breast cancer every year (WHO, 2015) of whom slightly over 20%, or one in 5, will develop arm lymphedema. This estimates to 286,000 women (DiSipio et al. 2013) yearly with new onset of lymphedema. Lymphedema is a chronic condition that causes multiple physical and psychological issues for the patient, such as pain, heaviness, tightness, decreased range of motion, impaired daily function, and impeded social relationships (Hayes et al. 2012). In a study by Roses et al. (1999), arm lymphedema was found to represent a constant reminder of the cancer. Maunsell et al. (1993) also demonstrated that lymphedema contributed to anxiety and depression. Furthermore, the lymphedema can compromise tissue oxygenation and the immune system. This puts patients at a high risk of bacterial cellulitis and recurrent episodes of infections (Tassenoy et al. 2009), and higher mortality (Hayes et al., 2011). In a survey by Moffatt et al. (2003), approximately 30% of patients with lymphedema had been admitted to hospital in the previous year for intravenous antibiotics due to infections. The authors also reported that over 80% of lymphedema patients had to take time off work.

Currently, there is a lack of standardized criteria for detecting lymphedema following breast cancer. There are significant differences in study design, diagnostic methods and timing of lymphedema measurement with respect to breast cancer treatment. As such, no consensus exists on when and how to search for this condition. Apart from the absence of diagnostic criteria, there also remains limited knowledge on the pathology and natural progression of the disease, and there is no objective quantitative method of staging the disease nor diagnosing it early enough to allow for prevention, early treatment and possible reversibility of the condition (Dixon et al. 2015). The large gaps in the understanding and in the diagnosis of lymphedema are mainly due to a lack of objective measurement techniques.

The primary aim of this study was to compare the tissue composition changes in patients who have been diagnosed with breast cancer-related lymphedema (BCRL) using DXA, Perometer, a circumference tape measurements, and handgrip dynamometer to a group of healthy control women. The secondary aim of this study was to assess the correlation of lean tissue

measurements to both forearm strength and volume measurements of women with BCRL and women without.

Methods

1. Participants

For this study, we chose to include a total of 40 women separated into two groups: our experimental group which consisted of women diagnosed with breast cancer-related lymphedema and a healthy control group. We chose to recruit a total of 40 women for this study as this is a new area of research in which the main purpose was to provide pilot data. This study was a cross-sectional, observational study comparing the affected and unaffected arms of 20 patients diagnosed with stage 2 lymphedema. In addition, 20 healthy “controls” matched for BMI underwent the same battery of tests and assessments. The inclusion and exclusion criteria to participate in this study was as follows:

Inclusion Criteria

Experimental Group:

The inclusion criteria for our experimental group consisted of women diagnosed with stage 2 unilateral lymphedema following breast cancer treatment. Patients that demonstrated the following criteria were approached to participate in this study:

- Above the age of 18 years
- BMI of 25 or over
- Diagnosis of unilateral stage 2 lymphedema of the arm
- Fluent in English or French, or accompanied by someone who is fluent in English or French

We chose to include a BMI of 25 or over, as a higher BMI is an increased risk factor for developing lymphedema (Garza et al. 2017) and most patients fall into this BMI category.

Control Group:

The inclusion criteria for the control group consisted of healthy women with no diagnosis of lymphedema. Women displaying the following criteria were approached to participate in this study:

- Above the age of 18 years-old
- BMI of 25 or over
- Fluent in either English or French, or accompanied by someone who was fluent in English or French

Exclusion Criteria

The following exclusion criteria were applied to both groups:

- Diagnosis of recurrent cancer
- Currently under treatment for breast cancer
- Bilateral lymphedema of the arms
- Any diagnosis of the following diseases: heart, liver, or kidney disease

Our Control women were recruited from the Concordia University staff, the Montreal community and the McGill University Health Centre (MUHC) Cedars Breast Centre, through word of mouth by approaching colleagues, friends and women accompanying patients to their appointments. The experimental group was mainly recruited from the MUHC Lymphedema Program and the MUHC Cedars Breast Centre. A total of 41 women agreed to participate in this study; 20 women met criteria for the experimental group and the remaining 21 met the criteria in the control group. All 41 women were included in this study.

2. Procedures

All procedures were carried out at the McGill Nutrition and Performance Laboratory (MNUPAL). Procedures and assessments were explained and informed consent was obtained. Participants' age, date of birth and medical history were recorded, followed by the measurement of their height and weight from which BMI was then calculated. The weight scale used was the

Detecto Scale Model 750 (± 0.1 kg). The height scale used was the Seca Wall Mounted height scale (± 0.1 cm).

Participants then underwent two DXA measures using the Lunar Prodigy Advance hardware (December 2005) and the Encore 2006 v.10.50.086 software. The first consisted of a full body scan, where patients were instructed to lie supine with bodies aligned within the four quadrants of the machine. Patient's arms were placed by their side with their hands stacked and fingers together. All jewelry was removed for the scan. The scan took a total of 6 minutes. The second scan consisted of the right and left femoral hip. Patients were again instructed to lay supine properly centered within the four quadrants of the machine. Patients' hips were internally rotated for this scan and the feet were strapped along the triangular contraption to ensure the hips remained in proper position for the scan. This data was taken to assess the incidence of osteoporosis and will be used for future research studies.

Following the DXA scan, patient underwent volumetric measurements with the Pero-System Type 350 NT (Peroplus 2000 built 2014.01h). The Perometer was used once on each arm. Patients were asked to sit with their legs uncrossed, with their feet flat on the floor with the knees flexed at a 90-degree angle. The Perometer was then adjusted accordingly to the patient's height such that their arm was abducted to 90 degrees with the palm facing down and with the tip of the middle finger resting on the appropriate location of the machine. The machine was then moved along the length of the patient's arm to obtain a volume measure of the entire arm.

The next step included the arm circumference measurements. Patients were instructed to sit comfortably on a chair with their back rested and their arms in a supinated position on their thighs. Measurements were taken with a 100-cm cloth tape measure (± 0.1 cm) and recorded in centimeters. A total of 6 circumference measurements were taken on each arm, at the following landmarks:

- 1- The palm, in line with the web space of the thumb
- 2- The wrist
- 3- 10 cm above the wrist landmark
- 4- The crease of the elbow

- 5- 10 cm above the elbow landmark
- 6- At the highest point in the arm, in line with the axilla and at the midline of the deltoid

These landmarks are illustrated in figure 1 and have been shown to provide inter-rater reliability (Khan, 2014).

FIGURE 1: Circumference tape landmarks marking the arm segments. The numbers on the figure represent the landmarks indicated in the text



The research assistant was seated in front of the participant and measured the circumference of the arm by placing the tape around the landmark. Tension was applied on one end of the tape and the measurement was recorded to the nearest 0.1 cm. The six landmark measurements were first taken from the affected arm (experimental group) and repeated on the unaffected arm.

The last step in the assessment was the handgrip strength measurement to assess the subject's strength generated from the muscles of the hand, forearm, and upper arm. The subjects were seated with their back rested and the forearm flexed at a 90-degree angle at the elbow placed on the chair's arm rest. Subjects were asked to squeeze the handgrip dynamometer (Jamar Hydraulic Hand Dynamometer +/- 0.1 kg) as hard as they could for a total of 2 seconds. The handgrip test was repeated twice, on both arms alternating arms between measurements with a 10 second rest period between each reading. The second readings were used for this analysis.

3. Statistical Analyses

Demographic data was compared between both groups using mean \pm standard deviation and independent t-tests. Within-group comparisons were completed using paired t-tests. Comparisons in Perometer, HGS, and DXA fat and lean measures were done between both arms in the control and the experimental groups using paired t-tests. Ninety five percent confidence intervals were used to assess body composition ratios in the control group and in the experimental group. A series of One-Way Analysis of Variance and Post-hoc Tukey tests were also used to compare the differences in arm circumferences in both arms in both groups. Pearson product moment correlations were used to assess the following relationships: lean mass and Perometer arm volume measurements, and handgrip strength and lean mass.

4. Ethics and Funding

This study obtained ethics approval from both the McGill University Health Centre and from Concordia University. Funding was obtained from the Dr. Louis G. Johnson Foundation and the PERFORM Centre Equipment Grant.

Results

The results in this study are presented in 4 parts:

1. Demographic and Body Composition Data

Of the 41 participants in this study, 20 had been diagnosed with stage 2 breast cancer-related lymphedema. One of the women in the experimental group refused to undergo the DXA scan. She was therefore excluded in the assessment of DXA measurements.

A comparison between both groups is presented in table 1. Independent t-tests were used to compare the means in age, height, weight, BMI, percent body fat, total fat, total lean and BMD amongst both the experimental and the control group. A P value smaller than 0.05 was

considered significant. Handedness was recorded in all participants, except for one in the experimental group that was missed. This was defined by asking the participant “which hand do you write with?”. The side affected with lymphedema was also recorded.

TABLE 1: Demographic and body composition data (mean \pm standard deviation) between women diagnosed stage 2 breast cancer related lymphedema compared to women without lymphedema.

	Women with BCRL (n=20)	Women without BCRL (n=21)	P Value
Age	56 \pm 14.8	48 \pm 20.8	0.184
Height (m)	1.62 \pm 0.07	1.59 \pm 0.06	0.198
Weight (kg)	84.6 \pm 18.4	73.9 \pm 11.1	0.03*
BMI (kg/m ²)	32.1 \pm 7.2	29.0 \pm 4.2	0.101
Body Fat (%)	47.5 \pm 6.9	42.4 \pm 6.4	0.023*
Total Fat (kg)	39.1 \pm 13.1	30.5 \pm 8.1	0.021*
Total Lean (kg)	41.6 \pm 5.8	40.1 \pm 4.5	0.363
BMD (g/cm ²)	-0.673 \pm 1.077	-0.110 \pm 1.411	0.200
Right Handed (%)	84	100	-
Lymphedematous limb is on the dominant side (%)	47	NA	-

2. Measurement Comparisons

Paired t-tests were used to compare the handgrip strength measurements, Perometer volume measures of the arm, arm fat measures obtained from DXA as well as arm lean measures obtained from DXA between one and the other arm in both the experimental and the control groups. In the experimental group, the affected arm was compared to the unaffected arm whereas the dominant (right) arm was compared to the non-dominant (left) arm in the control group.

Handgrip Strength:

There was no significant difference in handgrip strength between the dominant (right) and non-dominant (left) arms of the control group participants (23.8kg \pm 7.2 vs 23.3kg \pm 5.8,

p=0.755). There was also no significant difference between the affected and unaffected arms in the group with BCRL (22.9kg \pm 7.7 vs. 24.2kg \pm 5.1, p=0.414). Handedness did not affect the significance of these results (p=0.837 when the affected arm was dominant, p=0.111 when the affected arm was non-dominant).

Arm Volume:

There was no significant difference in the Perometer-measured volume of the dominant (right) arm compared to the volume of the non-dominant (left) arm in the control group women (3420mL \pm 990 vs 3355 mL 914, p= 0.738). There was; however, a significant difference found between the affected and unaffected arms in the BCRL group, with the affected arm having a significantly larger volume compared to the unaffected arm (3613mL \pm 909 vs. 3161 mL \pm 939, p=0.010). The trend was persistent when controlling for handedness, as is shown in table 2. The decrease in the significance of the p value is explained by the decrease in the number of subjects when considering handedness.

TABLE 2: Volumes of the affected and unaffected arms of women with lymphedema

	Mean volume of the affected arm (mL)	Mean volume of the unaffected arm (mL)	n	P value
Women with lymphedema	3613	3161	20	0.010
Lymphedematous limb was the dominant limb	3811	3220	9	0.078
Lymphedematous limb was the non-dominant limb	3474	3148	10	0.088

Arm Fat and Arm Lean Measurements:

Measurements of arm fat and arm lean were extracted from the DXA scans. For the control group, we found no significant differences between the dominant (right) and non-dominant (left) arms for both arm fat and arm lean measures. There was; however, a trend that was identified. In fact, results demonstrated that the right arm had more fat ($1.267\text{kg} \pm 0.374$ vs $1.223\text{kg} \pm 0.77$, $p=0.066$) and more lean tissue mass compared to the left arm ($1.863\text{kg} \pm 0.294$ vs 1.799 ± 0.3320 , $p=0.057$).

In the BCRL group, there were no significant differences in arm fat (1.863 ± 0.624 vs 1.917 ± 1.363 , $p=0.834$), nor arm lean (2.160 ± 0.558 vs. 1.971 ± 0.507 , $p=0.253$) measurements between the affected and unaffected arms. When taking handedness in consideration, we found a significant difference in these measurements, but only when the affected arm was not corresponding to the dominant limb. In fact, the lymphedema limb was found to have more fat and more lean tissue when compared to the unaffected side. The significance was not seen when the affected arm was the dominant limb, as shown on table 3.

TABLE 3: (A) DXA fat measures and (B) DXA lean measures on the affected and unaffected arms of women with lymphedema

A	Mean arm fat in the affected arm (Kg)	Mean arm fat in the unaffected arm (Kg)	n	P value
Women with Lymphedema	1.863	1.917	20	0.834
Lymphedematous limb is the dominant limb	1.785	2.157	9	0.500
Lymphedematous limb is the non-dominant limb	1.870	1.624	10	0.038

B	Mean arm lean in the affected arm (Kg)	Mean arm lean in the unaffected arm (Kg)	n	P value
Women with Lymphedema	2.160	1.971	20	0.253
Lymphedematous limb is the dominant limb	2.139	2.051	9	0.796
Lymphedematous limb is the non-dominant limb	2.126	1.829	10	0.026

Body Composition Ratios:

Confidence intervals were computed to compare the body composition obtained from the DXA measurements between the dominant (right) and non-dominant (left) arms of the control women as well as the affected and unaffected arms of the women diagnosed BCRL. A boxplot statistic was used to omit the outliers. *See table 4 for a summary of these results.* Using 95% confidence intervals, all the differences achieved statistical significance with or without exclusion of outliers. For the control women, results showed both 3.9% (95%CI: 0.2-7.5%) more fat and 3.9% (95%CI: 0.2-7.5%) more lean tissue in the dominant (right) arm compared to the non-dominant (left) arm. For the BCRL group, despite no difference being detected in absolute arm fat and arm lean measurements, the body fat composition was 12.9% (95%CI: 6.2-19.6%) larger in the affected limb compared to the opposite limb. Lean composition was also 13% (95%CI: 6.2-19.8%) larger in the affected limb.

TABLE 4: Body composition ratios between the dominant and non-dominant arm of the control group and the affected and unaffected arms of the BCRL group.

	Control n=21 (dominant/non-dominant)	95%CI	BCRL (outliers omitted) (affected/unaffected)	95%CI
Arm Fat	1.039	1.002, 1.075	1.129	1.062, 1.196
Arm Lean	1.039	1.002, 1.075	1.130	1.062, 1.198

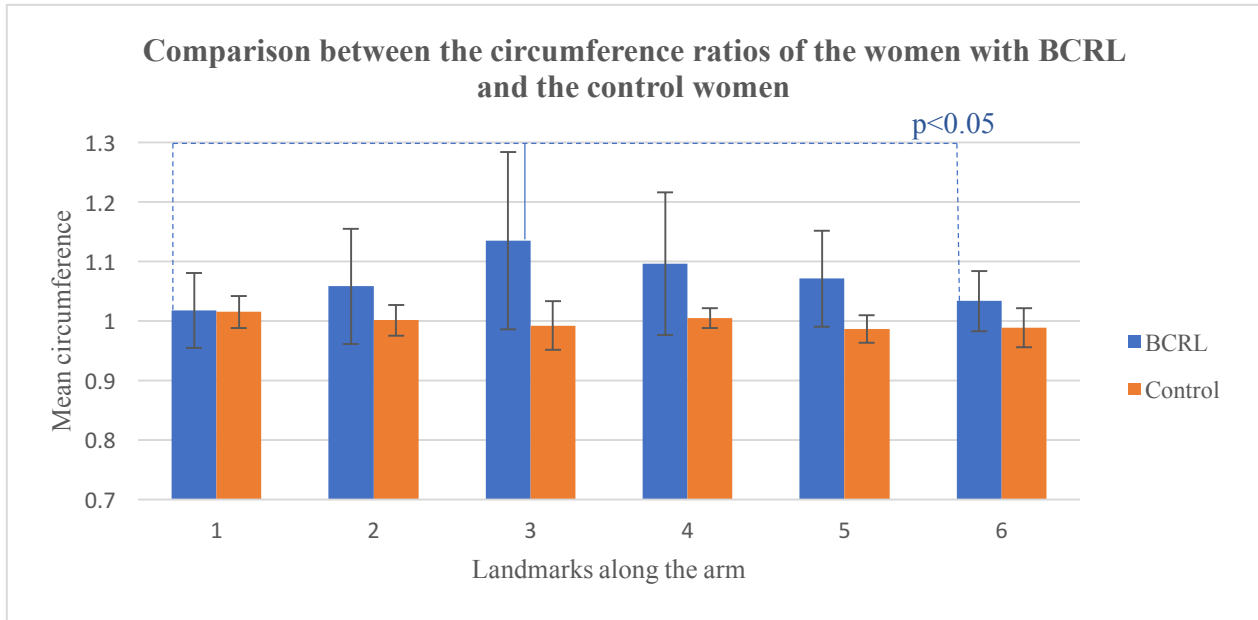
A one-way ANOVA was also used to compare arm composition (lean and fat) by using the ratio of the dominant over non-dominant arm of the control women, and the ratio between the affected to unaffected arms of women with BCRL. A significant difference was found between the control and the BCRL groups [$F(3, 68)=4.87, p=0.004$].

A post hoc Tukey test was used to identify the differences amongst the ratios. The two ratios for fat tissue (1.13 ± 0.121) and lean tissue (1.13 ± 0.123) for the group diagnosed with BCRL was found to be different than the two ratios for fat (1.039 ± 0.08) and lean tissue (1.039 ± 0.08) of the control group ($p<0.05$), showing that the difference in fat and lean composition between arms of the lymphedema patients was significantly larger than in the control group.

Circumference Measurements

Differences in arm circumference measurements were assessed in 6 different locations along the arm in order to verify if the lymphedema was spread uniformly along the arm or regionally affected. We chose to only look at circumference rather than indirectly compute the volume as this would serve as a more practical and efficient technique in a clinical setting. A One-Way Analysis of Variance showed significant differences along the arms of the control group [$F(5, 120)=3.0770, p=0.012$] and along the arms of the women with BCRL [$F(5/114)=3.6751, p=0.004$]. Tukey-Kramer Multiple comparison test was used to identify the locations of these differences. For the control women, the following circumference ratio (right arm/left arm) differences were noted: location 1 (palm) was found to be statistically larger from location 5 (mid arm) and location 6 (below shoulder), but locations 5 and 6 were not different from each other, as illustrated on figure 2a. For the women diagnosed with lymphedema, the following circumference ratio (affected/unaffected) were noted: location 3 (mid-forearm) with a mean ratio of 1.134 ± 0.149 was found to be statistically larger than locations 1 and locations 6, as shown on figure 2b. Location 1 was found to have the lowest arm circumference ratio with a mean ratio of 1.018 ± 0.063 . Location 1 and location 6 were both shown to be different than location 3, but were not different to each other. Hence the bulk of the increase in size in the lymphedematous arm was in location 3 (mid forearm).

FIGURE 2: Chart illustrating the arm circumference ratio of dominant over non-dominant arm in the healthy control women across the 6 locations along the limb and the ratio of the affected over unaffected arm in women diagnosed with stage 2 BCRL across the 6 locations along the limb



The locations that were predominately altered by the lymphedema were not affected by whether the lymphedematous limb was the dominant arm. When the dominant arm was also the affected arm, there was a slightly larger arm circumference across the 6 locations as compared to the non-dominant limb, as is illustrated on table 5.

TABLE 5: Arm circumference ratios of the affected over unaffected sides of women with lymphedema

Mean Arm Circumference Ratio (affected/unaffected)	Location 1	Location 2	Location 3	Location 4	Location 5	Location 6
All	1.012	1.058	1.135	1.096	1.072	1.033
Affected arm was the dominant arm	1.044	1.083	1.136	1.115	1.080	1.042
Affected arm was the non-dominant arm	0.995	1.039	1.135	1.077	1.060	1.026

Correlations

Pearson correlations were used to determine whether lean mass correlated with either handgrip strength or arm volume, both in the control group and the experimental group. The following correlations were calculated:

Handgrip strength vs. Lean tissue

For the control group, there was a strong correlation between the hand grip strength on the left arm and the lean mass on the left arm ($r=0.868$, $p=0.000001$, $n=19$) and there was a moderate to strong relationship between the handgrip strength of the right arm and the lean mass on the right arm ($r=0.667$, $p=0.0018$, $n=19$)

For the women with BCRL, there was no linear correlation between the handgrip strength in the unaffected arm and the lean mass in the unaffected arm ($r=0.087$, $p=0.722$, $n=19$). There was also no linear correlation between the handgrip strength of the affected lymphedema arm and the lean mass in the affected arm ($r=- 0.03$, $p=0.87$, $n=19$).

Lean tissue vs. Arm Volume

For the control group, there was a moderate to strong correlation between the lean mass on the right arm and the volume of the right arm ($r=0.7$, $p=0.0008$, $n=19$), as well as between the lean mass on the left arm and the volume of the left arm ($r=0.71$, $p=0.0006$, $n=19$). We also found a moderate to strong correlation between the measurement of the sum of the fat and lean tissue in the right arm and the volume of the right arm ($r=0.7246$, $p=0.00017$, $n=19$). A similar correlation was found between the sum of the fat and lean tissue in the left arm and the volume of the left arm ($r=0.732$, $p=0.00016$, $n=21$).

For the women with BCRL, there was a moderate to strong correlation between the sum of fat and lean tissue in the affected arm and the volume measure of the affected arm ($r=0.675$, $p=0.002$, $n=18$). There was a strong correlation between the sum of fat and lean tissue mass in the unaffected arm and the volume measurement of the unaffected arm ($r=0.86$, $p=0.00001$, $n=18$). There was a moderate correlation between the lean mass in the affected arm and the volume measure in the affected arm ($r=0.39$, $p=0.1$, $n=18$), but a weak correlation between the lean mass in the unaffected arm and the volume of the unaffected arm ($r=0.224322$, $p=0.37$, $n=18$).

Discussion

The purpose of this study was to investigate the composition of the lymphedematous arm in terms of arm fat mass, arm lean mass, forearm strength and arm volume in women diagnosed with stage 2 breast cancer-related lymphedema (BCRL). Multiple comparison tests were done between the arm affected with lymphedema and the arm that was unaffected. The same tests were done on a group of healthy control women.

The results of this study had two main findings:

- 1) The presence of lymphedema is more prevalent in the mid-forearm area:

The most common method to assess lymphedema is arm circumference measurements using a tape circumference. This method allows the clinician to obtain an overall volume measurement of the arm, from which the overall volume of the affected arm is compared to the overall volume of the unaffected arm. This is then used to determine the severity of the lymphedema. In our study, we computed the ratio of the affected over the unaffected arm at each of the six locations and compared the differences amongst each of the ratios. Interestingly location 3 (mid forearm) stood out from locations 1 and 6, where location 3 had the highest circumference ratio difference, regardless of hand dominance. This means that the circumference of the arm at the level of the mid-forearm area was significantly different than the extremities of the arm, that is the palm and the shoulder and the ratio between the affected over the unaffected arm was the greatest at the mid-forearm level. We found that there was 14% more lymphedema present at the level of the mid-forearm on the affected arm compared to the unaffected arm. When looking at the palm of the hand, we found that the unaffected arm was only 2% smaller in terms of circumference compared to the affected arm. This finding correlates with the finding from the study conducted by Czerniec, et al. (2015), where they also found the forearm, more specifically the region 10-20 cm away from the wrist, to contain the highest fat difference as measured by the DXA and BIS between the affected and unaffected arms compared to the rest of the arm. These findings may suggest that lymphedema onset may start around the mid-forearm area. This location should then be examined in more detail and may indicate that lymphedema begins to accumulate distally to proximally, except for the hand and palm region. This may be explained by anatomical and histological features (variable tissue compliance in these regions, differences in density of vasculature in these regions, increased muscular motions in the hand) that may help in preventing the accumulation in fluid in the hand. In clinical practice, when trying to detect early onset lymphedema, the mid-forearm region may perhaps be the location to begin the assessment.

2) Handgrip strength does not correlate with lean mass in the lymphedema arm

Prior to this study we hypothesized that there would be a strong correlation between handgrip strength and lean mass. One would think that if an individual had increased muscle mass, they would score higher on the handgrip dynamometer. In fact, Raj et al (2016) assessed the strength of the knee extensors of 36 participants using a Biodex and correlated it to the muscle thickness

that was measured using an Ultrasound device. The author's study showed significant correlations between the isometric and isokinetic strength of the quadriceps muscles and the muscle thickness. Similarly, in our control group, we found strong correlations between handgrip strength and lean mass. However, there was no correlation between the measurement in handgrip strength and the DXA measurement of lean mass in our lymphedema group. One possibility for this unexpected finding is that the excess fluid in the lymphedematous arm could be impeding muscle function and thus reduce handgrip strength. However, another possibility exists because lean mass as measured through the DXA includes not only muscle mass, but other tissue components as well. Specifically, lean tissue is defined as muscle connective tissue, fluid, proteins, glycogen, water and non-bone minerals. We believe that the increased fluid and inflammatory tissue components in lymphedema are what are causing this lack of correlation. In a study by Newman et al. (2013), the authors found a 15.6% more lean mass, as measured through a DXA, in the affected lymphedema arms of 24 women with BCRL as compared to the unaffected side and also suggested that the large difference between the two arms was mainly due to the fluid component in the lymphedematous limb. Furthermore, in our study we also found no such correlation between handgrip strength and lean mass in both the affected as well as the unaffected arm, suggesting the possibility that there may also be excess fluid in the unaffected arm. This may mean that the opposite limb may have a slight lymphedema as well, and that these women who were diagnosed with stage 2 unilateral lymphedema may in fact have a minor form of bilateral lymphedema. Similar questions have been raised in past research. In fact, Batse (2010) also suggested poor lymphatic function on the unaffected limb of women with BCRL. Further research would have to be done to investigate this in more detail. In a study conducted by Hoffner et al. (2017), water-fat magnetic resonance imaging was used to quantify and localize fat and water in the limbs of seven patients with arm lymphedema and six patients with leg lymphedema. Measurements of the healthy limb along with the lymphedematous limb were taken at baseline and five different time points following surgical liposuction. The authors were able to identify how water and muscle volumes in lymphedema change over time following liposuction and noticed a decrease in subfascial water/muscle compared to baseline starting at 3 months. The water-fat MRI technique that was used in that study, did not differentiate between the muscle tissue and water. It would be interesting to assess an imaging technique that would be able to identify each component separately and assess the changes in fluid over time in both the

lymphedema arm and contralateral arm over time to see if fluid may be accumulating in the contralateral limb as well.

In our study, we found there to be no significant difference in either lean nor fat measurements between the lymphedematous and the contralateral arms; however, the affected limb was significantly larger in volume. Here again, it leads us to think that reason for this large increase in volume may be related to the differences in fluid component. When looking at these same outcome measurements in our group of control women, these differences were not significant. We believe we found no significant differences in lean measurements and fat measurements in the lymphedema group because our sample size was small. When taking handedness into consideration, we did identify a significant difference when the arm affected with lymphedema was the non-dominant arm, where we found that it had more lean and fat tissue than the dominant unaffected arm. This is supported by a study conducted by Dylke et al (2013), where the researchers found that the volumes of fat and lean tissue are related to whether the affected side happens to be the dominant limb, and on the severity of the lymphedema. Using DXA and BIS, the authors compared the arms of 56 women diagnosed with stage 2 lymphedema to 44 women with no history of breast cancer and no lymphedema. The authors found there to be a correlation with all the tissue volumes (interlimb fat, interlimb lean and total volume) between the severity of the lymphedema and the side affected (fat: $F=3.22$, $p=0.04$; lean: $F=10.70$, $p<0.001$; total: $F=11.07$, $p<0.001$). In order to assess the effect on limb dominance, the authors assessed the tissue composition first on the dominant arms of the control women and found significantly less fat ($t=-2.90$, $p=0.005$), but more lean tissue ($t=6.9871$, $p<0.001$) on the dominant arm compared to the non-dominant. When looking at the lymphedema group, the authors found that when the dominant arm was the affected limb, there was significantly more fat ($t=3.694$, $p<0.001$), but less lean tissue (-1.508 , $p=0.14$) than the dominant arms of the control women without lymphedema. However, the non-dominant and unaffected lymphedema arm did not show significant difference when compared to the non-dominant arm of the controls (fat: $p=0.15$, lean: $p=0.09$, overall volume= 0.89). Although this study looks at the effect of arm dominance on lymphedema, it uses the arm of a healthy woman as a control, and compares it to the affected lymphedema arm of the patient. This can lead to some limitations as it does not consider general variations in body composition that are possible between two different people.

In our study, we looked at the differences between the arms of the controls separately than the differences in the arms of the women with lymphedema. We identified a trend where the dominant arms of the control had more lean tissue and fat tissue than their non-dominant side. This could be explained by the fact the dominant arm is used more often to complete general activities of daily living. Research has previously shown that the dominant arm of a healthy population has more lean tissue than the non-dominant arm (Taaffe et al. 1994). In the experimental group, we found a significantly larger amount of arm fat and arm lean tissue when the non-dominant arm was the arm affected with lymphedema. Czerniec et al. (2015), also found similar results, where the women who had lymphedema on their non-dominant arm had greater differences in absolute fat mass as compared to the women whose dominant arm was affected. This could be explained by the fact that these women may be less likely to use or exercise their non-dominant arm, leading to higher fatty tissue and higher lean tissue where the fluid component may be affecting the lean value. We could assume that the non-dominant arm has a larger amount of lymphedema present (more fluid affecting the lean value, more fatty tissue deposits) due to the lower amount of use and movements on a non-dominant arm as compared to a dominant arm. It is known that exercise helps treat and prevent lymphedema (Park et al. 2008, Johansson et al. 2002).

We also compared the tissue composition of the two limbs of both groups using ratios of the affected over the unaffected arms of the BCRL group and right over left arms of the healthy control women for measurements of arm fat and arm lean. When looking at the ratio between the affected and unaffected arm, we found there to be larger fat and lean composition in the affected arms compared to the unaffected arms. There was also a similar but much smaller difference in the right arm, or in this case the dominant limb of the control women compared to the left arm. The difference found in the lymphedema group was significantly larger than that found in the control group. These results are similar to the findings by Czerniec et al (2015) where they also found there to be significantly more fat mass and lean tissue, as measured through a DXA, in the affected lymphedema side compared to the unaffected side.

Conclusion

In this study, we assessed the tissue composition of the arms of women diagnosed with breast cancer-related lymphedema in order to obtain a better understanding of the structural lymphedematous changes. We compared the affected arms to the opposite unaffected limbs of the women with lymphedema and completed the same tests on a group of healthy controls. To our knowledge, no other study has used such a comparison with both groups of women. This study has led us to believe that the swelling and structural changes caused by lymphedema following breast cancer seem to mainly involve the mid-forearm region of the arm. Handgrip strength was found not to correlate with lean mass in lymphedema patients in both the affected and unaffected arm, a finding thought secondary to the fact that lean mass calculation by DXA is increased by the excess fluid in lymphedema. This study has also raised another new interesting hypothesis about the spread of the fluid accumulation in the affected arm towards the unaffected side. The data presented in this study is pilot data and it has raised multiple new questions regarding this condition. In future studies, we would like to re-assess these changes and address new questions regarding the fluid changes in the arm using other modalities such as ultrasound on a larger cohort of women.

III

Tissue Strain in a Cohort of Stage 2 Breast Cancer Related Lymphedema Patients Using Ultrasound Elastography

Abstract

Background: Classic ultrasonography has recently emerged as a potential tool to diagnose and assess the treatment outcomes in patients with lymphedema, but clinicians still rely on subjective measurement techniques such as palpation to determine fluid accumulation in the lymphedematous limb. Recent advancements in ultrasound elastography show promising results in evaluating body composition changes and have shown to provide more quantifiable information on tissue elasticity or strain. The purpose of this study was to assess the muscle, fat and skin strain in women diagnosed with breast cancer-related stage 2 lymphedema. **Methods:** A total of 20 women with unilateral stage 2 breast-cancer related lymphedema were recruited to participate in this study. Patients underwent measurements of fat and lean tissue through a DXA scan, volume measures through a Perometer, and 7 of them were randomly selected to undergo strain measures through Ultrasound. Ultrasound elastography measures were taken on both the affected and unaffected limb at six different landmarks along the length of the arm. **Results:** When comparing the affected and unaffected limbs through DXA or Perometer, no significant differences were found. There was; however, a significantly higher strain in the unaffected arm in terms of skin strain (0.405 ± 0.185 vs. 0.577 ± 0.176 , $p=0.01$), fat strain (0.396 ± 0.156 vs. 0.525 ± 0.134 , $p=0.01$) and muscle strain (0.402 ± 0.138 vs. 0.540 ± 0.069 , $p=0.009$) all at the mid-distal arm. Furthermore, the Tukey-Kramer multiple comparison test showed that the effect of less compressibility and harder tissue on the affected limb was greater in the distal arm than the proximal arm ($p=0.05$), by having lower fat and muscle strain values. **Conclusion:** Ultrasound elastography could provide additional information in tissue elasticity that cannot be detected by other measurement techniques and potentially be useful in understanding the pathogenesis of the condition as well as the ability to diagnose and follow patients.

Introduction

With the recent interest in ultrasonography as a tool for body composition, novel ultrasound techniques have been developed to assess tissue elastic properties. Ultrasound elastography can be defined as an imaging method that measures the elasticity of compliant tissue (Cespedes et al. 1993). It is a technique that measures the tissue deformation by compressing and decompressing it and has been shown to differentiate between hard and soft tissues (Adriaenssens

et al. 2012). In fact, pressure, produced by physiological motions, pulsation of blood vessels or external mechanical compressions on the tissue, produces strain and displacement within the tissue. This tissue deformation is then detected by pulse-echo ultrasound (Brandenburg et al. 2014). The returning echoes are analyzed before being converted into a B-mode image (Park et al. 2011) and provide a measurement known as strain. The strain is smaller in harder tissues. It is by measuring this strain distribution that the tissue hardness can be estimated and can be used for disease diagnosis. In fact, real time sonoelastography has been used for tumor detection and differentiation between benign and malignant lesions. It is based on the principle that tissue hardness is related to pathologies (Park et al. 2011). Ultrasound elastography is becoming a promising tool for determining the material and mechanical properties of tissues and has been applied in multiple clinical settings, for example in the assessment of various musculoskeletal disorders such as congenital muscular torticollis, early detection of osteoarthritis, peripheral nerve lesions and myopathies (Park et al. 2011). The technique also shows promising results in predicting muscle response to treatment and monitoring muscle responses to clinical interventions (Brandenburg et al. 2014).

Although ultrasound has only recently begun to be researched in the diagnosis and staging of breast cancer-related lymphedema, preliminary results are shown to be valid and reliable (Li et al. 2012). Further research is needed to investigate the use of elastography as a way to specifically quantify the staging of lymphedema based on the body composition of the upper extremity following breast cancer treatment. The first step in this process remains to gain an understanding in the different structural changes that occur in the limb affected by lymphedema and how this compares to an unaffected limb. Lymphedema patients are usually diagnosed in the late phase of stage 1 or early phase of stage 2. This is the point where the disease may still be reversible. It is towards the end of stage 2 that the disease becomes chronic and controlling its progression becomes the only treatment option. Stage 2 lymphedema is characterized by tissue changes, including the initial development of fibrosis and the deposition of adipose tissue (Dixon et al. 2015). In current clinical practice, the most common methods used to diagnose and stage the condition is based on subjective palpation and pitting tests to assess the hardening, elasticity and fluid content of the tissue, as well volumetric measurement techniques such as circumferential tape measurements and Perometer volume measures. These methods all fail to

provide objective quantifiable data on the underlying tissue characteristics, and as a result the condition tends to lead to a late diagnosis of lymphedema that is past the point of reversibility (Dixon et al 2015).

Given the current state of the clinical art in assessing and staging lymphedema and the lack of any reliable objective method that can be used repeatedly in a safe and economic manner, we proposed in this study to use ultrasound, more specifically ultrasound quantitative techniques such as elastography to assess the elasticity of lymphedematous arms in order to obtain additional knowledge on the tissue changes that occur in stage 2 lymphedema. In particular, we wished to assess tissue thicknesses (e.g., skin, subcutaneous layers and skeletal muscles), as well as the elastic tissue properties.

Methods

1. Participants

A total of 20 women diagnosed with breast cancer-related lymphedema were included in this study. Our main purpose was to provide pilot data for a new area of research. The study was an observational study. The inclusion and exclusion criteria to participate in this study were as follows:

Inclusion Criteria

The inclusion criteria consisted of women diagnosed with stage 2 unilateral lymphedema following breast cancer treatment. Patients that demonstrated the following criteria were approached to participate in this study:

- Age 18 years or over
- BMI of 25 or over
- Diagnosis of unilateral stage 2 lymphedema
- Fluent in English or French, or accompanied by someone who is fluent in English or French

We chose to include a BMI of 25 or over as a higher BMI is an increased risk factor for lymphedema (Garza et al. 2017) and most patients fall into this category.

Exclusion Criteria

The following exclusion criteria was applied:

- Diagnosis of recurrent cancer
- Currently under treatment for breast cancer
- Bilateral lymphedema of the arms
- Any diagnosis of the following diseases: heart, liver, or kidney disease

All the women who participated in the study were recruited from the McGill University Health Centre (MUHC) Lymphedema Program and the MUHC Cedars Breast Centre. A total of 20 women agreed to participate in a larger study. Due to time and financial restraints, we collected additional ultrasound data on 7 women. The seven women were randomly selected, by picking a number out of a hat, to represent the cohort.

2. Procedures

Procedures were carried out at the McGill Nutrition and Performance Laboratory. Procedures and assessments were explained and informed consent was obtained. Participants age, date of birth and medical history were recorded, followed by the measurement of their height and weight from which BMI was then calculated. The weight scale used in this study was a Detecto Scale Model 750 (+/- 0.1kg). The tool we used to measure the participants' height was a Seca Wall Mounted Height Scale (+/- 0.1cm).

Those who underwent ultrasound measurements, were asked to sit on a chair with both feet flat on the floor and their back rested on the chair. The measurements were taken on both arms, with the arm that was being assessed resting straight on a table at the level of the heart and the palm of the hand facing up. The researcher was sitting on a stool in front of the participant. Landmarks were taken at 6 different locations along both arms. The researcher started by marking the landmarks on the participants arm using a crayon and a 100-cm long cloth tape measure (+/- 0.1cm). The following six landmarks were identified:

- 1- 20% of the distance between the 5th digit to the styloid process of the wrist
- 2- 20% of the distance between the styloid process to the tip of the olecranon

- 3- 20% of the distance between the olecranon and the styloid process
- 4- 20% of the distance between the olecranon and the acromioclavicular joint
- 5- 40% of the distance between the acromioclavicular joint and the olecranon
- 6- 20% of the distance between the acromioclavicular joint and the olecranon

These landmarks are displayed on figure 1 below:

FIGURE 1: Ultrasound landmarks along the segment of the arm. The numbers in the figure represent the landmarks indicated in the text.



Hypoallergenic ultrasound gel was placed at the point of contact between the ultrasound transducer head and the skin to facilitate the diffusion of the sound pulses into the tissue. A gel pad was also used to provide a standard elasticity measure and to enhance the quality of the scans. The ultrasound probe was placed on the surface of the gel pad, where an additional layer of ultrasound gel was also applied. All data was collected using an Alpinion E Cube system (Bothell, WA) and the L3-12H transducer. A center frequency of 10 MHz was selected along with a sampling rate of 40 MHz. Images were taken first in B-mode, where an amount of pressure was applied on the ultrasound gel, small enough to not cause any distortion to the skin. A second sequence of images were then collected to obtain the elasticity measures. To do this, three pulses of slight pressure were applied straight down on the gel pad. This sequence was applied on each of the 6 locations and were repeated twice. The first time all images were taken in short-axis. The second time all images were taken in long axis. The strain readings were obtained as extensively described in Chapter IV.

Patients also underwent a full body DXA scan using the Lunar Prodigy Advance hardware (December 2005) and the encore 2006 v.10.50.086 software. Patients were instructed to lie supine with bodies aligned within the four quadrants of the machine. Patient's arms were

placed by their side with their hands stacked and fingers together. All jewelry was instructed to be removed for the scan. The scan took a total of 6 minutes.

In addition, patients underwent measurements with the perometer Pero System Type 350 NT (Peroplus 2000 built 2014.01h). The perometer was used once on each arm. Patients were asked to sit with their legs uncrossed, with their feet on the floor at a 90-degree angle. The perometer was then adjusted accordingly to the patient's height such that their arm was able to extend at a 90-degree angle, in an abducted position with the palm facing down and with the tip of the middle finger resting on the appropriate location of the machine. The machine was then moved along the length of the patient's arm to grasp a volume measure of the entire arm.

Handgrip strength measurements were also collected. The subjects were seated with their back rested and forearm placed at a 90-degree angle on the chair's arm rest. Subjects were asked to squeeze the handgrip dynamometer (Jamar Hydraulic Hand Dynamometer +/- 0.1 kg) as hard as they can for a total of 2 seconds. The handgrip test was repeated twice, alternating both arms. Only the strongest value was recorded for this study.

3. Statistical Analyses

Demographic data was compared between the 7 randomly chosen subjects and the entire group of 20 women using mean \pm standard deviation and independent t tests. Measurements of tissue strain were recorded from the ultrasound scans. Tissue strain included muscle strain, skin strain and fat strain. All these measurements were calculated using MATLAB. The ultrasound gel pad was used as standard elasticity. Prior to completing any of these calculations the elasticity of the gel pad alone was measured using a CIRS phantom. All strain calculations were measured by our trained computer engineer on the research team. Tissue strain measurements of the arm affected with lymphedema was compared to the arm without lymphedema at each of the 6 locations, using paired t-tests. A series of strain ratios comparing the affected over the unaffected arm for each tissue over the 6 locations was also completed. A One-Way ANOVA followed by a Tukey-Kramer multiple comparison test were used to determine if there were any differences in muscle strain, fat strain and skin strain along the length of the arm.

4. Ethics and Funding

Ethics approval was obtained from the McGill University Health Centre and Concordia University. We obtained funding for this study from the Dr. Louis G. Johnson Foundation and the PERFORM Centre Equipment Grant.

Results

Ultrasound data was collected from 20 women diagnosed with breast cancer-related lymphedema; of which 7 were randomly selected and calculations of fat strain, muscle strain and skin strain were obtained. The 7 randomly selected subjects were representative of the group of twenty as demonstrated by demographic data (*see table 1*). Although the cohort of 7 women had an older mean age and a slightly lower BMI, these differences were not significant ($p>0.05$). One participant refused to do the DXA scan, as a result she was excluded from the DXA analyses.

TABLE 1: Comparisons between the cohort of 20 women recruited in this study and the 7 randomly selected women that were analyzed

	Women with BCRL (n=20)	Randomly selected women (n=7)	P Value
Age	56 ± 14.8	65.3 ± 10.5	0.143
Height (m)	1.62 ± 0.07	1.61 ± 0.087	0.698
Weight (kg)	84.6 ± 18.4	81.1 ± 24.2	0.752
BMI (kg/m ²)	32.1 ± 7.2	30.9 ± 8.4	0.726
Body Fat (%)	47.5	47.5	0.996
Total fat (Kg)	39.1	38.1	0.885
Total lean (Kg)	41.6	39.6	0.484

1. Comparing affected to unaffected arm

The arm affected with lymphedema was compared to the opposite arm, using the unaffected arm as a control. Both arms were compared in terms of arm volume, handgrip

strength, arm fat and arm lean. There were no significant differences between the affected arm compared to the unaffected arm. The results are summarized in table 2:

TABLE 2: General comparisons between the affected lymphedema arm and the unaffected arm

	Affected Arm \pm SD	Unaffected Arm \pm SD	Paired t-test
Perometer (mL)	3655 \pm 849	3278 \pm 1327	0.162
Grip Strength (Kg)	20.57 \pm 9.57	22 \pm 5.99	0.735
DXA Arm fat (Kg)	1.59 \pm 0.817	2.324 \pm 2.288	0.378
DXA Arm Lean (Kg)	1.830 \pm 0.430	1.95 \pm 0.714	0.778

Comparisons in arm strain measurements were assessed between both arms. Strain measurements in terms of skin, fat and muscle were obtained at each of the 6 locations along each limb. Paired t-tests were used to compare the strain value of each location on the affected arm to the unaffected arm. Skin strain on the affected limb was significantly different to the unaffected limb at locations 1, 2, and 3. Fat strain on the affected limb was significantly different to the unaffected limb at locations 1, 3, 4 and 5. A trend was noted at locations 2 and 6. Muscle strain on the affected arm was significantly different then the unaffected arm at locations 1, 2, 4, and 5. A trend was identified at location 6. Results are summarized in table 3. The affected arm had lower strain values, representing less compressibility and thus harder tissue.

TABLE 3: Comparisons of the affected and unaffected tissue strain measurements for skin, fat and muscle

Tissue	Location	Affected	Unaffected	Paired t-tests
Skin	1	0.405 \pm 0.185	0.577 \pm 0.176	0.001 *
	2	0.302 \pm 0.158	0.465 \pm 0.194	0.046 *
	3	0.317 \pm 0.131	0.666 \pm 0.386	0.049 *
	4	0.396 \pm 0.218	0.467 \pm 0.160	0.367
	5	0.405 \pm 0.225	0.557 \pm 0.208	0.179
	6	0.54 \pm 0.301	0.738 \pm 0.312	0.101
Fat	1	0.396 \pm 0.156	0.525 \pm 0.134	0.011*
	2	0.238 \pm 0.131	0.605 \pm 0.498	0.083 (trend)
	3	0.228 \pm 0.053	0.488 \pm 0.207	0.009*
	4	0.368 \pm 0.222	0.579 \pm 0.243	0.012*
	5	0.496 \pm 0.314	0.957 \pm 0.296	0.004*
	6	0.724 \pm 0.583	1.43 \pm 0.759	0.062 (trend)
Muscle	1	0.402 \pm 0.138	0.540 \pm 0.069	0.009 *
	2	0.316 \pm 0.174	0.634 \pm 0.260	0.007*
	3	0.584 \pm 0.550	0.880 \pm 0.270	0.185
	4	0.655 \pm 0.376	1.165 \pm 0.636	0.019*
	5	0.695 \pm 0.395	1.329 \pm 0.487	0.007*
	6	0.877 \pm 0.226	1.585 \pm 0.835	0.091 (trend)

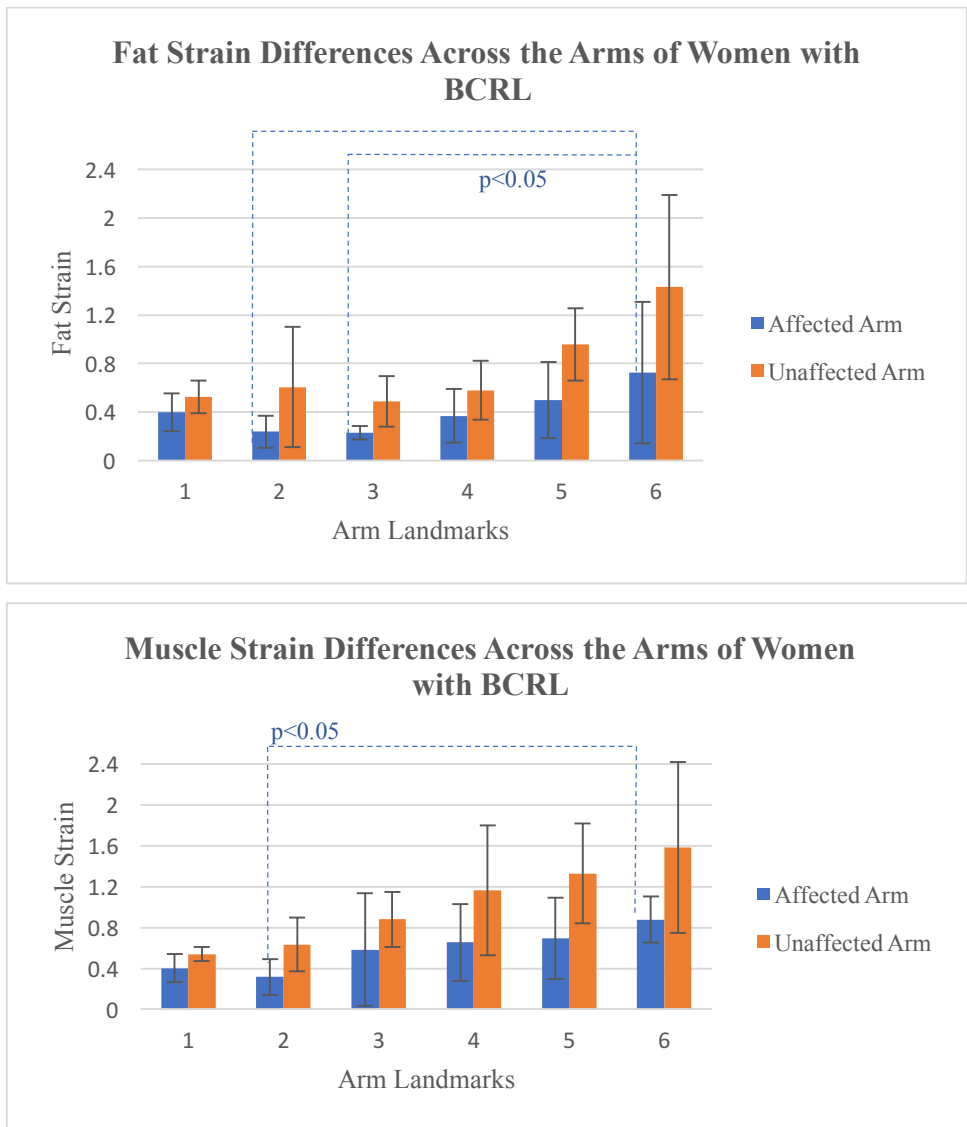
2. Comparing different locations along the arm

The strain values along the 6 locations of each arm were also compared. A one-way analysis of variance was used to compare the 6 different locations along the length of the arm affected with lymphedema. The same was then done on the unaffected arm. There were no significant differences along the length of the arm and across the 6 different locations in terms of skin strain measurements on both the affected and unaffected arms.

In terms of fat strain, differences were identified across the 6 locations in both the affected and the unaffected arms. The Tukey-Kramer multiple comparison test showed that the strain on the affected arm was lower in location 2 and location 3 compared to location 6 ($p < 0.05$), meaning the distal locations 2 and 3 have less compressibility and harder tissue compared to the proximal location 6 (figure 2a). When looking at the unaffected arm, differences in fat strain were also seen. The Tukey post Hoc test showed that location 6 was significantly higher than locations

1, 2, 3, and 4 ($p < 0.05$). Differences across the 6 locations along the length of the arm were also seen in terms of muscle strain. According to the Tukey post hoc test, location 6 was shown to be significantly greater than location 2 on the affected arm ($p < 0.05$), as shown on figure 2b. On the unaffected arm, location 6 was shown to be significantly larger when compared to location 1 and location 2 ($p = 0.05$).

FIGURE 2: (A) Fat strain differences found across the 6 landmarks along the affected and unaffected arms. (B) Muscle strain differences found across the same 6 landmarks along the affected and unaffected arms of women with stage 2 breast cancer-related lymphedema



3. Comparing strain ratios of affected over unaffected arm

A ratio of the affected over the unaffected arm in terms of skin strain, fat strain and muscle strain at all 6 locations was computed. Comparisons were then using a one-way ANOVA.

Overall the skin strain ratio had 28% less strain on the affected lymphedema arm compared to the unaffected side (mean skin strain ratio: 0.724). This strain was consistent throughout the affected arm as evidenced by the lack of any strain differences among the 6 different locations (range: 0.581-0.854). A lesser strain represents less compressibility and harder tissue in the affected arm.

Overall the fat strain ratio was 41% less strain on the affected arm compared to on the unaffected arm (mean fat strain ratio: 0.585). This strain was also consistent throughout the affected arm as evidenced by the lack of any strain differences among the 6 different locations (range: 0.502-0.745).

Overall there was a 37% less strain skeletal muscle on the affected arm, compared to on the unaffected arm (mean skeletal muscle strain: 0.63). This strain was also consistent throughout the affected arm as evidenced by the lack of any strain differences among the 6 different locations (range:0.531-0.734).

4. Global mean differences in skin, fat and muscle tissue

The final part of the study was to assess the global mean differences in skin, fat and muscle tissue of all 7 subjects across the 6 different locations, using a paired t-test. The mean skin strain ratio of the affected arm (0.395 ± 0.212) was found to be significantly lower than that of the unaffected arm (0.592 ± 0.268), $p=0.000029$, $n=42$. The mean fat strain ratio of the affected arm (0.409 ± 0.327) was found to be significantly lower than that of the unaffected arm (0.764 ± 0.516), $p=0.031$, $n=42$. The mean muscle strain ratio of the affected arm (0.544 ± 0.329) was significantly lower than that of the unaffected arm (1.023 ± 0.6000), $p=0.00002$, $n=42$.

Overall, the strain of the affected arm (0.449 ± 0.300) was significantly lower than that of the unaffected arm (0.777 ± 0.486), $p=0.000001$, $n=42$, consistent with the less compressible, harder tissue of the affected arm.

Discussion

The purpose of this study was to assess the tissue strain measurements of the arms of women diagnosed with lymphedema following breast cancer surgery using ultrasound elastography. The data collected consisted of pilot data in order to observe the underlying differences in skin strain, fat strain and muscle strain in the affected lymphedematous arm as compared to the unaffected side.

We found there to be multiple differences in all three strain types between both arms. For all three strain measurements, there is a noted decrease in strain or compressibility in the distal affected limb when compared to the unaffected limb. These structural changes align the those seen in the previous research in chapter 2 where there were noticeable differences of lymphedematous properties in the mid-forearm region.

In this study, we found overall differences in strain ratios between both arms where there was less skin strain and fat strain on the affected arm and less muscle strain on the affected arm suggesting that lymphedema decreases tissue compliance. This could be explained by the fact the women may be less inclined to use their arm affected with lymphedema due to the symptoms of heaviness and discomfort felt from the pathology and therefore lead to muscle atrophy on the affected side. The increase in fat deposits on the lymphedematous limb from the damage to the lymphatic system could also explain the differences found in the fat strain. These are novel findings. As to our knowledge, there have been no studies that have investigated the strain compositions of the different tissue components in patients with lymphedema. Most studies in the lymphedema population that use ultrasound focus on the changes in thickness of the dermis and subcutis area of the skin using classic B-mode ultrasound (Hacard et al. 2013, Suehiro et al. 2015, Bok et al. 2016). B-mode ultrasound could pose difficulties with spatial resolution (Tassenoy et al. 2016). It has been previously shown that ultrasound elastography has the ability to better detect tumors and cysts than classic B-mode ultrasonography (Hall et al. 2003).

Although there have been some studies that used ultrasound elastography on lymphedema patients, none of them to our knowledge, assessed the differences between the affected and unaffected sides of lymphedema showing the potential changes that could occur in the terms of the tissue structures from the pathology. The main studies involving lymphedema patients that focused on elastography were used to either detect the pathology or to compare the technique to other ultrasound techniques. In a study conducted by Righetti et al (2007) poroelastography was assessed as a tool to detect lymphedema. Poroelastography is defined as a type of elastography in which a time sequence is obtained from a poroelastic material under compression and may provide information on the permeability of the material (Righetti et al. 2005). A poroelastogram represents the images of the change in Poisson ratio over time, in which the Poisson ratio is defined as the ratio between the lateral to axial strain when a downward compression is applied to an elastic material. The rate of change in the Poisson ratio may provide information on the movement of fluid within the tissue (Park et al. 2011). In their study, Righetti et al. (2007) investigated seven females and one male with lymphedema, along with five females without lymphedema. Poroelastographic images were taken on the thighs and forearms of each individual. The authors used a 7.5 MHz array transducer and a 20 MHz sampling frequency. The authors hypothesized that lymphedematous tissue could be classified according to their poroelastic materials based on the tissue properties. The authors described the tissue as a coupled phenomenon composed of a solid matrix deformation and a fluid translocation. Based on the tissue elastic properties, the compressibility of the tissue and the porosity of the matrix, the poroelastograms could be used to distinguish lymphedematous tissue from normal tissue.

In another study conducted by Adriaenssens et al (2012), ultrasound elastography was compared to high frequency ultrasound. Data was collected from twenty women with breast edema following breast cancer surgery from the University Hospital of Brussels. The authors assessed both breasts before and after the breast cancer surgery and tested whether ultrasound elastography can quantitatively measure early breast edema following breast cancer surgery and irradiation as compared to the untreated breast. Measurements were performed on both breasts and on four different quadrants defined as the upper inner quadrant, lower inner quadrant, lower outer quadrant and upper outer quadrant. For the elastography measures, the ultrasound transducer was compressed five times onto the skin. The elastogram displayed both a strain color

image, comparing the strain values of tissues with different elasticity, and a strain graph. Using a standardized region of interest box, ratios were calculated on all quadrants of the breast. The authors used a 12MHz linear transducer for both the high frequency ultrasound technique and the elastography method. The authors assessed multiple outcomes using a 4-point categorical questionnaire and the above-mentioned ultrasound techniques. The authors identified an increase in subjective swelling, an increase in mean skin thickness an increase in the mean echogenicity on the lymphedematous breast. The authors also found significant increase in interstitial fluid following breast cancer surgery. The authors also stated that ultrasound elastography was significantly correlated with the visibility of the echogenic line as measured from the high frequency ultrasound. It was therefore concluded that ultrasound elastography could be an objective tool for early diagnosis of breast edema. Although these two studies provided additional knowledge and insight to detect lymphedema, they failed to provide any additional details on structural tissue components that result from lymphedema.

Johnson et al (2015) assessed lymphedema using ultrasound. The authors measured the tissue texture by using entropy (a measure of randomness within the ultrasound image representing the organization of the tissue) and average pixel intensity (reflecting the brightness or echogenicity of the structure) as variables. The authors tested the correlations of the ultrasound measures compared to the physiotherapists' clinical assessments and also compared the ultrasound image data of the affected lymphedematous arm to the unaffected arm. Ultrasound entropy measures showed a significant difference between the affected (mean=6.09; CI: 5.98-6.21) and unaffected arms (mean=6.17; CI: 6.05-6.28), $p=0.03$. Entropy measures also correlated well with the patient's self-reporting of edema and fibrosis at the lateral elbow (Spearman's $\rho=0.35$; $p=0.05$). The authors therefore concluded ultrasound to be a promising tool to measure lymphedema tissue texture in a safe and effective manner. Again, this study did not provide any information on the different tissue components in the lymphedematous limb.

There have been studies that have assessed structural compositions in a healthy cohort, such as in the study conducted by Hwang et al (2014), where the soft tissue thickness was measured through ultrasound in the arms of 20 healthy women and was compared to perometry volume measures. Circumference measures were taken at 10 cm above and below the elbow

crease by two different examiners and on sixteen different sites using a tape measure. The amount of soft tissue was found using a transducer with a frequency of 7.5 MHz and the soft-tissue thickness was measured from the distance between the skin and the fascia of the muscle. The cross-sectional area of the tissue was then calculated. The authors found the use ultrasound as a measure of soft tissue thickness to have a strong intra-rater and inter-rater reliability. The study also showed strong correlation coefficients between ultrasound and perometry. The authors also found strong correlations between the cross-sectional area measures and circumference measures above the elbow. The authors concluded that ultrasonography could be an alternate way to measure the status of soft tissue. They identified multiple advantages to this technique. In fact, they described ultrasound as a safe technique that can be used repeatedly and efficiently. Furthermore, they suggested that using cross-sectional measurement from ultrasound gives an adequate volume measure. Finally, the authors suggested that this method allows observations of structural and tissue property changes in a cost-effective manner, as opposed to the traditional measures of perometry and tape measuring that do not take tissue structure or properties in consideration and as compared to expensive methods such as MRI and CT. The main limitation that was stated in this technique was that the volume measure taken from the ultrasound was an indirect measure, as they were unable to directly measure the entire limb.

In our study, we found there to be no significant differences between affected and unaffected arms of the women with lymphedema in terms of volume, handgrip strength, arm fat and arm lean when measured through the Perometer, handgrip strength and DXA. When looking at measurements taken via ultrasound elastography we found significant differences between the two arms. Ultrasound elastography is therefore a more sensitive tool that could provide additional quantitative and qualitative data on the structural components of the arm and is a safe and efficient technique that could potentially be used for early detection of breast cancer related lymphedema, as well as to assess and follow women who have been previously diagnosed with BCRL. Furthermore, the high definition of the strain elastography technique may be helpful to identify those who have more inflammatory and quickly progressive lymphedema, and therefore may need more attention and more frequent follow-ups with therapists. These results may also aid in the early diagnosis of patients who may have signs of malignant lymphedema as an early

sign of recurrent cancer. Malignant lymphedema not only progresses more quickly, but also appears more inflammatory (Weissleder H et al. 2008, Shallwani S et al. 2017).

Conclusion

These preliminary findings suggest that ultrasound elastography is a technique that could be used to assess the tissue changes in the arms of women who have been diagnosed with breast cancer-related lymphedema, as it provides additional information on the tissue strain (fat, muscle and skin) that you would not get from other techniques that are currently used to monitor and assess the condition.

IV

Assessment of Mechanical Properties of Tissue in Breast Cancer-Related Lymphedema Using Ultrasound Elastography

Assessment of Mechanical Properties of Tissue in Breast Cancer-Related Lymphedema Using Ultrasound Elastography

Hoda S. Hashemi, Stefanie Fallone, Mathieu Boily, Anna Towers, Robert D. Kilgour, and Hassan Rivaz

Abstract—Breast cancer-related lymphedema (BCRL) is a consequence of a malfunctioning lymphatic drainage system resulting from surgery or some other form of treatment. In the initial stages, minor and reversible increases in fluid volume of the arm are evident. As the stages progress over time, the underlying pathophysiology dramatically changes with an irreversible increase in arm volume most likely due to a chronic local inflammation leading to adipose tissue hypertrophy and fibrosis. Clinicians have subjective ways to stage the degree and severity such as the pitting test which entails manually comparing the elasticity of the affected and unaffected arms. Several imaging modalities can be used but ultrasound appears to be the most preferred because it is affordable, safe and portable. Unfortunately, ultrasonography is not typically used for staging lymphedema because the appearance of the affected and unaffected arms is similar in B-mode ultrasound images. However, novel ultrasound techniques have emerged, such as elastography that may be able to identify changes in mechanical properties of the tissue related to detection and staging of lymphedema. This paper presents a novel technique to compare the mechanical properties of the affected and unaffected arms using quasi-static ultrasound elastography to provide an objective alternative to the current subjective assessment. Elastography is based on Time Delay Estimation (TDE) from ultrasound images to infer displacement and mechanical properties of the tissue. We further introduce a novel method for TDE by incorporating higher-order derivatives of the ultrasound data into a cost function, and propose a novel optimization approach to efficiently minimize the cost function. This method works reliably with our challenging patient data. We collected Radio-Frequency (RF) ultrasound data from both arms of seven patients with Stage 2 lymphedema, at six different locations in each arm. The ratio of strain in skin, subcutaneous fat and skeletal muscle divided by strain in the standoff gel pad was calculated in the unaffected and affected arms. The p -values using a Wilcoxon sign-rank test for the skin, subcutaneous fat, and skeletal muscle were 1.24×10^{-8} , 1.77×10^{-8} , 8.11×10^{-7} respectively, showing differences between the unaffected and affected arms with a very high level of significance.

H. S. Hashemi is with the Department of Electrical and Computer Engineering, University of British Columbia, V6T 1Z4, BC, Canada

S. Fallone and R. D. Kilgour are with the Department of Exercise Science, Concordia University, Montreal, QC, H3G 1M8, Canada

M. Boily is with the Department of Radiology, McGill University Health Centre (MUHC), Montreal, QC, H4A 3J1, Canada

A. Towers is the the Director of the Lymphedema program at the Department of Oncology, McGill University, Montreal, QC, H4A 3J1, Canada

A. Towers and R. D. Kilgour are with the McGill Nutrition and Performance Laboratory, Montreal, QC, H4A 3J1, Canada

H. Rivaz and R.D. Kilgour are PERFORM Centre researchers, Concordia University, Montreal, QC, H3G 1M8, Canada

H. Rivaz is with the Department of Electrical and Computer Engineering, Concordia University, Montreal, QC, H3G 1M8, Canada

Email: H. S. Hashemi: hoda@ece.ubc.ca

Email: H. Rivaz: hrivaz@ece.concordia.ca

Index Terms—Breast Cancer, Lymphedema, Quasi-Static Ultrasound Elastography, Time Delay Estimation, TDE, Efficient Second-Order Minimization.

I. INTRODUCTION

Breast cancer related lymphedema (BCRL) is manifested by a noticeable increase in excess arm volume due to treatment (e.g., surgery, radiation therapy) effects on the functioning of the lymphatic fluid drainage system [1]. This swelling can occur soon after treatment or may take several years to develop [2]. Regardless of its time to appearance, BCRL typically progresses through several clinical stages (Stages 0-3) with the initial stages (Stages 0-1) characterized by mild fluid accumulation that can be reversed by simply elevating the arm [3]. However, the successive stages (Stages 2-3) are defined by irreversible swelling that is not totally related to fluid accumulation but to suspected changes in tissue morphology of the arm such as in the skin, subcutaneous fat, and skeletal muscle. These tissue adaptations may be directly related to an abnormal pathophysiology resulting in localized inflammation of the arm leading to adipose tissue hypertrophy and pathological fibrotic changes [4]. Clearly, a shift in staging from Stage 0-1 to Stage 2-3 represents a significant change in the clinical course of this condition and warrants future investigation into the ways in which BCRL is detected and staged.

Currently, BCRL staging consists of a simple subjective assessment procedure involving an assessment of tissue pitting. Using this method, if the skin becomes “pitted” after applying finger pressure to the area, then the patient is categorized into a certain stage. This technique lacks precision and a vision of what is happening beneath the level of the skin. Thus, more sophisticated methods must be explored. There are imaging modalities that have been used in the past to detect lymphedema including magnetic resonance imaging (MRI), computed tomography (CT), and ultrasonography [5]–[7]. While MRI and CT show structural changes to tissues, their clinical utility is limited due to their considerable cost and limited availability. On the other hand, ultrasound can provide real-time measures, is portable and does not emit radiation. Furthermore, recent advances in ultrasonography such as elastography may help better assess mechanical properties of the skin, subcutaneous fat and skeletal muscle of the arm and to aid the clinician in staging lymphedema based upon changes in tissue morphology.

Ultrasound imaging can be used to investigate changes in the subcutaneous tissue that are associated with lymphedema,

which include increased thickness of the dermis, a shift from hypo- to hyperechogenicity of the subcutis, and fluid retention located in the dermis, interlobular space, and superficial fascia [8]–[10]. However, ultrasonic appearance of these changes can be negligible and hard to detect.

Certain ultrasound-based techniques have been used to tackle these problems. Poroelastographic techniques are employed to explore changes in mechanical properties of the tissue [11]–[13]. Recent work has also applied compression with the ultrasound probe, and measured the thickness of the skin and subcutis in the upper extremity [14]–[17]. These studies show that skin thickness and subcutis layers are different in the unaffected versus affected arms. However, these methods use B-mode ultrasound to manually measure tissue thickness. This measurement can be performed with greater accuracy by using Radio-Frequency (RF) data instead of B-mode images, and by using Time Delay Estimation (TDE) methods that are widely used in ultrasound elastography [18]–[25]. Such automatic TDE estimation will also be less time consuming and less subjective than manually measuring tissue thickness. Another difficulty in manually measuring skin thickness lies in normalization of the applied pressure. When comparing the thickness of the two arms, the applied pressure should be equal. Therefore, new research has proposed to use pressure sensors to generate equal pressure in both arms [26]. In this work, we propose an alternative approach wherein we use an acoustic gel pad to normalize the applied pressure on the tissue. In addition to normalizing the applied pressure, the gel pad will increase the quality of the ultrasound data at the skin.

TDE from RF data is a challenging task that is the heart of almost all ultrasound elastography methods, and as such, is an active field of research. The most common approach divides the RF data in one of the images into (usually overlapping) windows, and performs TDE by finding the best corresponding window in the other image using either intensity or phase of the RF data [27]–[29]. The second class uses optimization techniques to calculate a displacement field [30]–[34]. In addition to its wide application in almost all elastography methods, TDE has many applications such as segmentation [35] and motion compensation [36]. Our group has developed several techniques in the second class, which are usually less susceptible to decorrelation noise compared to the window-based methods [37].

Herein, we calculate TDE from the RF signal using a novel method, and estimate strain values for the gel pad, skin, subcutaneous fat, and skeletal muscle layers in the affected and unaffected arms. We use the strain values to study differences between the two arms. To the best of our knowledge, this is the first time that this approach is used in studying the differences in different layers of subcutaneous tissues between the affected and unaffected arms. More specifically, the contributions of this work are:

- 1) Introducing a novel method based on ultrasound elastography for comparing affected and unaffected arms in patients with lymphedema.
- 2) Proposing a novel method for TDE of quasi-static elastography that works reliably with the challenging patient data.

The new technique for estimation of the displacement map between two frames of RF data is based on minimization of a regularized cost function that has two terms of data similarity and continuity of TDE. It is based on our recent work entitled GLocal Ultrasound Elastography (GLUE) [38]. We introduce two novel techniques to improve GLUE. First, second-order Taylor expansion is used in the cost function, compared to first-order Taylor expansion used in GLUE. We show that inclusion of second-order Taylor terms makes the optimization problem intractable, and therefore propose a novel method for linearizing the cost function. Second, we utilize Efficient Second-order Minimization (ESM), an optimization technique that is widely shown to have superior convergence properties in computer vision and image registration [39]–[41]. We call our new method GLUE2, and show using simulation and phantom experiments that it outperforms GLUE. To focus the clinical results on differences between the mechanical properties of the unaffected and affected arms, we only present the results of GLUE2. More detailed comparisons of GLUE and GLUE2 is provided in the Supplementary Material.

To improve the quality of the superficial tissue and to normalize the compression applied to the arm during elastography, we use a gel pad, which does not contain any scatterers and appears dark in ultrasound images. It is important to measure the strain in the gel pad to normalize the manual compression, which unfortunately is not straightforward using window-based methods. To solve this problem, previous work has proposed post-processing steps to fill-in these dark regions [42]. However, both GLUE and GLUE2 are able to reliably calculate the displacement field in the gel pad since they automatically rely on the regularization term if no data term is available. Therefore, in addition to providing high-quality strain images, our proposed method is ideally suited for staging lymphedema.

A much shorter version of this work is recently published in a conference [43]. The differences are as follows. First, the introduction and literature review of this paper are more comprehensive. Second, this paper includes results of finite element and Field II simulations as well as data from seven patients, whereas the conference paper did not include simulation results and was further limited to two patients only. And last, the results are discussed in substantial more detail in this extended paper.

II. METHODS

In this section, we first briefly describe the closely related previous work of GLUE [38]. We then present GLUE2.

A. GLocal Ultrasound Elastography (GLUE)

Let I_1 and I_2 be images of size $m \times n$ that correspond to images obtained before and after some deformation. Also, let $a_{i,j}$ and $l_{i,j}$ denote be axial and lateral displacements of sample (i, j) , where $i = 1 \dots m$ and $j = 1 \dots n$. First, an estimate of the displacement field in the axial ($a_{i,j}$) and lateral ($l_{i,j}$) directions are calculated using the Dynamic Programming Analytic Minimization (DPAM) method [44]. DPAM calculates TDE by optimization of a cost function that incorporates both

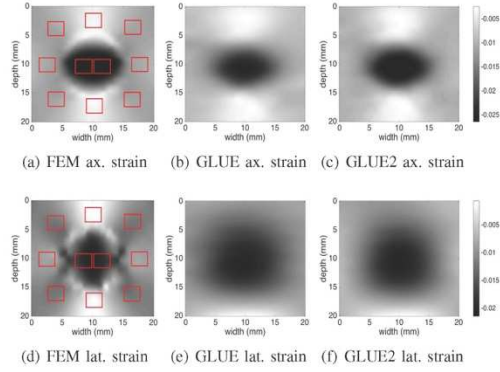


Fig. 1. Results of the Field II and Finite Element Method (FEM) simulation experiment. (a)-(c) show axial strains corresponding to respectively ground truth, GLUE and GLUE2. (d)-(f) show lateral strains corresponding to respectively ground truth, GLUE and GLUE2. The red windows in (a) and (d) are used for SNR and CNR calculations.

amplitude similarity and displacement continuity. The simultaneous estimation is performed for individual RF-lines, limiting the algorithm to utilize only a small fraction of the information available from the entire image in every optimization. The goal of GLUE is to find subsample $\Delta a_{i,j}$ and $\Delta l_{i,j}$ displacements such that the tuple $(a_{i,j} + \Delta a_{i,j}, l_{i,j} + \Delta l_{i,j})$ which refines DPAM estimates $(a_{i,j}, l_{i,j})$ and provides more accurate axial and lateral displacement estimates for all the samples of the RF frame simultaneously. The GLUE cost function is defined as:

$$C(\Delta a_{1,1}, \dots, \Delta a_{m,n}, \Delta l_{1,1}, \dots, \Delta l_{m,n}) = \sum_{j=1}^n \sum_{i=1}^m \{D(i, j) + R(i, j)\} \quad (1)$$

where the data term D is:

$$D(i, j) = [I_1(i, j) - I_2(i + a_{i,j} + \Delta a_{i,j}, j + l_{i,j} + \Delta l_{i,j})]^2, \quad (2)$$

and the regularization term R is:

$$R = \alpha_1 (a_{i,j} + \Delta a_{i,j} - a_{i-1,j} - \Delta a_{i-1,j})^2 + \beta_1 (l_{i,j} + \Delta l_{i,j} - l_{i-1,j} - \Delta l_{i-1,j})^2 + \alpha_2 (a_{i,j} + \Delta a_{i,j} - a_{i,j-1} - \Delta a_{i,j-1})^2 + \beta_2 (l_{i,j} + \Delta l_{i,j} - l_{i,j-1} - \Delta l_{i,j-1})^2, \quad (3)$$

and α and β are regularization weights in axial and lateral directions respectively. The first-order 2D Taylor expansion around $(i + a_{i,j}, j + l_{i,j})$ gives:

$$I_1(i, j) - I_2(i + a_{i,j} + \Delta a_{i,j}, j + l_{i,j} + \Delta l_{i,j}) \approx I_1(i, j) - I_2(i + a_{i,j}, j + l_{i,j}) - I'_{2,a} \Delta a_{i,j} - I'_{2,l} \Delta l_{i,j}, \quad (4)$$

where $I'_{2,a}$ and $I'_{2,l}$ are the derivatives of the I_2 at the point $(i + a_{i,j}, j + l_{i,j})$ in the axial and lateral directions. Inserting Eq. 4 in Eq. 1 will make the cost function quadratic with respect to variables $\Delta a_{i,j}$ and $\Delta l_{i,j}$, and therefore can be efficiently optimized by setting its derivative to zero.



Fig. 2. CIRS phantom and the acoustic gel pad.

B. Incorporation of the Second-Order Taylor Expansion into the Cost Function

Minimizing the cost function provides us the displacement map. GLUE uses the first order Taylor expansion (Eq. 4) to approximate the nonlinear data term of cost function with a linear term. Including higher order derivatives of Taylor expansion reduces the error in the estimated data term. As a result, having more accurate cost function by including higher order derivatives for the data term can improve the accuracy of displacement estimation. However, doing so will make the derivative of Eq. 1 nonlinear, and therefore the optimization problem becomes intractable given that this equation typically has millions of variables. For example, an RF frame of size 1000×500 has a total of 500,000 samples. Each sample Eq. 1 results in two variables (i.e. the axial and lateral displacements). Therefore, the cost function in this case has 1 million variables.

We therefore propose a novel technique to incorporate the second-order Taylor expansion into the cost function while keeping the problem computationally efficient. Our proposed cost function is:

$$C = \sum_{j=1}^n \sum_{i=1}^m \{w(i, j)D(i, j) + R(i, j)\} \quad (5)$$

where w is the weight of each data term:

$$w(i, j) = \frac{1}{\epsilon + |I''(i, j)_{2,a}| + |I''(i, j)_{2,l}|} \quad (6)$$

where ϵ is a small positive constant to prevent the denominator from becoming zero, and $|I''_{2,a}|$ and $|I''_{2,l}|$ are the absolute values of second-order derivatives in the axial and lateral directions respectively. The weight w reduces the contribution of regions of the RF-data with high second-order derivatives where Eq. 4 does not hold. Therefore, this method utilizes second-order derivatives while keeping the cost function quadratic and tractable. This idea has some similarities to a previous work that utilized areas of the images wherein cost functions approximations are more accurate [45].

C. Efficient Second-order Minimization (ESM)

We also utilize the Efficient Second-order Minimization (ESM) optimization method [39] for the first time for TDE. ESM is shown to have superior convergence properties [40].

[41], [46] compared to the asymmetric Gauss-Newton optimization method used in GLUE.

Let $p = (i + a_{i,j}, j + l_{i,j})$ denote a vector containing the coordinate of a pixel after an approximate displacement $(a_{i,j}, l_{i,j})$, and consider $p + \Delta p = (i + a_{i,j} + \Delta a_{i,j}, j + l_{i,j} + \Delta l_{i,j})$ as its refined location after a small displacement estimate $(\Delta a_{i,j}, \Delta l_{i,j})$. ESM uses the following Taylor expansion to linearize the data term [39]:

$$I_2(p + \Delta p) = I_2(p) + \frac{1}{2}\{I'_{2,a}(p) + I'_{1,a}(p)\}\Delta a_{i,j} + \frac{1}{2}\{I'_{2,l}(p) + I'_{1,l}(p)\}\Delta l_{i,j} \quad (7)$$

Utilizing Eq. 7 in our cost function of Eq. 5, we have:

$$C(\Delta a_{1,1}, \dots, \Delta a_{m,n}, \Delta l_{1,1}, \dots, \Delta l_{m,n}) = \sum_{j=1}^n \sum_{i=1}^m \{w(i,j)[I_1(i,j) - I_2(i + a_{i,j}, j + l_{i,j}) - \frac{1}{2}\{I'_{2,a}(p) + I'_{1,a}(p)\}\Delta a_{i,j} - \frac{1}{2}\{I'_{2,l}(p) + I'_{1,l}(p)\}\Delta l_{i,j}]^2 + R(i,j)\} \quad (8)$$

where $I'_{1,a}$, $I'_{2,a}$, $I'_{1,l}$ and $I'_{2,l}$ are calculated at the point $(i + a_{i,j}, j + l_{i,j})$. This equation is a quadratic equation with respect to the unknowns $\Delta a_{i,j}$ and $\Delta l_{i,j}$, and therefore can be efficiently optimized by setting its derivative with respect to the unknowns to zero. ESM (Eq. 7) uses the derivatives of both images i.e. $I'_2(p) = \frac{1}{2}(I'_{2,a}(p) + I'_{1,a}(p))$. This equation can be utilized in both axial and lateral directions. By taking derivatives from this equation and obtaining $I''_2(p)$ in both axial and lateral directions, we modify the weight of the data (Eq. 6) term as follows:

$$w(i,j) = \frac{1}{\epsilon + \frac{1}{2}[I''(i,j)_{2,a} + I''(i,j)_{1,a}] + \frac{1}{2}[I''(i,j)_{2,l} + I''(i,j)_{1,l}]} \quad (9)$$

Once the displacement field is estimated, it is common to estimate its spatial gradient to generate strain images. We consider several displacement measurements and perform a least square regression to calculate the strain image [47]. Generally, large kernels are used to reduce noise amplification of the derivative operator. They generate smooth strain fields, but make the boundary of two different types of tissue blurred. In this work, the window length of 93 is used for differentiable kernel to strike a balance between smoothness and contrast of the strain image. Note that GLUE and GLUE2 estimate displacements for all samples of RF data, and therefore, 93 is the number of samples in the RF data and not number of windows typically used in popular window-based TDE methods.

The results are not sensitive to the values of the parameters. A good combination of the tuneable parameters of the GLUE2 technique are set to $\alpha_1 = 0.2$, $\alpha_2 = 0.1$, $\beta_1 = 0.2$, and $\beta_2 = 0.1$. The parameter ϵ is set to 0.07 in simulations, 0.8 for phantom experiment and 0.012 for the *in-vivo* patient data. Higher values of this parameter are more suitable for homogenous tissues, whereas lower values are more suitable in layered inhomogenous tissues discussed in Section IV. Changing the value of ϵ by 100% for the patient data will change the CNR and SNR values in the strain map by less than only 2%. Therefore, the results are not sensitive to the value of this parameter. For the parameters of the DPAM method we

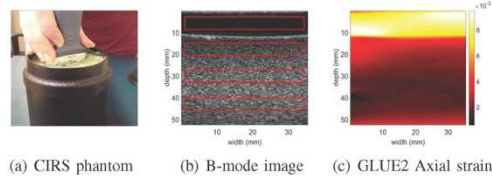


Fig. 3. B-mode image and axial strain obtained from the ultrasound probe placement on the gel pad. CIRS elastography phantom and the ultrasound B-mode image are shown in (a) and (b). The axial strain obtained from GLUE2 is depicted in (c). The red windows in (b) are used for calculation of SNR and CNR.

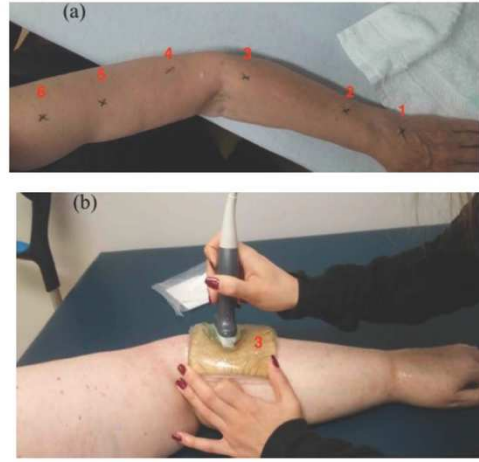


Fig. 4. Data collection from patients. (a) shows the six skin landmarks where ultrasound data collection was performed, and (b) shows RF data collection from an arm affected with lymphedema.

set $\alpha_{DP} = 0.15$, $\alpha = 5$, $\beta = 1$, and $\gamma = 0.005$. Ultrasound machines usually have presets for different organs (breast, thyroid, prostate, transcranial, etc.) for optimized imaging. The aforementioned parameters can be stored alongside these imaging presets in a commercial implementation of GLUE2.

GLUE2 is implemented in MATLAB, and our current implementation takes approximately 0.8 sec to run on a 4th generation 3.6 GHz Intel Core i7 for two RF frames of size 1000x100 to generate a 2D displacement map of the same size. The code can be optimized by implementing it in C++, and also by parallelism and use of GPU to run in real-time.

D. Simulation and Experimental Data

Simulation, phantom and *in-vivo* data from seven patients with stage 2 lymphedema are used to validate the performance of our proposed method. The simulated ultrasound images are generated using Field II [48], and ABAQUS (Providence, RI) Finite Element Method (FEM) software packages. We distribute more than 10 scatterers per cubic mm in the simulated

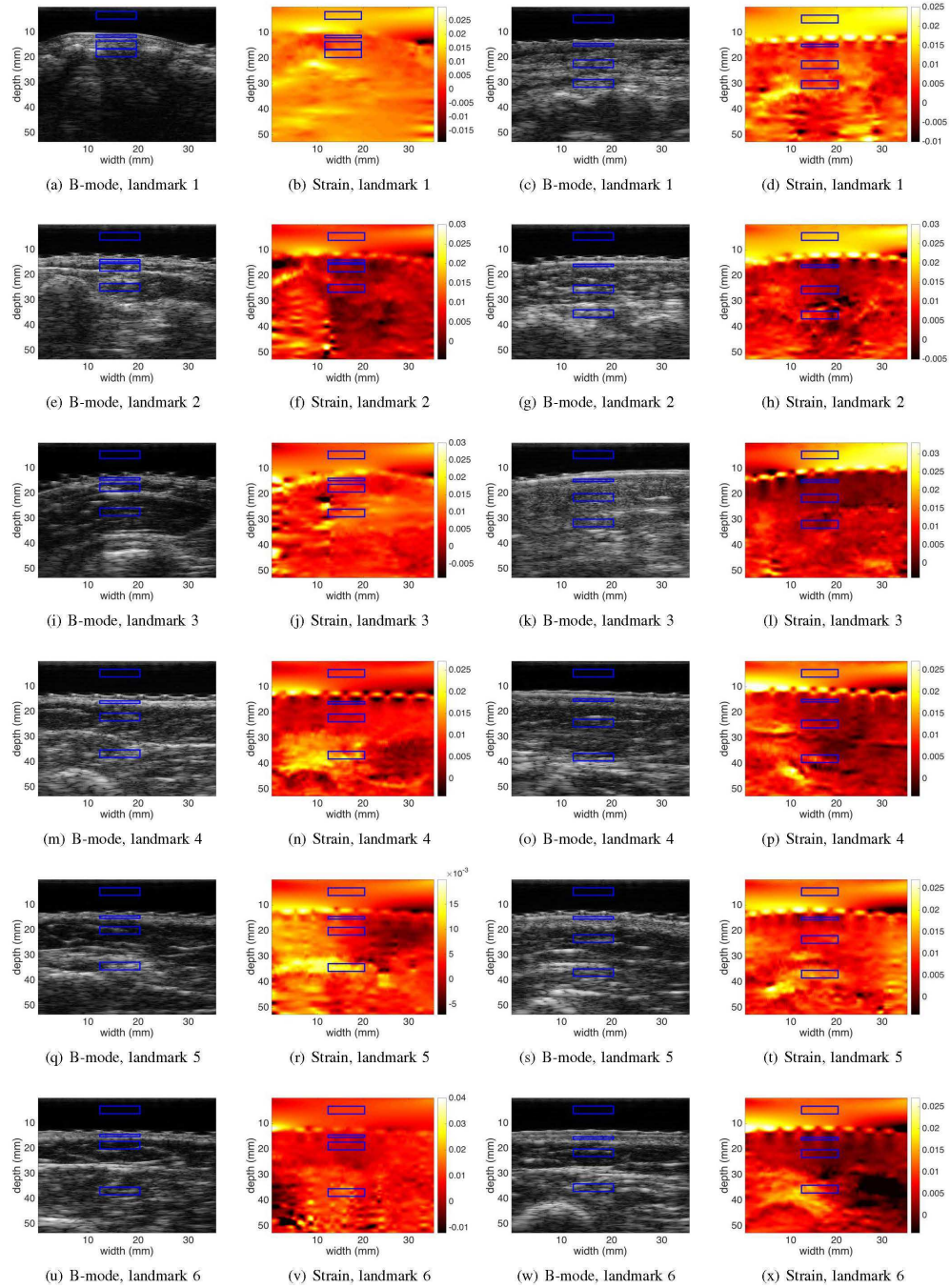


Fig. 5. Ultrasound and strain images of the 6 landmarks shown in Figure 4 in the unaffected arm (first and second columns) and affected arm (third and fourth columns).

phantom [49], and mesh the phantom for FEM analysis. We then displace the mesh nodes using the FEM package and calculate the displacement of each scatterer through interpolation of the neighboring nodes.

In phantom and *in-vivo* data collections, RF data was collected with an Alpinion E-Cube system (Bothell, WA) using the L3-12H transducer at the centre frequency of 10 MHz and the sampling rate of 40 MHz. The patient data were collected at the McGill University Health Centre (MUHC) Lymphedema clinic. Ethics approval was obtained from MUHC, and all subjects provided written consent to participate in this study. In all phantom and *in-vivo* experiments, the ultrasound probe was hand-held and was used to compress the tissue.

E. Normalization of the Compression Level Using Strain Ratio

According to the Hooke's law for linear elastic materials, $S = \frac{F}{A \cdot E}$, where S is the strain, F is the perpendicular force, A is the area, and E is the Young's modulus. Note that according to this equation, increasing the force increases the strain, and therefore strain values from different experiments cannot be compared since the force can vary. However, assuming that the gel pad is linear elastic and that the applied force varies slowly so that viscous damping can be ignored, the force in the gel pad is equal to the force applied to the tissue, and therefore, dividing the strains by the strain in the gel pad allows comparison of strain values under different forces. We validate this theoretical prediction through real phantom experiments. To this end, we use the unit-less metric strain ratio (SR) to quantitatively compare the results of the affected and unaffected limb in patient data. SR is calculated for the skin, subcutaneous fat and skeletal muscle tissue using the following equations:

$$SR_s = \frac{\bar{S}_s}{\bar{S}_g}, SR_f = \frac{\bar{S}_f}{\bar{S}_g}, SR_m = \frac{\bar{S}_m}{\bar{S}_g} \quad (10)$$

where \bar{S}_g , \bar{S}_s , \bar{S}_f and \bar{S}_m are the spatial average of the strain in the gel pad, skin, subcutaneous fat and skeletal muscle. All the spatial average values are calculated within a window of size 8mm×3mm in the corresponding regions of the strain image except for the skin which has less thickness and the window of size 8mm×1mm is used in calculations.

III. RESULTS

This section includes results on simulation and phantom data, as well as results on women who are suffering from BCRL. The unitless metrics signal to noise ratio (SNR) and contrast to noise ratio (CNR) [50] are used to quantitatively assess the quality of strain images:

$$CNR = \frac{C}{N} = \sqrt{\frac{2(\bar{s}_t - \bar{s}_b)^2}{\sigma_t^2 + \sigma_b^2}}, SNR = \frac{\bar{s}_t}{\sigma_t} \quad (11)$$

where \bar{s}_b and \bar{s}_t are the spatial strain average of the background and target windows, and σ_b^2 and σ_t^2 are the spatial strain variance of the background and target windows.

A. Simulation Results

The strain images are calculated from the displacement fields obtained from GLUE and GLUE2 and are shown in

Figure 1. These images, especially at the lesion boundaries, show that GLUE2 provides strain images that are sharper and have more contrast which makes it easier to distinguish the lesion from background. SNR and CNR values calculated using the background windows in Figure 1 (a) and (d) are reported in the Supplementary Material. These results show that GLUE2 improves the CNR in the axial strain from 18.15 to 52.74, i.e. a 190% improvement.

B. Phantom Results

For experimental validation, RF data is acquired from a CIRS elastography phantom (Norfolk, VA) with a Young's Elasticity Modulus of 7KPa as shown in Figure 2. The results are shown in Figure 3. (a) and (b) show the phantom and B-mode image respectively. The phantom is a uniform tissue which leads to an approximately uniform strain depicted in (c) for GLUE2. Unlike the simulation experiment, this phantom is uniform, and hence, it is hard to visually compare the results of GLUE and GLUE2. For this reason, and to keep the paper concise, we do not visually compare GLUE and GLUE2 and only compare them quantitatively. The SNR and CNR are calculated for 3 regions using the windows shown in (b). Please refer to Supplementary Material for the CNR and SNR measurements. The proposed method has 28% and 24% improvements in terms of CNR and SNR over the previous technique, GLUE.

To illustrate the advantage of SR over strain values, we compare their values in the phantom study at four different strain levels using GLUE2 (Table 1). Basically, the strain values will increase if the applied pressure on the tissue is intensified. It causes problems for comparison of the strain values between two different ultrasound images for affected and unaffected arms because when sonographers take ultrasound images from patients, the applied force on the tissue is different for every ultrasound image. We therefore normalize the strain values of the tissue within an image against the strain values of the gel pad. This normalization makes the strain values less dependent to the applied pressure. In Table 1, \bar{S}_p are the average values of the strain in the phantom, which change substantially from 0.07% to 0.38% at different compression levels (an increase of 443%) as expected. However, SR values depict a much slower increase from 0.27 to 0.33 (an increase of only 22%). Note that theoretically, SR should not change at all and the small changes are likely caused by nonlinearities in mechanical properties of the gel pad or phantom. Therefore, SR can be used to reduce the impact of different levels of compression.

C. Patient Data

The study population was composed of women with Stage 2 breast cancer-related lymphedema. All participants in this study had a Body Mass Index (BMI) greater than 24 kg/m² and ranged in age from 54 to 81 years old. All the patients underwent breast cancer surgery and treatment more than 6 years ago. We placed the 6 following landmarks on both arms to mark the location of the data collection (Figure 4):

TABLE I
COMPARISON OF STRAIN AND SR AT 4 DIFFERENT COMPRESSION LEVELS. THE 443% INCREASE IN PHANTOM STRAIN S_p (FROM 0.07% TO 0.38%) IS SUBSTANTIALLY REDUCED TO 22% INCREASE IN SR (FROM 0.27 TO 0.33).

Compression level	$S_p, \%$	SR
1	0.07	0.27
2	0.18	0.30
3	0.29	0.31
4	0.38	0.33

- (a) 20% of the distance between the styloid process of the 5th digit and tip of it
- (b) 20% of the distance between the styloid process of the 5th digit and olecranon
- (c) 20% of the distance between olecranon and styloid process of 5th digit
- (d) 20% of the distance of olecranon and acromioclavicular joint (AC) joint
- (e) 40% of the distance of AC joint and olecranon
- (f) 20% of the distance of AC joint to olecranon

Figure 5 shows the strain results of patient 1 for the unaffected arm in the first and second columns and for the affected arms in third and fourth columns, respectively. It is difficult to visually show the difference between GLUE and GLUE2 strain images. Therefore, to keep the paper concise, we only show the strain images of GLUE2. The windows show the location of the boxes used for calculating average strain and are placed on skin, fat and muscular regions. The location of these windows is verified by a fellowship-trained musculoskeletal radiologist (M. B.). We calculate SR for all seven patients in all 6 landmark locations, and show the results in Table III. Figure 6 visualizes the difference between strain values of unaffected and affected arms as box plots, where the strain values in Table III are used to calculate U-A for every landmark in skin, subcutaneous fat, and muscle regions. The six landmarks (from L1 to L6) are demonstrated in the horizontal axes.

Since the data cannot be assumed to have a normal Gaussian distribution, we performed the nonparametric paired Wilcoxon sign-rank test to compare the SR values of the unaffected and affected arms. The results show that SR has significantly higher values for the unaffected compared to the affected arm. Figure 6 shows that there is statistically significant difference between SR values in the affected and unaffected arms in all 6 locations in the subcutaneous fat tissue. The reason that differences in the skin (part (a)) is not as significant as fat and muscle (parts (b) & (c)) is likely because the skin layer is very thin, which can cause more variance in the SR estimates. Another reason is that this figure is only considering 7 patients, which is too small to test statistical hypothesis. To solve this problem, we consider differences at all 6 locations to increase the number of samples from 7 to $6 \times 7 = 42$, and show the results in Table III. Significant differences between the affected and unaffected arms were found for skin, subcutaneous fat and skeletal muscle SR values. The p -values for the skin, subcutaneous fat, and skeletal muscle are as follows: 1.24×10^{-5} , 1.77×10^{-8} , 8.11×10^{-7} , well below

the 0.05 threshold for statistical significance. This strongly confirms the substantial difference between SR values of the unaffected and affected arms.

To compare the ratio of SR measurements at different locations, we divide the average SR values of the unaffected arm by the affected arm from Table III and show them in Table IV. One can see that all values are more than one, meaning that SR is more in the unaffected arm. A visualization of this Table is demonstrated in Figure 7. The ratio is shown for the skin, fat, and muscle tissue types. In these seven women, the optimal location for acquiring data to distinguish the affected from the unaffected arm is the landmark 3 for the skin tissue type, landmark 2 for both subcutaneous fat and skeletal muscle area (Table IV). To obtain the overall best location, we add these three ratios at the skin, fat and muscle regions, and show the results in the last column of Table IV. The values demonstrate that locations 2, 3 and 5 have the highest difference between the two arms.

Another interesting observation from this table is that subcutis fat provides the highest difference between the SR values of the affected and unaffected arms with a very high ratio of 2.50. This is in agreement with the results of Figure 6 which showed a statistically significant difference between unaffected and affected arms for a small population of only 7 samples.

IV. DISCUSSION

The cost function of GLUE2 has two competing terms of data fidelity and continuity prior which guide the TDE towards a smooth field that also satisfies similarity of RF data. The gel pad does not have scatterers and appears dark in the B-mode image. In this region, the data term cannot guide the displacement and therefore the TDE is solely guided by the continuity prior. Window-based cross correlation methods may therefore create noisy TDEs in such regions [42]. Therefore, GLUE2 is ideally suited for the proposed study. This scenario happens also in other real-life applications such as in imaging cysts or other highly hypoechoic regions. If the gel pad contains scatterers, both data and regularization terms will guide displacement estimation and hence force normalization will likely be improved. This will be investigated in a future study.

The number of variables in the cost function is 2×10^5 for a typical RF frame of size 1000×100 . Therefore, optimization of Eq. 8 entails solving a linear system with a large coefficient matrix of size $2mn \times 2mn$ given an RF frame of size $m \times n$. One of the advantage of our method is that this large coefficient matrix is a sparse matrix with nonzero elements on a diagonal band of the size $4n+1$. Therefore, the optimization step is computationally efficient.

Eq. 9 allows us to incorporate second-order derivatives of the data term into our cost function with negligible additional computational cost. If we set ϵ to a large number, we reduce the impact of the second-order derivatives. Therefore, ϵ should be set to larger values when imaging organs that generate a mostly linear data term. Our experiments corroborated this analysis and showed that higher values of ϵ are more suitable for homogenous tissues, whereas lower

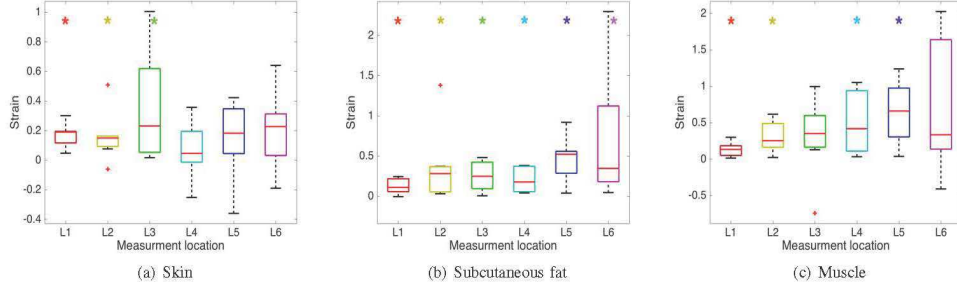


Fig. 6. Visual representation of Table III. The difference of strain values for unaffected and affected arms (U-A) are demonstrated as the box plots for every landmark (U: unaffected, A: affected). (a), (b), and (c) show these values for skin, fat, and skeletal muscle respectively. At each landmark L1 to L6, an asterisk * indicates significant difference ($p < 0.05$) between the affected and unaffected arms.

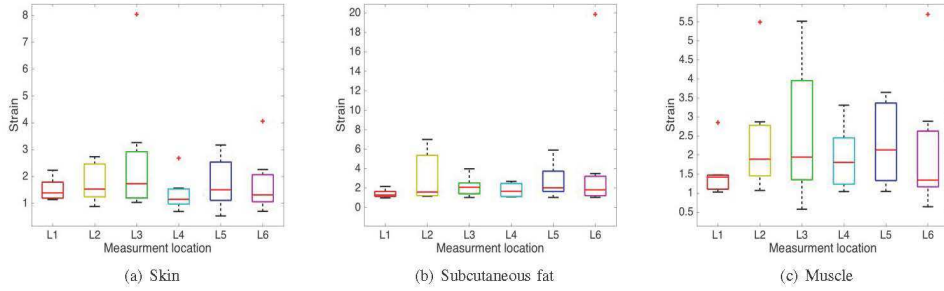


Fig. 7. Visual representation of Table IV. The ratio of SR values for the unaffected and affected arms (U/A) are demonstrated as the box plots for every landmark (U: unaffected, A: affected). (a), (b), and (c) show these values for skin, fat, and skeletal muscle.

values are more suitable in layered inhomogenous tissues. When a high/low value is considered regarding the tissue type (homogenous/inhomogenous) as the value of ϵ , it can be changed by 100% without noticeable difference in the results, which shows that the results are not sensitive to this parameter. Ultrasound machines often require specifying the imaging organ to load the optimized imaging parameters. The optimal value of all parameters of GLUE2, including ϵ , can be loaded in a similar fashion when imaging different organs.

The landmarks in Figure 4 are identified using a measuring tape. Therefore, the location of these landmarks in the two arms might be slightly different. Our hypothesis is that since tissue properties vary continuously, small differences in these locations do not generate large differences in strain measurements. Another limitation is that the direction of the ultrasound probe can lead to different SR measurements since tissue is anisotropic. To mitigate this, the sonographer should hold the probe perpendicular to the skin. In the future, we will estimate 3D ultrasound strain images [51], [52] to tackle these limitations of 2D imaging.

Although this study is limited to seven women with documented Stage 2 breast cancer-related lymphedema, the findings have uncovered several important and novel results that have allowed us to gain insight into the differences in tissue properties between the unaffected limb (non-lymphedematous)

compared to the affected limb (lymphedematous limb). It would appear that the SR values in the affected limb are consistently and significantly lower in the skin, subcutaneous fat and skeletal muscle layers. The reduction in SR suggests a less compliant tissue when compared to a more normal or healthier tissue. This reduction was noted at every landmark location suggesting that the tissue abnormalities that are contributing to the firmer tissue properties are not specific to just a single area of the arm but can be found from the most distal (wrist) to the more proximal regions of the upper arm. Of particular interest are the lower skin SR findings in the affected compared to the unaffected limb (Table III). The pitting test has been shown to differentiate between the affected and unaffected arms in stage 3, but not always in stage 2 [53]. Our findings therefore may indicate that the proposed elastography technique is more sensitive than the pitting test. Of course, these findings are representative of only 5 women; thus more data is needed to make a more definitive conclusion.

There are several factors that can explain the overall lower SR values in the lymphedemic arm. Because of the probable inflammatory processes that are present in the affected limb, it would not be surprising that inflammatory-induced fibrotic tissue has accumulated among the tissue layers thereby causing the displacement to be less pronounced. Also, additional layering of subcutaneous fat once again brought on by localized

TABLE II
SR VALUES FOR THE LANDMARKS 1 TO 6 IN SKIN, FAT, AND MUSCULAR TISSUES (A = AFFECTED AND U = UNAFFECTED).

Location 1	Skin		Fat		Muscle	
	U	A	U	A	U	A
Patient 1	0.4469	0.2653	0.4203	0.3789	0.5848	0.3957
Patient 2	0.7946	0.6047	0.7469	0.5789	0.5479	0.5327
Patient 3	0.3565	0.3086	0.4547	0.2096	0.4619	0.1618
Patient 4	0.4323	0.2367	0.5503	0.4399	0.5732	0.4034
Patient 5	0.7747	0.6791	0.6048	0.6094	0.5717	0.5452
Patient 6	0.6918	0.4978	0.5617	0.3276	0.6157	0.4876
Patient 7	0.5467	0.2451	0.3387	0.2331	0.4273	0.2941
Average	0.58	0.41	0.53	0.39	0.54	0.40
Location 2						
Patient 1	0.2569	0.0939	0.2298	0.1984	0.3632	0.3393
Patient 2	0.4481	0.5086	0.7551	0.4741	1.104	0.6675
Patient 3	0.2949	0.1315	0.21	0.1783	0.5356	0.2834
Patient 4	0.4234	0.2832	0.4141	0.0591	0.7797	0.2714
Patient 5	0.5634	0.4866	1.654	0.2715	0.755	0.1375
Patient 6	0.8404	0.3308	0.5432	0.1707	0.4831	0.3489
Patient 7	0.4327	0.2826	0.4343	0.3141	0.4218	0.1684
Average	0.47	0.30	0.60	0.24	0.64	0.32
Location 3						
Patient 1	0.8289	0.103	0.6437	0.1616	1.2174	0.2207
Patient 2	0.6282	0.3282	0.4779	0.2299	0.5544	0.2848
Patient 3	0.5488	0.3169	0.4796	0.2509	1.0987	0.748
Patient 4	0.268	0.2427	0.1786	0.1724	0.5451	0.4156
Patient 5	0.5209	0.5038	0.6688	0.3108	1.1335	0.5181
Patient 6	1.4490	0.4443	0.7150	0.2698	1.0047	1.7480
Patient 7	0.4196	0.2802	0.2545	0.2033	0.7022	0.1544
Average	0.67	0.32	0.49	0.23	0.89	0.59
Location 4						
Patient 1	0.3601	0.3148	0.6104	0.2362	1.47	0.4441
Patient 2	0.735	0.5103	0.9173	0.5475	0.9107	0.8769
Patient 3	0.357	0.3108	0.2815	0.232	0.6512	0.6103
Patient 4	0.2983	0.1905	0.3321	0.1544	0.8401	0.4215
Patient 5	0.3757	0.4082	0.454	0.4127	1.1081	0.4258
Patient 6	0.5738	0.8255	0.8513	0.7699	2.4662	1.1511
Patient 7	0.5699	0.2125	0.6093	0.2262	0.7115	0.3941
Average	0.47	0.39	0.58	0.37	1.16	0.66
Location 5						
Patient 1	0.6451	0.5063	0.6169	0.3623	1.8268	0.5882
Patient 2	0.5168	0.3337	1.1071	0.5452	1.475	0.4045
Patient 3	0.6173	0.1945	1.0203	0.4715	2.1202	1.4337
Patient 4	0.2467	0.2333	0.4975	0.1166	0.9293	0.2691
Patient 5	0.5547	0.1935	1.1065	0.1873	0.9591	0.4493
Patient 6	0.9160	0.6077	1.3439	0.8208	0.9089	0.8714
Patient 7	0.4058	0.7646	1.0107	0.9715	1.0877	0.8498
Average	0.56	0.40	0.95	0.50	1.32	0.69
Location 6						
Patient 1	0.4075	0.1804	0.2622	0.1119	0.9612	0.805
Patient 2	0.4459	0.635	1.0297	0.9843	1.3224	0.9867
Patient 3	0.9892	0.7533	1.7792	1.2837	2.9419	1.019
Patient 4	0.3840	0.3656	0.7674	0.4212	0.9671	0.8361
Patient 5	1.0570	0.9826	1.8921	1.615	1.7234	0.9296
Patient 6	1.0357	0.6968	1.8652	0.5327	0.7279	1.1360
Patient 7	0.8505	0.2094	2.4187	0.1217	2.4554	0.4307
Average	0.74	0.54	1.43	0.72	1.58	0.88

TABLE III
RESULTS OF TABLE II SUMMARIZED FOR SKIN, FAT AND MUSCLE. SR VALUES ARE MEANS \pm STANDARD DEVIATION (N=42, 7 SUBJECTS \times 6 LOCATIONS FOR EACH TISSUE TYPE). P-VALUES DETERMINED USING A PAIRED WILCOXON SIGN-RANK TEST BETWEEN SUBJECTS.

Tissue	Affected Arm	Unaffected Arm	p-value
Skin	0.39 \pm 0.21	0.58 \pm 0.26	1.24 \times 10 ⁻⁸
Subcutaneous Fat	0.41 \pm 0.33	0.76 \pm 0.52	1.77 \times 10 ⁻⁸
Skeletal Muscle	0.59 \pm 0.37	1.02 \pm 0.60	8.11 \times 10 ⁻⁷

inflammation may also contribute to the lower SR. The change in tissue composition definitely implies an alteration in the anatomical structure that could lead to changes in functional capabilities especially with skeletal muscle function. From a clinical perspective, these findings can guide health care professionals to focus on specific target areas of the limb. These initial findings are encouraging and would direct us to

TABLE IV
SR RATIO OF THE UNAFFECTED ARM DIVIDED BY THE AFFECTED ARM (U/A) FOR EACH LANDMARK LOCATION. AVERAGE VALUES FROM TABLE II ARE USED TO COMPUTE THESE NUMBERS. HIGHEST NUMBERS ARE HIGHLIGHTED IN BOLD FONT.

Location	Skin (Ave.)		Fat (Ave.)		Muscle (Ave.)	
	U/A	U/A	U/A	U/A	Sum	
1	1.41	1.35	1.35	1.35	4.11	
2	1.56	2.50	2.00	2.00	6.06	
3	2.09	2.13	1.51	1.51	5.73	
4	1.21	1.57	1.76	1.76	4.54	
5	1.40	1.90	1.91	1.91	5.21	
6	1.37	1.99	1.79	1.79	5.15	

evaluate how these SR values would differ among the different stages of lymphedema and from a more basic perspective, how these values differ from the limbs of healthy women.

V. CONCLUSIONS

In this paper, we introduced the application of quasi-static ultrasound elastography for assessment of differences between affected and unaffected arms in patients with breast cancer-related lymphedema. We proposed the biomarker of SR (Strain Ratio), and showed that it is significantly different in the affected and unaffected arms. In addition, we proposed a novel method that utilizes the second-order derivative of the data term to improve the quality of the displacement estimation. We further introduced a new time-delay estimation method that reliably estimates strain images in patient data in less than a second. Future work will focus on using the SR biomarker for staging and early diagnosis of lymphedema.

ACKNOWLEDGEMENTS

This work was supported by the Dr. Louis G. Johnson Foundation and by the Richard and Edith Strauss Canada Foundation. The authors would like to thank Z. Vajihhi for her help in data collection and the women from the MUHC Lymphedema Program who participated in this study. We also thank Julian Lee from Alpinion USA for technical support.

REFERENCES

- A. G. Warren, H. Brorson, L. J. Borud, and S. A. Slavin, "Lymphedema: a comprehensive review," *Annals of plastic surgery*, vol. 59, no. 4, pp. 464–472, 2007.
- P. S. Mortimer, "The pathophysiology of lymphedema," *Cancer*, vol. 83, no. S12B, pp. 2798–2802, 1998.
- I. ISL, "The diagnosis and treatment of peripheral lymphedema," *Lymphology*, vol. 36, no. 2, pp. 84–91, 2003.
- S. G. Rockson, "Diagnosis and management of lymphatic vascular disease," *Journal of the American College of Cardiology*, vol. 52, no. 10, pp. 799–806, 2008.
- S. Dnewell, K. D. Hagspiel, J. Zuber, G. K. von Schulthess, A. Bollinger, and W. A. Fuchs, "Swollen lower extremity: role of mr imaging," *Radiology*, vol. 184, no. 1, pp. 227–231, 1992.
- R. Garza, R. Skoracki, K. Hock, and S. P. Povoski, "A comprehensive overview on the surgical management of secondary lymphedema of the upper and lower extremities related to prior oncologic therapies," *BMC cancer*, vol. 17, no. 1, p. 468, 2017.
- A. Szuba and S. G. Rockson, "Lymphedema: classification, diagnosis and therapy," *Vascular medicine*, vol. 3, no. 2, pp. 145–156, 1998.
- M. Gniadecka and B. Quistoff, "Assessment of dermal water by high-frequency ultrasound: comparative studies with magnetic resonance," *British Journal of Dermatology*, vol. 135, no. 2, pp. 218–224, 1996.
- M. Gniadecka, "Localization of dermal edema in lipodermatosclerosis, lymphedema, and cardiac insufficiency: high-frequency ultrasound examination of intradermal echogenicity," *Journal of the American Academy of Dermatology*, vol. 35, no. 1, pp. 37–41, 1996.

- [10] E. Fumiere, O. Leduc, S. Fourcade, C. Becker, C. Garbar, R. Demeure, F. Wilputte, A. Leduc, and C. Delcour, "Mr imaging, proton mr spectroscopy, ultrasonographic, histologic findings in patients with chronic lymphedema," *Lymphology*, vol. 40, no. 4, pp. 157–162, 2007.
- [11] R. Righetti, B. S. Garra, L. M. Mobbs, C. M. Kraemer-Chant, J. Ophir, and T. A. Krouskop, "The feasibility of using poroelastographic techniques for distinguishing between normal and lymphedematous tissues in vivo," *Physics in Medicine & Biology*, vol. 52, no. 21, p. 6525, 2007.
- [12] G. P. Berry, J. C. Bamber, P. S. Mortimer, N. L. Bush, N. R. Miller, and P. E. Barbone, "The spatio-temporal strain response of oedematous and nonoedematous tissue to sustained compression in vivo," *Ultrasound in Medicine and Biology*, vol. 34, no. 4, pp. 617–629, 2008.
- [13] L. Coutts, N. Miller, P. Mortimer, and J. Bamber, "Investigation of in vivo skin stiffness anisotropy in breast cancer related lymphoedema," *Journal of biomechanics*, vol. 49, no. 1, pp. 94–99, 2016.
- [14] R. H. Mellor, N. L. Bush, A. W. Stanton, J. C. Bamber, J. R. Levick, and P. S. Mortimer, "Dual-frequency ultrasound examination of skin and subcutis thickness in breast cancer-related lymphedema," *The breast journal*, vol. 10, no. 6, pp. 496–503, 2004.
- [15] W. Kim, S. Chung, T. Kim, and K. Seo, "Measurement of soft tissue compliance with pressure using ultrasonography," *Lymphology*, vol. 41, no. 4, p. 167, 2008.
- [16] C. Lim, H. Seo, K. Kim, S. Chung, and K. Seo, "Measurement of lymphedema using ultrasonography with the compression method," *Lymphology*, vol. 44, no. 2, p. 72, 2011.
- [17] F. Hacard, L. Machet, A. Caille, V. Tauveron, G. Georgescou, I. Rape-neau, M. Samimi, F. Patat, and L. Vaillant, "Measurement of skin thickness and skin elasticity to evaluate the effectiveness of intensive decongestive treatment in patients with lymphoedema: a prospective study," *Skin Research and Technology*, vol. 20, no. 3, pp. 274–281, 2014.
- [18] X. Pan, J. Gao, S. Tao, K. Liu, J. Bai, and J. Luo, "A two-step optical flow method for strain estimation in elastography: Simulation and phantom study," *Ultrasonics*, vol. 54, no. 4, pp. 990–996, 2014.
- [19] H. Rivaz, E. M. Boctor, M. A. Choti, and G. D. Hager, "Ultrasound elastography using multiple images," *Medical image analysis*, vol. 18, no. 2, pp. 314–329, 2014.
- [20] A. N. Ingle, C. Ma, and T. Varghese, "Ultrasonic tracking of shear waves using a particle filter," *Med. phys.*, vol. 42, no. 11, pp. 6711–6724, 2015.
- [21] M. G. Kibria and M. K. Hasan, "A class of kernel based real-time elastography algorithms," *Ultrasonics*, vol. 61, pp. 88–102, 2015.
- [22] J. Jiang and T. J. Hall, "A coupled subsample displacement estimation method for ultrasound-based strain elastography," *Physics in medicine and biology*, vol. 60, no. 21, p. 8347, 2015.
- [23] J. Porée, D. Garcia, B. Chayer, J. Ohayon, and G. Cloutier, "Noninvasive vascular elastography with plane strain incompressibility assumption using ultrafast coherent compound plane wave imaging," *IEEE transactions on medical imaging*, vol. 34, no. 12, pp. 2618–2631, 2015.
- [24] Z. Liu, C. Huang, and J. Luo, "A systematic investigation of lateral estimation using various interpolation approaches in conventional ultrasound imaging," *IEEE Transactions on Ultrasonics, Ferroelectrics, and Frequency Control*, 2017.
- [25] M. S.-E. Rabbi and M. K. Hasan, "Speckle tracking and speckle content based composite strain imaging for solid and fluid filled lesions," *Ultrasonics*, vol. 74, pp. 124–139, 2017.
- [26] C. Lim, B. Hwang, H. Park, D. Lee, J. Park, K. J. Lee, S. K. Kim, and K. S. Seo, "Optimal pressure for measuring objective lymphedema with postoperative ultrasonography in patients with breast cancer," *Computer Assisted Surgery*, vol. 21, no. sup1, pp. 102–110, 2016.
- [27] E. Konofagou and J. Ophir, "A new elastographic method for estimation and imaging of lateral displacements, lateral strains, corrected axial strains and poisson's ratios in tissues," *Ultrasound in Medicine and Biology*, vol. 24, no. 8, pp. 1183–1199, 1998.
- [28] T. Shina, K. R. Nightingale, M. L. Palmeri, T. J. Hall, J. C. Bamber, R. G. Barr, L. Castera, B. I. Choi, Y.-H. Chou, D. Cosgrove et al., "Wtumb guidelines and recommendations for clinical use of ultrasound elastography: Part 1: basic principles and terminology," *Ultrasound in Medicine and Biology*, vol. 41, no. 5, pp. 1126–1147, 2015.
- [29] R. Ahmed, R. Arfin, M. H. Rubel, K. K. Islam, C. Jia, D. Metaxas, B. S. Garra, and S. K. Alam, "Comparison of windowing effects on elastography images: Simulation, phantom and in vivo studies," *Ultrasonics*, vol. 66, pp. 140–153, 2016.
- [30] M. McCormick, N. Rubert, and T. Varghese, "Bayesian regularization applied to ultrasound strain imaging," *IEEE Transactions on Biomedical Engineering*, vol. 58, no. 6, pp. 1612–1620, 2011.
- [31] Z. Chen, Y. Chen, and Q. Huang, "Development of a wireless and near real-time 3d ultrasound strain imaging system," *IEEE transactions on biomedical circuits and systems*, vol. 10, no. 2, pp. 394–403, 2016.
- [32] B. Byram, G. E. Trahey, and M. Palmeri, "Bayesian speckle tracking, part i: An implementable perturbation to the likelihood function for ultrasound displacement estimation," *IEEE transactions on ultrasonics, ferroelectrics, and frequency control*, vol. 60, no. 1, pp. 132–143, 2013.
- [33] D. M. Dumont, K. M. Walsh, and B. C. Byram, "Improving displacement signal-to-noise ratio for low-signal radiation force elasticity imaging using bayesian techniques," *Ultrasound in Medicine and Biology*, vol. 42, no. 8, pp. 1986–1997, 2016.
- [34] C. Pellot-Barakat, F. Frouin, M. F. Insana, and A. Herment, "Ultrasound elastography based on multiscale estimations of regularized displacement fields," *IEEE transactions on medical imaging*, vol. 23, no. 2, pp. 153–163, 2004.
- [35] M. A. Hussain, A. J. Hodgson, and R. Abugarbieh, "Strain-initialized robust bone surface detection in 3-d ultrasound," *Ultrasound in Medicine and Biology*, vol. 43, no. 3, pp. 648–661, 2017.
- [36] J. Porée, D. Posada, A. Hodzic, F. Toumoux, G. Cloutier, and D. Garcia, "High-frame-rate echocardiography using coherent compounding with doppler-based motion-compensation," *IEEE transactions on medical imaging*, vol. 35, no. 7, pp. 1647–1657, 2016.
- [37] T. J. Hall, P. E. Barbone, A. A. Oberai, J. Jiang, J.-F. Dord, S. Goenezen, and T. Fisher, "Recent results in nonlinear strain and modulus imaging," *Current medical imaging reviews*, vol. 7, no. 4, pp. 313–327, 2011.
- [38] H. S. Hashemi and H. Rivaz, "Global time-delay estimation in ultrasound elastography," *IEEE Transactions on Ultrasonics, Ferroelectrics, and Frequency Control*, vol. 64, pp. 1625–1636, 2017.
- [39] S. Benhimane and E. Malis, "Real-time image-based tracking of planes using efficient second-order minimization," in *Intelligent Robots and Systems, 2004 (IROS 2004). Proceedings. 2004 IEEE/RSJ International Conference on*, vol. 1. IEEE, 2004, pp. 943–948.
- [40] C. Wachinger, P. Golland, C. Magnain, B. Fischl, and M. Reuter, "Multi-modal robust inverse-consistent linear registration," *Human brain mapping*, vol. 36, no. 4, pp. 1365–1380, 2015.
- [41] H. Zhou and H. Rivaz, "Registration of pre-and postresection ultrasound volumes with noncorresponding regions in neurosurgery," *IEEE journal biomedical and health informatics*, vol. 20, no. 5, pp. 1240–1249, 2016.
- [42] A. Nahiyani and M. K. Hasan, "Hybrid algorithm for elastography to visualize both solid and fluid-filled lesions," *Ultrasound in medicine & biology*, vol. 41, no. 4, pp. 1058–1078, 2015.
- [43] H. Hashemi, S. Fallone, M. Boily, A. Towers, R. Kilgour, and H. Rivaz, "Ultrasound elastography of breast cancer-related lymphedema," in *Biomedical Imaging (ISBI 2018), 2018 IEEE 15th International Symposium on*. IEEE, 2018, pp. 1491–1495.
- [44] H. Rivaz, E. M. Boctor, M. A. Choti, and G. D. Hager, "Real-time regularized ultrasound elastography," *Medical Imaging, IEEE Transactions on*, vol. 30, no. 4, pp. 928–945, 2011.
- [45] S. Benhimane, A. Ladikos, V. Lepetit, and N. Navab, "Linear and quadratic subsets for template-based tracking," in *IEEE Conference Computer Vision Pattern Recognition, 2007*. IEEE, 2007, pp. 1–6.
- [46] C. Mei, S. Benhimane, E. Malis, and P. Rives, "Efficient homography-based tracking and 3-d reconstruction for single-viewpoint sensors," *IEEE Transactions on Robotics*, vol. 24, no. 6, pp. 1352–1364, 2008.
- [47] F. Kallel and J. Ophir, "A least-squares strain estimator for elastography," *Ultrasonic imaging*, vol. 19, no. 3, pp. 195–208, 1997.
- [48] J. A. Jensen, "Field: A program for simulating ultrasound systems," in *10TH NordiBaltic Conference on Biomedical Imaging, Vol. 4, Supplementary Part 1: 351–353*. Citeseer, 1996.
- [49] H. Rivaz, E. M. Boctor, and G. Fichtinger, "Ultrasound speckle detection using low order moments," in *Ultrasonics Symposium, 2006. IEEE, 2006*, pp. 2092–2095.
- [50] J. Ophir, S. Alam, B. Garra, F. Kallel, E. Konofagou, T. Krouskop, and T. Varghese, "Elastography: ultrasonic estimation and imaging of the elastic properties of tissues," *Proceedings of the Institution of Mechanical Engineers, Part H: Journal of Engineering in Medicine*, vol. 213, no. 3, pp. 203–233, 1999.
- [51] H. Rivaz, I. Fleming, L. Assumpcao, G. Fichtinger, U. Hamper, M. Choti, G. Hager, and E. Boctor, "Ablation monitoring with elastography: 2d in-vivo and 3d ex-vivo studies," *Medical Image Computing and Computer-Assisted Intervention-MICCAI 2008*, pp. 458–466, 2008.
- [52] A. Ingle, T. Varghese, and W. A. Sethares, "Efficient 3-d reconstruction in ultrasound elastography via a sparse iteration based on markov random fields," *IEEE transactions on ultrasonics, ferroelectrics, and frequency control*, vol. 64, no. 3, pp. 491–499, 2017.
- [53] K. Levenhagen, C. Davies, M. Perdomo, K. Ryans, and L. Gilchrist, "Diagnosis of upper-quadrant lymphedema secondary to cancer: Clinical practice guideline from the oncology section of apta," *Rehabilitation Oncology (American Physical Therapy Association, Oncology Section)*, vol. 35, no. 3, p. E1, 2017.

V

Concluding Remarks

Lymphedema of the upper extremity is a condition negatively affecting the quality of life of many women who are breast cancer survivors. This chronic condition currently has no cure and research has described it to be as stressful as the initial diagnosis of breast cancer as well as a continuous reminder of the cancer (Park et al. 2008). Indeed, the swelling and complications caused by the damage to the lymphatic system lead to negative changes on the patient's self-image on top of the impact many already obtained from the mastectomy itself. In addition to the psychological and psychosocial burden, the patient also feels physical symptoms, such as pain, heaviness and numbness, for the remainder of their life.

The lack of standardization in diagnosing the condition and the lack of information about the various tissue changes that occur as a result of the condition, create multiple challenges in treating and monitoring the improvements or progression of the lymphedema. First, tissue changes of lymphedema occur much sooner than any visible swelling, causing clinicians to often diagnose the condition passed the point of possible reversibility and focusing treatment on maintenance. The reasons for this are numerous. In addition, there exist no standard defined criteria that stage the severity of the lymphedema that are agreed upon by researchers and clinicians. Furthermore, the currently used techniques to assess lymphedema are subjective and provide no information on the underlying tissue changes occurring beneath the skin. Indeed, the most common methods used include circumferential tape measurements and palpation. Circumferential tape measures provide information on the area and volume changes of the arm, but no information on whether these changes are due to alterations in fluid or blood flow, adipose tissue changes, or muscle atrophy or hypertrophy. Palpation is used to evaluate the edema and further stage the severity of the condition based on pitting, that is the ability of the tissue to bounce back after pushing down on the skin.

There is very little research done on lymphedema and a large gap as to understanding, diagnosing and monitoring the condition. Most studies focus on measuring the success of treatments such as decongestive or compression therapy on patients who have been diagnosed with the condition using relatively subjective techniques such as circumference measures. More recent studies have begun to use ultrasonography as a measurement tool to diagnose the condition or monitor treatment outcomes, and these early results suggest that tool is valid and reliable (Li et

al. 2012). However, these results are preliminary, and fail to compare the affected lymphedema side to the unaffected side or to compare to a group of healthy controls. This thesis project was therefore divided into two parts; (1) gaining an overall understanding of the underlying tissue changes in the affected lymphedema limb and how this compares to the opposite unaffected side (2) obtaining measures of tissue strain through novel ultrasound elastography to detect lymphedema and understand the effect of lymphedema on different tissue components (eg. fat, skin and muscle).

In the first study, we used multiple techniques including DXA, Perometer, arm circumference measurement techniques and handgrip strength to observe the changes in lean tissue, fat tissue, volume and strength. Interestingly, we found a significantly larger concentration of lymphedema around the mid-forearm area. This difference remained when controlling for the patients' dominant hand. The palm area was also found to have the smallest circumference ratio in the lymphedematous arm. This finding suggests that the onset of lymphedema may begin to form around the mid-forearm area and further spread proximally, apart from the hand. We believe there are protective anatomical factors regarding the early development of the lymphedema in the hand such as the fascia, or blood vessels, or perhaps the more frequent hand movements propel the fluid more proximally. Another of our interesting and this time surprising finding is the lack of correlation between handgrip strength and lean mass in the women diagnosed with lymphedema, as opposed to the strong correlation we found in the control group. We believe the difference between the two groups is due to the fact that lean tissue as measured by DXA is composed not only of muscle mass, but also includes fluids, minerals and proteins, and that the fluids may be falsely raising the DXA measured estimate of muscle mass. The study also raised a question as to whether excess fluid might also begin to develop in the unaffected side.

These novel findings open multiple areas of new research regarding the pathogenesis of lymphedema, the spread of lymphedema and could also provide additional information about early diagnosis (given earlier findings in the mid-forearm) and which can potentially lead to identifying the best treatment alternative for the patient. These results are pilot data, stemming from a small cohort of women. Future research is needed to assess each of these questions in

more detail, with a larger number of patients, and by controlling for additional variables, that we did not take into consideration in this study, such as age, a narrower BMI window, and the type of breast-cancer treatment that the patient underwent.

The second study was focused specifically on the use of ultrasound elastography to observe the elasticity, or strain of the different tissue compositions in the lymphedematous limb in order to provide additional insight and details on the changes occurring in the affected limb. To our knowledge no such study has been conducted in this type of population. First, we established a novel elastography method that focused on better time delay estimation and better quality of displacement estimation by using a second-order derivative and reliably estimated strain images (Hashemi et al. 2019). We then used this method in patients with unilateral breast-cancer related lymphedema at stage 2 to compare the affected arm to the unaffected arm. The results showed promising findings in terms of using this tool to assess the condition. We found differences in skin strain, fat strain and muscle strain between both the affected limb and the unaffected limb, where there was significantly lower strain in the affected arm, meaning the tissue was harder, and less compressible the healthy limb, and these differences were more prominent in the lower-forearm region, which aligns with the findings from the DXA from the first part of the study. Both studies suggest that this area may be the area first affected by lymphedema as this area has the largest circumference ratio and smallest strain values than the rest of the arm, meaning that the changes are occurring at a faster rate in that region. Again, this data was strictly for observational purposes and provided pilot data. Limitations of the study include the small sample size, and the lack of a comparison to a group of healthy controls. We did; however, try to factor in these limitations, by using the healthy unaffected arm of women with unilateral lymphedema to act as a control limb, and the cohort of 7 women used in this study were representative of the larger cohort of 20 women that were recruited, when examined for differences in age, height, weight, BMI, and body composition (body fat%, lean mass, and fat mass).

Overall, this project presented multiple novel findings in the area of breast cancer-related lymphedema and raised multiple questions regarding the onset of lymphedema, the spread of lymphedema and the possibility of the condition spreading to involve other regions. Furthermore,

it provided positive and promising results regarding the use of the more objective ultrasound tool to be used as method to diagnose, assess and monitor lymphedema as opposed to the classic subjective techniques that are currently used in this field. Ultrasonography has proven to be useful in providing more quantifiable data, is quick, easy to use, portable and more affordable than other available technologies. Future studies focusing on reliability and reproducibility of this tool in a larger sample of population are required, along with studies comparing both a group of women affected by condition as well as a group of healthy controls. It would also be interesting to study the correlations of volume segments along the arm and to see if they correlate with the strain measurements taken from the ultrasound elastography, especially in terms of the differences that were identified in the mid-forearm regions. Clinical observations have also suggested possible early manifestation of lymphedema right above the elbow (personal communication, Dr. Anna Towers, March 2019). It would be interesting to study that region in additional detail along with the mid-forearm region and to complete a longitudinal study using ultrasound elastography, where we would follow patients from their initial breast cancer treatment in order to see the changes in strain over time. As research progresses in this domain, we will gain a larger overall understanding of lymphedema, be able to stage the patients based on severity, be better able to follow disease progression, and substantially determine the best treatment alternatives for these patients.

VI

References

Abe T, Thiebaud RS, Loenneke JP. Age-related change in handgrip strength in men and women: is muscle quality a contributing factor? *Age*. 2016; 38(28): 1-7. doi: 10.1007/s11357-016-98911-4

Adriaenssens N, Belsack D, Buyl R, Ruggiero L, Breucq C, De Mey J, Lievens P, Lamote J. Ultrasound elastography as an objective diagnostic measurement tool for lymphedema of the treated breast following breast conserving surgery and radiotherapy. *Radiol Oncol*. 2012; 46(4): 284-295. Doi: 10.2478/v10019-012-0033-z

Ancukiewicz M, Russell TA, Otoole J, Specht M, Singer M, Kelada A, Murphy CD, Pogahar J, Gioioso V, Patel M, Skolny M, Smith BL, Taghian AG. Standardized method for quantification developing lymphedema in patients treated for breast cancer. *Int. J. Radiation Biol. Phys*. 2011; 79(5): 1436-1443. doi:10.1016/j.ijrobp.2010.01.011

Armer JM, Stewart BR, Shook RP. 30-month post-breast cancer treatment lymphoedema. *J Lymphoedema*. 2009; 4P 14-18.

Batse David O. An interstitial hypothesis for breast cancer related lymphedema. *Pathophysiology*. 2010; 17(4): 289-294. doi:10.1016/j.pathophys.2009.006.

Brandenburg JE, Eby SF, Song P, Zhao H, Brault J, Chen S, An KN. Ultrasound Elastography: The New Frontier in Direct Measurement of Muscle Stiffness. *Arch Phys Med Rehabil*. 2014; 95(11): 2207-2219. doi:10.1016/j.apmr.2014.07.007

Bok SK, Jeon Y, Hwang P. Ultrasonographic evaluation of the effects of progressive resistive exercise in breast cancer-related lymphedema. *Lymphatic Research and Biology*. 2016; 14(1): 18-24. doi: 10.1089/lrb.2015.0021

Canadian Cancer Society. Retrieved March 16, 2019:
<http://www.cancer.ca/en/cancer-information/cancer-type/breast/statistics/?region=qc&ts=180129161424>

Cespedes I, Ophir J, Ponnekanti H, Maklad N. Elastography: elasticity imaging using ultrasound with application to muscle and breast in vivo. *Ultrasonic Imaging*. 1993; 15: 73-88. doi: 10.1177/016173469301500201.

Chevillat AL, McGarvey CL, Petrek JA, Russo SA, Thiadens SR, Taylor ME. The grading of lymphedema in oncology clinical trials. *Semin Radiat Oncol*. 2003; 13: 214-225. doi: 10.1016/S1053-4296(03)0038-9

Common Toxicity Criteria (CTC) v.3.0. Retrieved December 1, 2015:

http://ctep.cancer.gov/protocolDevelopment/electronic_applications/docs/ctcae3.pdf

Czerniec SA, Ward LC, Meerkin JD, Kilbreath SL. Assessment of Segmental Arm Soft Tissue Composition in Breast Cancer-Related Lymphedema: A Pilot Study Using Dual Energy X-ray Absorptiometry and Bioimpedance Spectroscopy. *Lymphatic Research and Biology*. 2015; 3(1): 33-39. doi: 10.1089/lrb.2014.0033

Di Sipio T, Rye S, Newman B, Hayes S. Incidence of unilateral arm lymphedema after breast cancer: a systematic review and meta-analysis. *Lancet Oncol*. 2013; 14: 500-515. doi: 10.1016/S1470-2045(13)70076-7

Dixon JB, Weiler MJ. Bridging the divide between pathogenesis and detection in lymphedema. *Seminars in Cell & Developmental Biology*. 2015; 38: 75-82. doi: 10.1016/j.semcdb.2014.12.003

Dylke ES, Ward LC, Meerkin JD, Nery RN, Kilbreath SL. Tissue Composition Changes and Secondary Lymphedema. *Lymphatic Research and Biology*. 2013; 11(4): 211-218. doi: 10.1089/lrb.2013.0018

Dynamic Ultrasound Group. *Physics, instrumentation and basic technique*. Retrieved March 28, 2016, from: <http://dynamicultrasound.org/dugphysics.html>.

Ferreira de Abreu Junior G, Benjamin de Brandao Pitta G, Araujo M, Araujo Castro A, Ferreira de Azevedo Junior W, Mirando Junior F. Ultrasonographic changes in the axillary vein of patients with lymphedema after mastectomy. *Rev. Col. Bras. Circ.* 2015; 42(2): 081-092. doi:10.1500/0100-69912015002004

Garza R, Skoracki R, Hock K, Povoski SP. A comprehensive overview on the surgical management of secondary lymphedema of the upper and lower extremities related to prior oncologic therapies. *BMC Cancer.* 2017; 17:468. doi: 10.1186/s12885-017-3444-9

Gomes PRL, Junior IFF, Silva CB, Rocha APR, Salgado ASI, Carmo EM. Short-term changes in handgrip strength, body composition, and lymphedema induced by breast cancer surgery. *Rev Bras Ginecol Obstet.* 2014; 36(6): 244-250. doi:10.1590/S0100-720320140005004

Hacard F, Machet L, Caille A, Tauveron V, Georgescu G, Rapeneau I, Samimi M, Patat F, Vaillant L. Measurement of skin thickness and skin elasticity to evaluate the effectiveness of intensive decongestive treatment in patients with lymphedema: a prospective study. *Skin Research and Technology.* 2014; 20: 274-281. doi: 10.1111/srt.12116

Hashemi HS, Fallone S, Boily, Towers A, Kilgour RD, Rivaz H. Assessment of Mechanical Properties of Tissue in Breast-Cancer Related Lymphedema Using Ultrasound Elastography. *IEEE TUFFC;* 2019, 66(3): 541-550. doi:10.1109/TUFFC.2018.2876056

Hayes S, Di Sipio T, Rye S, López JA, Saunders C, Pyke C, Bashford J, Battistutta D, Newman B. The prevalence and prognostic significance of secondary lymphedema following breast cancer. *Lymphat Res Biol.* 2011; 9: 135-141. doi: 10.1089/lrb.2011.0007

Hayes SC, Johansson K, Stout NL, Prosnitz R, Armer JM, Gabram S, Schimtz KH. Upper-body morbidity after breast cancer: incidence and evidence for evaluation, prevention, and management within a prospective surveillance model of care. *Cancer.* 2012; 118(suppl): 2237-2249. doi: 10.1002/cncr.27467

Hoffner M, Peterson P, Mansson S, Brorson H. Lymphedema Leads to Fat Deposition in Muscle and Decreased Muscle/Water Volume After Liposuction: A Magnetic Resonance Imaging Study. *Lymphatic Research and Biology*. 2017. doi:10.1089/lrb.2017.0042

Hwang JH, Lee CH, Lee HH, Kim SY. A new soft tissue volume measurement strategy using ultrasonography. *Lymphat Res Biol*. 2014; 12(2):89-94. doi:10.1089/lrb.2013.0030

Ikai M, Fukunaga T. Calculation of muscle strength per unit cross-sectional area human muscle by means of ultrasonic measurement. *Int. Z. Angew. Physiol*. 1968; 38: 355-360

Jang D-H, Kim M-W, Oh S-J, Kim JM. The influence of arm swelling duration on shoulder pathology in breast cancer patients with lymphedema. *PLoS One*. 2015; 10(11): e0142950. doi: 10.1371/journal.pone.0142950

Johansson K, Ohlsson K, Ingvar C, Albertsson M, Ekdahl C. Factors associated with the development of arm lymphedema following breast cancer treatment: a match pair case-control study. *Lymphology*. 2002; 35: 59-71.

Johnson CK, DeSarno M, Ashikaga T, Dee J, Henry SM. Ultrasound and clinical measures for lymphedema. *Lymphatic Research and Biology*. 2015; 00: 1-10. doi: 10.1089/lrb.2015.0001

Khan, S. Inter-rater variability of circumferential volume measurements at the Lymphedema Clinic and the Cedars Breast Clinic, McGill University Health Centre. Presented at the Annual Conference of the Lymphedema Association of Quebec, September 20, 2014.

Li X, Karmakar MK, Lee A, Kwok WH, Critchley LA, Gin T. Quantitative evaluation of the echo intensity of the median nerve and flexor muscles of the forearm in the young and the elderly. *Br J Radiol*. 2012; 85:e140-e145. doi: 10.1259/bjr/30878012

- Lu Q, Delproposto Z, Hu A, Hu J. MR Lymphography of lymphatic vessels in lower extremity with gynecologic oncology-related lymphedema. *PLOS one*. 2012; 7(11): e50319. doi:10.1371/journal.pone.00530319
- Maunsell E, Brisson J, Deschenes L. Arm problems and psychological distress after surgery for breast cancer. *Can J Surg*. 1993; 36: 315-320
- Minetto MA, Caresio C, Menapace T, Hajdarevic A, Marchini A, Molinari F, Maffioletti N. Ultrasound-based detection of low muscle mass for diagnosis of sarcopenia in older adults. *Physical Medicine & Rehabilitation*. 2015. doi: 10.1016/j.pmrj.2015.09.014
- Moffatt CJ, Franks PJ, Doherty DC, Williams AF, Badger C, Jeffs E, Bosanquet N, Mortimer PS. Lymphoedema: an underestimated health problem. *QJM*. 2003; 96:731-738.
- Newman AL, Rosenthal L, Towers A, Hodgson P, Shay CA, Tidhar D, Viganò A, Kilgour RD. Determining the precision of dual energy x-ray absorptiometry and bioelectric impedance spectroscopy in the assessment of breast cancer related lymphedema. *Lymphat Res Biol*. 2013; 11(2): 104-109. doi: 10.1089/lrb.2012.0020
- Nicolaides AN. Investigation of chronic venous insufficiency a consensus statement. *American Heart Association*. 2000; 102: e126-e163. doi: 10.1161/01.CIR.102.20.e126v
- Niimi K, Hirai M, Iwata H, Miyazaki K. Ultrasonographic findings and the clinical results of treatment for lymphedema. *Ann Vasc Dis*. 2014; 7(4): 369-375. doi:10.3400/avd.oa.14-00104
- Park GY, Kwon DR. Application of real-time sonoelastography in musculoskeletal diseases related to physical medicine and rehabilitation. *American Journal of Physical Medicine and Rehabilitation*. 2011; 90(11):875-886. doi:10.1097/PHM.0b013e31821a6f8d
- Park J, Lee WH, Chung HS. Incidence and risk factors of breast cancer lymphedema. *Cancer*

Nursing. 2007; 17: 1450-1459. doi: 10.1111/j.1365-2702.2007.02187x

Porrino J, Walsh J. Masive localized lymphedema of the thigh mimicking liposarcoma.

Radiology Case Reports II. 2016: 391-397. doi:

<http://dx.doi.org/10.1016/j.radcr.2016.08.009>

Raj IS, Bird SR, Shield AJ. Ultrasound Measurements of Skeletal Muscle Architecture are Associated with Strength and Functional Capacity in Older Adults. *Ultrasound in Med & Bio.* 2016; 1-9. <http://dx.doi.org/10.1016/j.ultrasmedbio.2016.11.013>

Rastelli F, Capodaglio P, Orgiu S, Santovito C, Caramenti M, Cadioli M, Falini A, Rizzo G, Lafortuna CL. Effects of muscle composition and architecture on specific strength in obese older women. *Exp Physiol.* 2015; 100(10):1159-1167. doi: 10.1113/EP085273

Righetti R, Garra B, Mobbs LM, Kraemer-Chant CM, Ophit J, Krouskop TA. The feasibility of using proelastographic techniques for distinguishing between normal and lymphedematous tissues in vivo. *Phys Med Biol.* 2007; 53: 6525-6541. doi: 10.1088/0031-9155/52/21/013

Righetti R, Ophir J, Krouskop TA. A method for generating permeability elastograms and Poisson's ratio time-constant elastograms. *Ultrasound in Medicine and Biology.* 2005; 31(6): 803-816. doi: <https://doi.org/10.1016/j.ultrasmedbio.2005.02.004>

Roses DF, Brooks AD, Harris MN, Shapiro RL, Mitnick J. Complications of Level I and II Axillary Dissection in the Treatment of Carcinoma of the Breast. *Ann Surg.* 1999; 230(2) 194-200.

Sagen A, Karesen, R, Skaane Per, Arna Risburg M. Validity for the simplified water displacement instrument to measure arm lymphedema as a result of breast cancer surgery. *Arch Phys Med Rehabil.* 2009; 90: 803-809. doi: <https://doi.org/10.1016/j.apmr.2008.11.016>

- Semelka RC, Armao DM, Elias J, Huda W. Imaging strategies to reduce the risk of radiation in CT studies, including selective substitutions with MRI. *Journal of Magnetic Resonance Imaging*. 2007; 25: 900-909. doi: 10.1002/jmri.20895
- Shallwani S, Towers A. Self-management strategies for malignant lymphedema: a case report with one- year and four-year follow-up data. *Physiotherapy Canada*. 2017; 70(3): 1-8. doi:10.3138/ptc.201694
- Stout NL, Pfalzer LA, McGarvey C, Springer B, Gerber LH, Soballe P. Preoperative assessment enables the early diagnosis and successful treatment of lymphedema. *Cancer*. 2008; 112: 2809-2819. doi: 10.1002/cncr. 23494
- Suehiro K, Morikage N, Murakammi M, Yamashita O, Harada T, Ueda K, Samura M, Hamano K. A study of increase in leg volume during complex physical therapy for leg lymphedema using subcutaneous tissue ultrasonography. *Journal of Vascular Surgery*. 2015: 295-302. doi: 10.1016/j.jvsv.2015.02.001
- Szuba A, Rockson SG. Lymphedema: classification, diagnosis and therapy. *Vascular Medicine*. 1998; 3: 145-156.
- Taaffe DR, Lewis B, Marcus R. Quantifying the effect of hand preference on upper limb bone mineral and soft tissue composition in young and elderly women by dual x-ray absorptiometry. *Clinical Physiology and Functional Imaging*. 1994; 14(4): 393-404.
- Tassenoy A, De Mey J, Stadnik T, De Ridder F, Peeters E, Van Schuerbeek P, Wylock P, Van Eeckhout GP, Verdonck K, Lamote J, Baeyens L, Lievens P. Histological findings compared with magnetic resonance and ultrasonographic imaging in irreversible postmastectomy lymphedema: A case study. *Lymphat Res Biol*. 2009; 7: 145-151. doi: 10.1089/lrb.2008.1025

- Tassenoy An, De Striker D, Adriaenssens N, Lievens P. The Use of Noninvasive Imaging Techniques in the Assessment of Secondary Lymphedema Tissue Changes as Part of Staging Lymphedema. *Lymphatic Research and Biology*. 2016; 14(3): 127-133. doi: 10.1089/lrb.2016.0011
- Tortora GJ, Nielson MT. *Principles of Human Anatomy* (12th ed). Hoboken, New Jersey: John Wiley & Sons, Inc, 2012.
- Visser M, Fuerst T, Lang T, Salamone L, Harris T. Validity of fan-beam dual-energy X-ray absorptiometry for measuring fat-free mass and leg muscle mass. *Journal of Applied Physiology*. 1999; 87(4): 1513-1520. Doi: <https://doi.org/10.1152/jappl.1999.87.4.1513>
- Ward L.C. Bioelectrical Impedance Spectrometry for the Assessment of Lymphoedema: Principles and Practice. In: Greene A., Slavin S., Brorson H. (eds) *Lymphedema*. Springer, Cham. 2015. doi: https://doi.org/10.1007/978-3-319-14493-1_12
- Weissleder H, Shuchardt C, eds (2008). *Lymphedema Diagnosis and Therapy*. Viavital-Verlag GmbH. 2008; 4. Essen Germany.
- World Health Organization. *Breast Cancer Awareness Month in October*. WHO, 2015 Retrieved from: http://www.who.int/cancer/events/breast_cancer_month/en/
- Young A, Hugues I, Russell P, Parker MJ, Nichols PJR. Measurement of quadriceps muscle wasting by ultrasonography. *Rheumatology and Rehabilitation*. 1980; 19(3): 141-148. doi: 10.11093/rheumatology/19.3.141